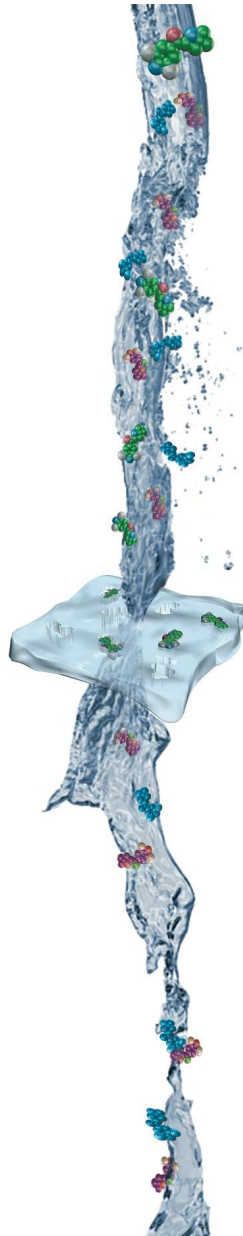


Molecularly imprinted polymers and reactive scavengers in pharmaceutical clean-up



Rüstem Keçili

**Molecularly imprinted polymers and reactive
scavengers in pharmaceutical clean-up**

Dissertation

zur Erlangung des akademischen Grades

Doktor der Naturwissenschaften

(Dr. rer. nat.)

der Technischen Universität Dortmund

vorgelegt von

Rüstem Keçili

aus Eskisehir, Türkei

Dortmund 2012

Molecularly imprinted polymers and reactive scavengers in pharmaceutical clean-up

Ph.D. Thesis submitted to
the Faculty of Chemistry
at the Technical University of Dortmund
for obtaining the degree of
Doctor of Philosophy in Chemistry

Supervisors

Priv. Doz. Dr. Börje Sellergren
(Technical University of Dortmund, Germany)

Dr. Ecevit Yilmaz
(Biotage AB, Sweden)

Rüstem Keçili

Dortmund 2012

This work was carried out between September 2009 and October 2012 at Biotage AB, Lund, Sweden and at the Faculty of Chemistry, Technical University of Dortmund, Germany.

Die vorliegende Doktorarbeit wurde am Institut für Umweltforschung und der Firma MIP Technologies (Biotage), Schweden, angefertigt und eingereicht an der Fakultät für Chemie der Technischen Universität Dortmund.

Gutachter der Dissertation:

1. Gutachter: Priv. Doz. Dr. Börje Sellergren
2. Gutachter: Prof. Dr. Ralf Weberskirch

Tag des öffentlichen Promotionskolloquiums:

11. Dezember 2012

Erklärung

Hiermit erkläre ich, dass ich die vorliegende Dissertation selbständig und nur mit den angegebenen Hilfsmitteln angefertigt habe. Die Arbeit wurde bisher in gleicher oder ähnlicher Form keiner anderen Prüfungskommission vorgelegt und auch nicht veröffentlicht.

Dortmund, 30. Oktober 2012



Rüstem Keçili

To my family

ACKNOWLEDGEMENTS

First of all, I would like to thank my industrial supervisor Dr. Ecevit Yilmaz for all his advice, constant guidance, support, encouragement, optimism and for giving me the great opportunity to work at Biotage AB (Sweden). Despite his busy schedule at the company he always had time to help me. His guidance both in scientific and non-scientific matters has been invaluable.

Further, I would like to thank my academic supervisor, Priv. Doz. Dr. Börje Sellergren, for giving me the opportunity to work in his group and for all the support and scientific advice during my Ph.D. project.

I would like to express my sincere gratitude to Prof. Anthony Rees and to Prof. Ola Karlsson for giving me the opportunity to work at the company. Thanks also to Dr. Steve Jordan for his support during this project.

I would like to thank Prof. Dr. Ralf Weberskirch for kindly acting as second examiner of my Ph.D. thesis.

Special thanks to Dr. Johan Billing for his wealth of knowledge, for all his help and useful advice on organic and polymer chemistry during this project.

I would like to thank David Nivhede and Dr. Mats Leeman for all their help regarding analytical issues and the instrumentation during my Ph.D. work.

I would like to thank all my colleagues at Biotage for the great atmosphere, their useful advice, help and kindness.

Many thanks to Dr. György Székely for all his support during my Ph.D. work.

I would like to thank Sudhirkumar Shinde for all his help and advice during my Ph.D. work in Dortmund.

I would also like to thank all my co-workers and friends in Dortmund for providing me with a friendly working environment in Germany and for their help and support: thanks so much to Mahadeo, Emelie, Fatemeh, Eric, Carla, Javier, Ricarda, Annabell, Reza, Malak, Abed and Patrick.

Special thanks to Prof. Dr. Ridvan Say, Prof. Dr. Arzu Ersöz, Assoc. Prof. Dr. Lutfi Genc, Assoc. Prof. Dr. Deniz Hur, Asst. Prof. Dr. Sibel Emir Diltemiz, Asst. Prof. Dr. Ayca Atilir Özcan, Dr. Sibel Buyuktiryaki, Dr. Ali Özcan, Senay Arikan Eser, Özlem Bicen Unluer and Guner Saka for all their support during my Ph.D. work.

Financial support of the European Commission under FP7-Marie Cure Actions, Contract PITN-GA-2008-214226 [NEMOPUR] for the work presented in this thesis is gratefully acknowledged.

Last but not the least I am grateful to my family for their endless support.

SUMMARY

Genotoxic compounds (GTIs) are impurities that may be present at low levels in pharmaceutical products. A rather diverse group of compounds have been identified that may pose a threat to the safety of the pharmaceutical product. In consequence, substances with a genotoxic potential have recently been the focus of a great deal of attention from regulators and pharmaceutical producers. It is therefore of great importance to either avoid or, as described in this present thesis, to remove such dangerous impurities. Hence, the elimination of undesired impurities from active pharmaceutical ingredients (APIs) is very important during the production process in the pharmaceutical industry

This thesis describes the development, identification and evaluation of adsorption materials that can have practical use towards the selective removal of such genotoxic impurities from pharmaceutical compounds by using molecularly imprinted polymers (MIPs) and reactive scavengers. In the scope of this thesis, three genotoxic compounds were investigated, namely methyl p-toluenesulfonate, acrolein and a set of aminopyridines.

The first part of the work had the focus on the removal of the GTI **methyl p-toluenesulfonate** from model APIs. In order to identify appropriate resins, first screening experiments of MIP libraries were done, then novel MIP resins were designed, synthesized and evaluated and lastly, reactive scavengers were evaluated. Although the MIP screening experiments did not result in any distinct hit resin, a non-imprinted resin was found that displayed good selectivity towards methyl p-toluenesulfonate over the model API 21-chlorodiflorasone. This resin was packed into an HPLC column and the chromatographic separation of GTI and API was successfully achieved. The preparation, characterization and application of novel MIPs that were designed for selectivity towards methyl p-toluenesulfonate were also carried out in this part of the work. Finally, the performance of modified polystyrene and silica based reactive scavengers were also tested. It was found that employing those reactive scavengers was the most

promising route here and the GTI methyl p-toluenesulfonate was successfully separated from the model API in organic solutions.

In the second part of work, the GTI **acrolein** was the target molecule. Here, the synthesis, characterization and binding behavior of novel MIPs that were designed to exhibit selectivity towards acrolein, was evaluated. In addition, the performance of aldehyde scavengers based on polystyrene and silica was tested in organic media. Also here, the selective removal of these genotoxic impurities from the model API iodixanol was best achieved by using the reactive scavengers.

In the third part of the study, a group of GTI compounds, namely the **aminopyridines** were investigated. Also here, screening experiments were conducted using MIP resin libraries to identify resins with the desired selectivity towards those potentially genotoxic impurities over pharmaceutical compounds. A quite potent hit resin was found from the screening experiments which exhibited a considerable imprinting effect. The resin displayed a broad selectivity towards all the five different aminopyridines in the presence of two model APIs piroxicam and tenoxicam.

Both the reactive scavengers that were identified for removal of methyl p-toluenesulfonate and acrolein and also the MIP selective towards the group of aminopyridines are promising candidates for practical industrial use in the pharmaceutical industry that can be envisaged to get employed in a real API purification processes.

ZUSAMMENFASSUNG

Genotoxische Verbindungen sind Verunreinigungen, die in geringen Konzentrationen in pharmazeutischen Produkten vorhanden sein können. Eine breite Palette von Verbindungen ist identifiziert worden, welche die Produktsicherheit bedrohen können. Die Entfernung von bedenklichen, genotoxischen Reststoffen in pharmazeutischen Wirkstoffen ist in der pharmazeutischen Industrie gegebenermassen von hohem Interesse und ist ein wichtiger Schwerpunkt auf der Tagesordnung der zuständigen Behörden und den Produzenten aus der pharmazeutischen Industrie. Es ist deswegen wichtig, sowohl die Bildung dieser Stoffe zu verhindern, als auch die Entfernung, wie in dieser Arbeit beschrieben wird, zu bewerkstelligen.

In der vorliegenden Arbeit wird die Entwicklung, Identifizierung und Untersuchung von Adsorptionsmaterialien beschrieben, die für die praktische Entfernung von genotoxischen Verunreinigungen (GTIs) aus pharmazeutischen Wirkstoffen (APIs) mit Hilfe von molekular geprägten Polymeren (MIPs) und reaktiven Harzen verwendet werden können. In dieser Arbeit werden drei genotoxische Verbindungen behandelt, nämlich Methyl-p-Toluolsulfonat, Acrolein und eine Gruppe von Aminopyridinen.

Der erste Teil der Arbeit beschäftigt sich mit der Entfernung von **Methyl-p-Toluolsulfonat** von Model-APIs. Um geeignete Adsorbentien zu ermitteln, wurden zuerst Screening Experimente mit MIP Bibliotheken durchgeführt. Dann wurden neuartige MIPs designed, synthetisiert und ausgewertet und als letztes wurden reaktive Scavengers untersucht. Aus dem Screening hat sich zwar kein Harz-Kandidat ergeben, der eine hohe Bindung aufweist, jedoch wurde ein Harz identifiziert, welches eine hohe Selektivität für das GTI gegenüber dem API aufweist. In der chromatographischen Anwendung konnte dieses Harz das GTI erfolgreich vom API trennen. In diesem Teil der Arbeit wurden auch neue MIPs synthetisiert, charakterisiert und untersucht, wie effektiv diese neuartigen MIPs das GTI vom API entfernen können. Als letzte Methode wurden im diesem Teil

der Arbeit reaktive Harze, basierend auf Polystyrol und Silika, auf ihre Leistungsfähigkeit bezüglich der selektiven Separation von Methyl-p-Toluolsulfonat gegenüber dem Modelwirkstoff API 21-Chlorodiflorason in organischen Lösungsmitteln untersucht. Hier erwies sich die Anwendung von reaktiven Harzen für die Aufreinigung als sehr wirksam und es konnte gezeigt werden, dass das genotoxische Methyl-p-Toluolsulfonat erfolgreich vom API entfernt werden konnte.

Im zweiten Teil der Arbeit wurde **Acrolein** als Zielmolekül untersucht. Hier wurden geprägte Polymere synthetisiert, charakterisiert und deren Bindungseigenschaften bezüglich Acrolein untersucht. Darüber hinaus wurden reaktive Harze, basierend auf Polystyrol und Silika, auf ihre Leistungsfähigkeit bezüglich der selektiven Separation von Acrolein vom Modelwirkstoff Iodixanol untersucht. Hier erwies sich die Anwendung von reaktiven Aldehyd-Harzen für die Aufreinigung als sehr wirksam.

Im dritten Teil der Arbeit wurde eine Gruppe von **Aminopyridinen** untersucht. Auch hier wurden Screening-Experimente mit MIP Bibliotheken durchgeführt, um selektive Harze für die Bindung von genotoxischen Aminopyridinen zu ermitteln. Es wurde ein leistungsstarkes, geprägtes Material identifiziert, welches Aminopyridine gut von den pharmazeutischen Wirkstoffen Piroxicam und Tenoxicam unterscheiden kann. Des Weiteren zeigte das selektive MIP auch deutliche Prägungseigenschaften.

In dieser Arbeit wurden reaktive Harze, welche Methyl-p-Toluolsulfonat und Acrolein selektiv entfernen können und auch ein MIP, welches Aminopyridine selektiv bindet, identifiziert. Diese sind vielversprechende Materialien, die in industriellen Aufreinigungsprozessen für pharmazeutische Wirkstoffe praktische Anwendung finden können.

CONTENTS

ACKNOWLEDGEMENTS	1
SUMMARY	4
ZUSAMMENFASSUNG	6
CONTENTS	8
1 INTRODUCTION	10
1.1 Genotoxic impurities in pharmaceuticals	11
1.1.1 Guidelines on limits for genotoxic impurities.....	13
1.1.2 Genotoxic impurity removal from pharmaceuticals	15
1.2 Genotoxic impurities selected for this study	16
1.2.1 Methyl p-toluenesulfonate	16
1.2.2 Acrolein.....	18
1.2.3 Aminopyridines.....	19
1.3 Molecularly imprinted polymers (MIPs).....	20
1.3.1 Approaches for the preparation of MIPs.....	23
1.3.2 MIPs for solid phase extraction (SPE).....	27
1.3.3 Previous examples of MIPs for genotoxic impurity removal	30
1.3.4 Screening of MIP libraries	31
1.4 Reactive scavengers	44
2 OBJECTIVES OF THE THESIS	47
3 MATERIALS	48
4 METHODS	50
4.1 Analysis of target GTIs and APIs.....	50
4.1.1 HPLC analysis.....	50
4.1.2 LC-MS/MS analysis.....	51
4.2 MIP library screening procedures	53
4.3 HPLC column packing	54
4.4 Flow through scavenging procedures for reactive scavengers.....	55
4.5 Batch scavenging procedures for reactive scavengers	56
4.6 Synthesis of urea based functional monomers	57
4.7 Preparation of methyl p-toluenesulfonate imprinted polymers.....	58
4.8 Characterization of the polymers.....	59
4.8.1 Nitrogen adsorption.....	60
4.8.2 Elemental analysis.....	61
4.8.3 Particle size analysis	61
4.8.4 Optical microscopy	61
4.8.5 Swelling experiments	61
4.8.6 Infrared spectroscopy	62
4.9 Batch rebinding procedure for the polymers.....	62
4.10 Comparison experiments of the binding behavior of the polymers and reactive scavengers.....	62
4.11 Synthesis of functional monomers for acrolein MIPs	63
4.12 Preparation of MIPs for acrolein	64
5 RESULTS AND DISCUSSION	67
5.1 MIP resins and reactive scavengers towards methyl p-toluenesulfonate.....	67
5.1.1 Screening of urea MIPs.....	67

5.1.2	Selectivity tests	71
5.1.3	Binding isotherms	74
5.1.4	Synthesis of methyl p-toluenesulfonate imprinted polymers.....	78
5.1.5	Binding behavior of the new polymers for methyl p-toluenesulfonate	85
5.1.6	Properties of the studied reactive resins.....	86
5.1.7	Scavenging behavior of the reactive resins.....	91
5.1.8	Comparison of MIPs and reactive resins for GTI removal.....	101
5.2	Removal of acrolein from APIs using designed MIPs and aldehyde scavengers	103
5.2.1	Analysis of acrolein.....	103
5.2.2	Synthesis of functional monomer for acrolein MIPs	104
5.2.3	Synthesis of MIPs for acrolein.....	105
5.2.4	Binding behavior of the polymers towards acrolein	109
5.2.5	Scavenging behavior of reactive resins.....	112
5.3	Fast identification of selective resins for removal of aminopyridines from APIs	119
5.3.1	Screening of resin chemistries	119
5.3.2	Screening of carboxylic acid MIPs	121
5.3.3	Binding and elution of aminopyridines and corresponding APIs from the candidate resins	123
5.3.4	Chromatographic evaluation of the polymers towards aminopyridines.....	131
6	CONCLUSIONS	136
7	APPENDIX	139
7.1	Abbreviations	139
8	PUBLICATIONS	141
8.1	Articles	141
8.2	Posters	141
9	REFERENCES	142

1 INTRODUCTION

Pharmaceutical companies and those who supply them with intermediates, constantly strive to produce active pharmaceutical ingredients (APIs) and intermediates of the highest purity. The synthesis of pharmaceutical compounds often involves the use of reactive reagents and also the formation of intermediates and by-products. Despite a range of work-up efforts in the production processes, low levels of some of these may be present in the final product as impurities. Consequently, the removal of undesired impurities from APIs is an important aspect of the production processes in the pharma industry and substances with undesired genotoxicity have recently received considerable attention from regulatory agencies and pharmaceutical companies. ^[1-6] In the development and manufacturing of APIs and their intermediates, purification processes constitute the bulk of the processing time and cost. The technological advances in analysis, which make detection of impurities at lower levels possible, exacerbate the time and cost demands. At the same time, there is a growing expectation among patients regarding the efficacy, safety and purity of medicines. These trends have created an urgent need for new molecular purification technologies in pharmaceutical production. Furthermore, chemical synthesis in the pharma industry is often carried out in organic solvents and involve products with high value that have to be separated from complex mixtures. This makes the purification steps more difficult because of the harsh operating conditions. The APIs are usually purified using various unit operations such as crystallization, chromatography, extraction, precipitation and distillation. However, all these processes often result in loss of API and therefore increase the total cost of the final product. Therefore, innovative technologies and processes with higher selectivity, fewer process steps and lower time and energy requirements are needed.

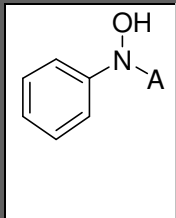
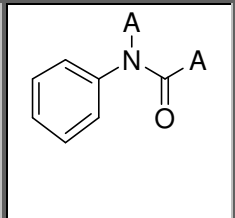
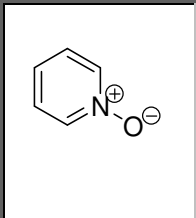
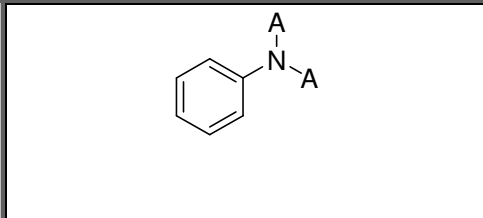
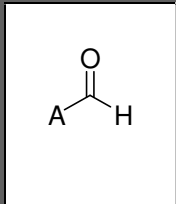
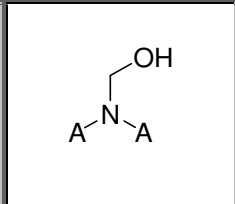
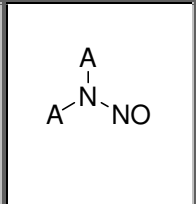
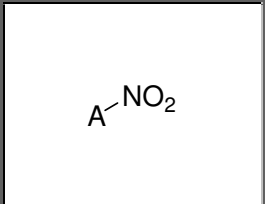
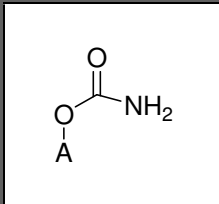
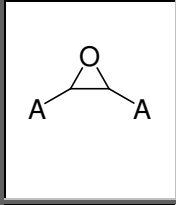
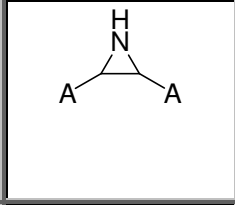
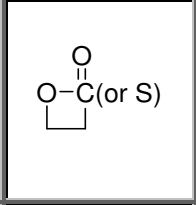
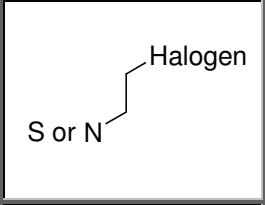
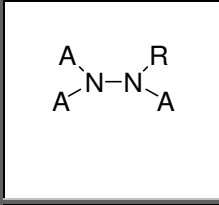
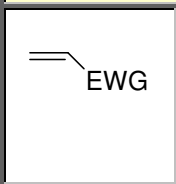
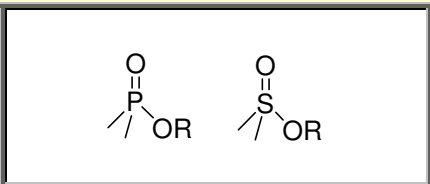
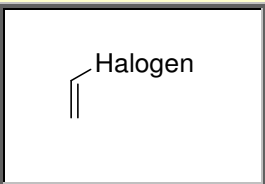
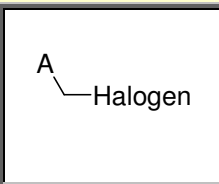
1.1 *Genotoxic impurities in pharmaceuticals*

Pharmaceutical genotoxic impurities (GTIs) are residuals that can occur in pharmaceutical compounds and may have the ability to induce genetic mutations, chromosomal breaks, or chromosomal rearrangements, and have hence the potential to cause cancer in humans.^[7-8] Therefore, any level of exposure to such impurities present in an active pharmaceutical ingredient (API) may be a significant toxicological problem.^[9-11] The analysis of these impurities in APIs has received increased attention^[12-14] and guidelines were recently issued.^[15] During the production of active pharmaceutical ingredients, reactive intermediates, catalyst, acids, or bases are often used and these compounds or their derivatives can potentially end up at trace levels in final pharmaceutical substances. The Viracept (nelfinavir mesylate) contamination accident can be given as an example that shows the potential dangers of genotoxic compounds present in a pharmaceutical compounds. In June 2007, excess levels of a genotoxic sulfonate ester (ethyl mesylate) formed from the reaction between residual ethanol and the methyl sulfonic acid counter ion in the production tank were detected in the active pharmaceutical ingredient of Viracept produced by Roche and this led to a temporary global recall of the product.^[16]

It is hence very crucial for process scientists to explore possible routes to avoid the use and generation of these genotoxic compounds during the manufacturing process and if genotoxic impurities are still present in the product, they need to be reduced to acceptable levels using one or more purification steps. Since a very large number of compounds are used or tested in drug synthesis and development, no full list of target compounds is available, and instead a list of “structural alert functionalities” is used.^[8, 17]

A range of important structurally alerting functional groups was recently published by a consortium of representatives of several large global pharmaceutical companies.^[8] This list is given in Table 1.1.

Table 1.1: Examples of structurally alerting functional groups ^[8]

Group 1: Aromatic Groups				
				
<i>N-Hydroxyaryls</i>	<i>N-Acylated aminoaryls</i>	<i>Aza-aryl N-oxides</i>	<i>Aminoaryls and alkylated aminoaryls</i>	
Group 2: Alkyl and Aryl Groups				
				
<i>Aldehydes</i>	<i>N-Methylols</i>	<i>N-Nitrosamines</i>	<i>Nitro Compounds</i>	<i>Carbamates</i>
				
<i>Epoxides</i>	<i>Aziridines</i>	<i>Propiolactones Propiosulfones</i>	<i>N or S Mustards (beta haloethyl)</i>	<i>Hydrazines and Azo compounds</i>
Group 3: Heteroatomic Groups				
				
<i>Michael-reactive Acceptors</i>	<i>Alkyl esters of phosphonates or sulfonates</i>	<i>Halo-alkenes</i>	<i>Primary halides (Alkyl and aryl-CH₂)</i>	

Legend: A= Alkyl, Aryl or H

Halogen= F, Cl, Br, I

EWG= Electron withdrawing group (CN, C=O, ester etc)

1.1.1 Guidelines on limits for genotoxic impurities

The European Medicines Agency's (EMA) International Conference on Harmonization (ICH) and The Pharmaceutical Research and Manufacturers Association (PhRMA) have published guidelines to provide limits for genotoxic impurities in pharmaceutical compounds.

The guideline published in 2006 by the EMA and the Committee for Medicinal Products for Human Use (CHMP) categorized impurities into two categories: ^[15] one category for the impurities which there is “sufficient evidence for a threshold-related mechanism” and the other one for impurities “without sufficient evidence for a threshold-related mechanism”.

The guideline recommends to regulate acceptable levels to an “as low as reasonably practicable” principle for genotoxic compounds without adequate confirmation for a threshold-related mechanism. This approach specifies that every effort should be made to prevent the formation of such compounds during the synthesis of pharmaceutical compounds.

On the other hand, a threshold of toxicological concern (TTC) has been established to provide threshold values for all compounds.

The concentration limits of genotoxic impurities in pharmaceutical compounds derived from the TTC values can be calculated from the estimated daily dose using the following equation (1):

$$\text{Concentration limit (ppm)} = \text{TTC } (\mu\text{g/day}) / \text{dose (g/day)} \quad (1)$$

The ICH guidelines ICHQ3A(R), Q3B(R) and Q3C(R) ^[18-20] have been provided for content and qualification of genotoxic impurities in new pharmaceutical compounds. Various threshold values were defined in the guideline ICH Q3A(R) to identify and establish the minimum qualification requirements for genotoxic impurities.

ICHQ3A(R) emphasizes that: “The level of impurity present in a new pharmaceutical compound that has been adequately tested in clinical studies

would be considered qualified. Impurities which are also substantial metabolites present in human or animal, clinical studies do need further qualification.”

ICHQ3B(R) addresses only impurities in new pharmaceutical products that are categorized as degradation impurities of the pharmaceutical compound or reaction products of the pharmaceutical compound.

Finally, ICHQ3C recommends acceptable levels of residual solvents in the pharmaceutical products.

In another approach, impurities were categorized by a published procedure for testing, classification, qualification requirements, and toxicological risk assessment of GTIs.^[8] The Pharmaceutical Research and Manufacturers Association (PhRMA) categorized impurities into five categories:

The impurities in *category 1* are genotoxic and carcinogenic.

Category 2 impurities are genotoxic but their carcinogenic potential is not known. These impurities should be controlled using TTC values.

The impurities in *category 3* contain structural alerts unrelated to the structure of the API and unknown genotoxicity. The impurities in this category contain functional groups that should be considered as genotoxic based on the structure.

Category 4 impurities contain structural alerts related to the API.

The impurities in *category 5* do not contain structural alerts and there is no sufficient evidence for their genotoxicity. These compounds are to be considered as normal impurities. If the compounds in the *category 3 or 4* which show genotoxicity or are not tested for genotoxicity, they should be considered in the *category 2*. If those compounds do not show any genotoxicity they are considered in the *category 5*.

As regulatory bodies are lowering the level of acceptable concentrations of GTIs in pharmaceutical formulation, their analysis is concurrently getting more and more technically demanding. Hence, sophisticated analytical work-up methods and the use of high-performance columns and advanced instrumentation will be increasingly required to meet those tightened demands.

1.1.2 Genotoxic impurity removal from pharmaceuticals

The prime aim of the production of active pharmaceutical ingredients is to deliver a clean and safe product. Careful purification and impurity removal is necessary to meet the strict demands on purity and safety of the compound. The general removal of genotoxic impurities consists of multistep processes such as recrystallization, fractional distillation, extraction, chromatography or membrane filtrations among others.

In a recrystallization process, the crude API is dissolved in an appropriate solvent at high temperature and the API crystals reform while the solution is allowed to cool. If the solvent has been chosen properly, impurities in the API remain in solution and the API crystals can be separated by filtration from the recrystallization media.

In the fractional distillation technique, API and GTI compounds are separated by controlled heating based on their different boiling points. The pure API is collected as a distillate during distillation, leaving the non-volatile compounds in the residue. This technique is not appropriate for heat-sensitive compounds.

Furthermore, chromatography and activated carbon based processes can be used for purification of APIs. However, although these techniques are commonly used and commercially available, they have some restrictions in cost, scale up, selectivity and sometimes they also lead to loss of API.

The use of adsorbents^[21-22] and reactive resins^[23] for the selective removal of undesired impurities from pharmaceutical compounds has previously been described. Molecularly imprinted polymers (MIPs), organic solvent nanofiltration (OSN), OSN-MIP hybrid systems and MIP-membrane composites have also recently been reported for selective removal of GTIs from API solutions.^[24-28]

Many pharmaceutical companies also take the route to re-design their production reaction process to avoid the generation of GTIs. Wherever this is possible to employ then the final clean-up is simplified or made redundant. As changes in the synthetic process are not always feasible or possible, subsequent clean-up steps are a main option that can be used.

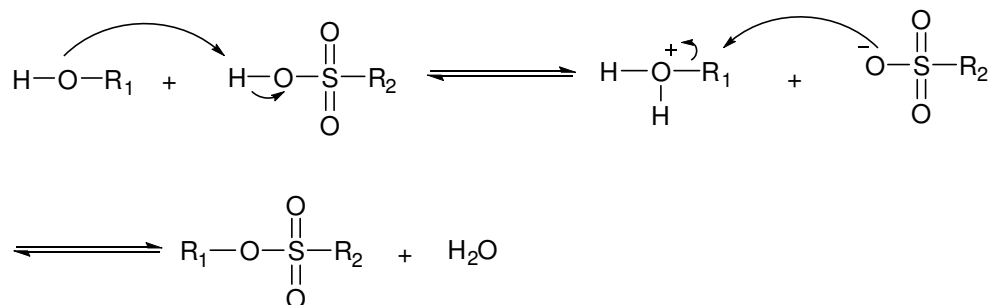
1.2 Genotoxic impurities selected for this study

1.2.1 Methyl p-toluenesulfonate

The compound p-toluenesulfonic acid (pTSA) is a chemical that is used for many organic reactions. Due to its strong acidity it is commonly used as a counter-ion or catalyst in the synthesis of pharmaceutical compounds. [29]

The presence of any residual alcohols such as methanol or ethanol, originating from the production processes or recrystallization steps, may result in the formation of undesired alkyl tosylates, which are known to be genotoxic impurities (GTIs). [8]

A general reaction mechanism for alkyl tosylate formation from pTSA and an alcohol is shown in scheme 1.1. The mechanism has been confirmed by Teasdale et al. [30] using ¹⁸O-labeled methanol.



R₁ - alkyl-methyl/ethyl/propyl etc.

R₂ - alkyl /aryl

Scheme 1.1: Reaction mechanism for alkyl tosylate formation [30]

These GTIs, due to their DNA alkylation ability, can induce carcinogenic and mutagenic effects. [31] Alkylation occurs on nitrogen and oxygen of deoxyguanosine in the DNA structure (Figure 1.1) Formation of these DNA adducts depends on the structure of the alkylating agent and on the alkylation mechanism. [32- 34]

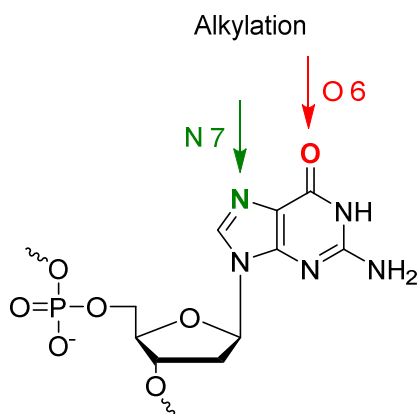


Figure 1.1: Alkylation sites of deoxyguanosine ^[35]

In this study, a model system combining methyl p-toluenesulfonate as the GTI and 21-chlorodiflorasone, used in the synthesis of corticosteroid drugs for the treatment of inflammatory skin diseases, as the API, has been chosen.

The chemical structures of these compounds are shown in Figure 1.2.

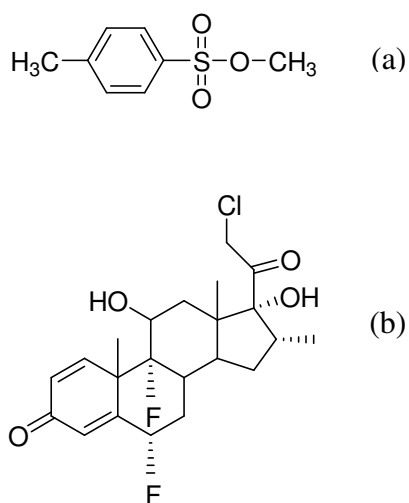


Figure 1.2: Structures of methyl p-toluenesulfonate (GTI) (a) and 21- chlorodiflorasone (API) (b)

1.2.2 Acrolein

Acrolein is an unsaturated aldehyde that is used abundantly in the industry ^[36] and is also used as a building block in the synthesis of pharmaceutical compounds. ^[37] The highly reactive C=C double bond and C=O carbonyl group moieties in the conjugated C=C–C=O system are responsible for its electrophilicity.

The chemical structures of acrolein and the model API iodixanol, commonly used as a dimeric X-ray contrast agent for tomography in diagnosis, ^[38] used in this study are shown in Figure 1.3.

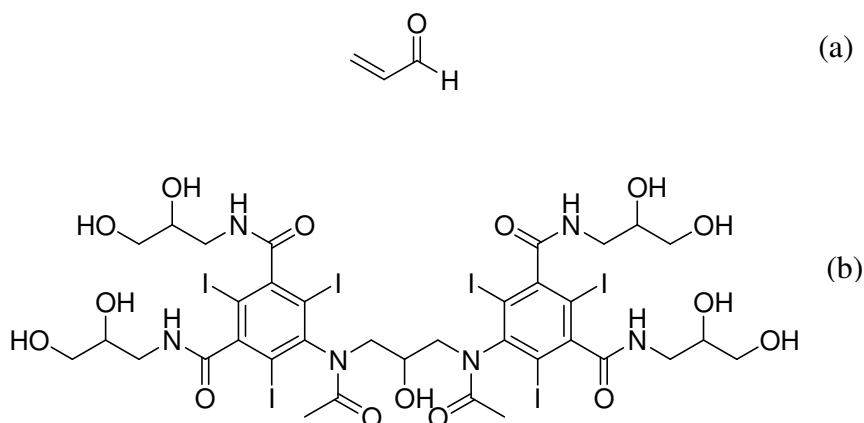
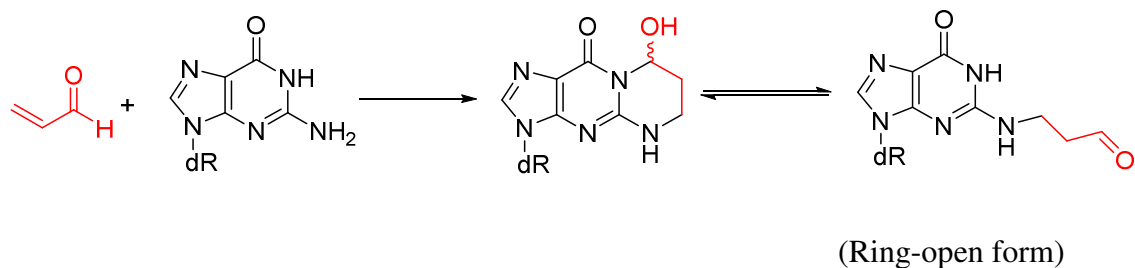


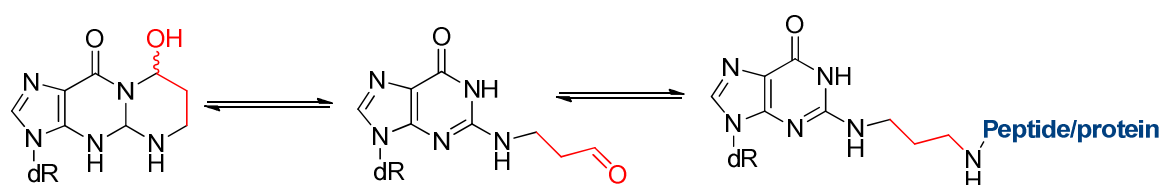
Figure 1.3: Structures of acrolein (GTI) (a) and iodixanol (API) (b)

Acrolein can rapidly penetrate through the cell membranes and subsequently disturbs the cellular redox balance via binding to reactive species. This leads to oxidative stress. ^[39] Acrolein can also rapidly react with the nucleophilic amino groups of deoxyguanosine residues in DNA followed by reversible cyclization resulting in the DNA adducts as exemplified in Scheme 1.2. ^[39]



Scheme 1.2: Reaction of acrolein (red) with deoxyguanosine (black) ^[39]

The active aldehyde side of the ring open form of the DNA adduct can react with peptide or protein moieties such as amino and thiol which leads to coupling of DNA to protein ^[39] (Scheme 1.3) causing inactivation of DNA replication and mutation induction since certain intracellular proteins have critical functions in DNA replication and transcription reactions.



Scheme 1.3: Acrolein DNA adducts induced DNA-peptide/protein cross-link ^[39]

The U.S. Department of Health and Human Services has recently issued a report of the toxicology studies for acrolein. ^[40] Although acrolein rapidly reacts with biological molecules, no clear evidence for carcinogenicity related to its oral intake has been found. ^[41]

1.2.3 Aminopyridines

Aminopyridines are commonly used as starting compounds in the synthesis of APIs and are potentially genotoxic impurities (PGIs) that can be present at trace levels in pharmaceutical compounds. ^[42,43] For example, 2-aminopyridine is a precursor in the synthesis of piroxicam and may also be present as a degradation impurity in the product. ^[44]

In this study, five different aminopyridines and the model APIs piroxicam and tenoxicam, both nonsteroidal anti-inflammatory drugs commonly used for the

treatment of various diseases such as rheumatoid arthritis, osteoarthritis and musculoskeletal disorders, ^[45,46] were examined. The chemical structures are shown in Figure 1.4.

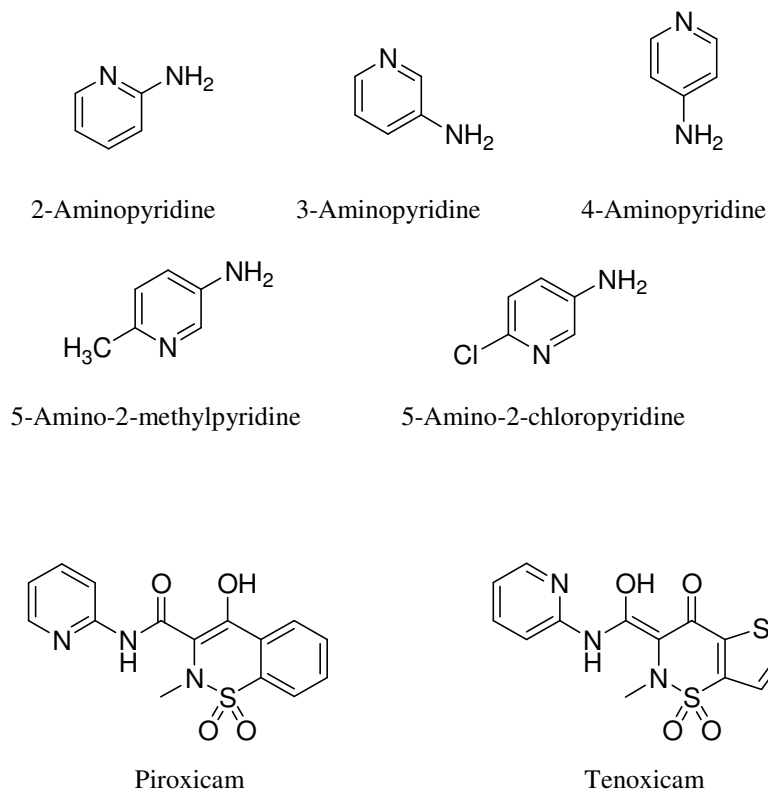


Figure 1.4: Structures of aminopyridines and model APIs

1.3 *Molecularly imprinted polymers (MIPs)*

Molecularly imprinted polymers (MIPs) are a type of selective adsorbents that possess binding sites within the polymer matrix that are adapted to the three-dimensional shape and functionalities of a target molecule. ^[47,48] The selectivity of these binding sites is established during preparation of the MIP. A template, either the target molecule or a derivative of it, and one or more monomers with certain functional groups are dissolved together in a solvent. These monomers bind to the template through covalent, ^[49-58] non-covalent, ^[59-67] electrostatic ^[68] or metal ion coordination ^[69-71] interactions and this complex is then solidified by means of copolymerization of the functional monomer with a cross-linker. The template is removed by extensive washing resulting in a MIP with free specific

binding sites. The obtained polymer displays an engineered selectivity to the analyte of interest (Figure 1.5).

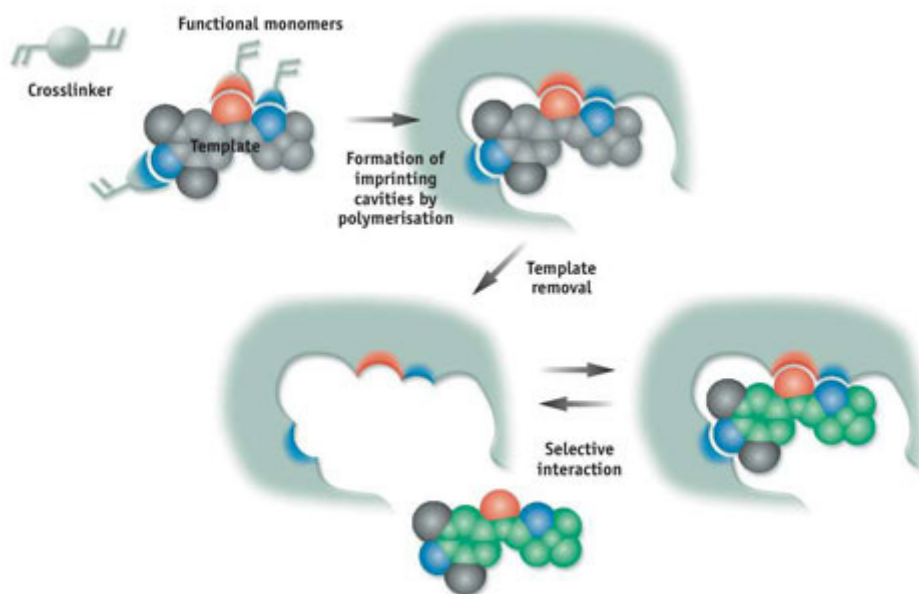


Figure 1.5: Principle of MIP synthesis ^[72]

The rebinding kinetics of the target molecule depends on the nature of the interactions involved in the rebinding process. ^[73]

Common initiators used in MIP synthesis are shown in Figure 1.6. They decompose into two free radical molecules when exposed either to heat or UV-light as shown in Figure 1.7 and the unpaired electrons on the free radicals react with the monomers and cross-linkers in order to form a polymer network during the polymerization.

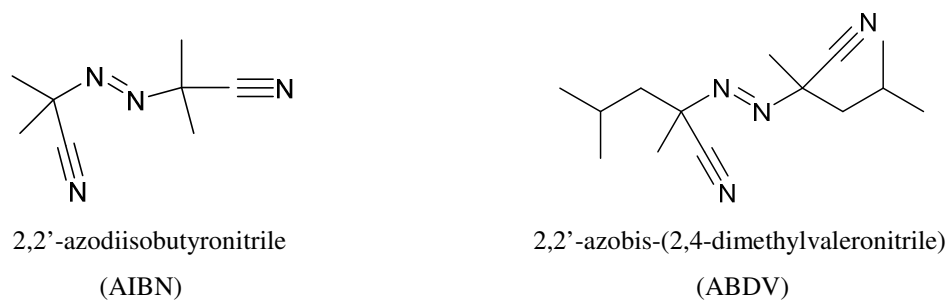


Figure 1.6: Initiators commonly used in MIP synthesis

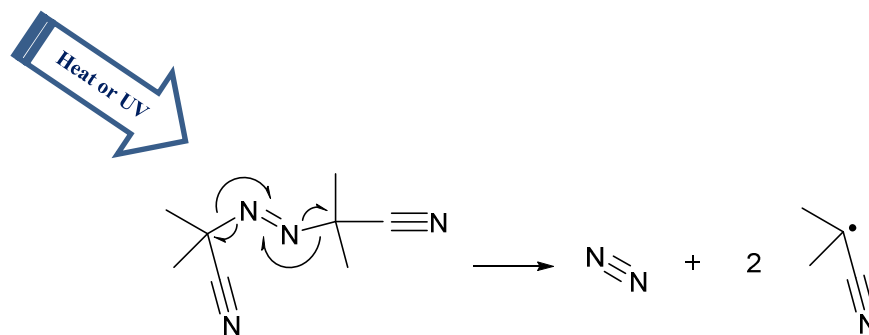


Figure 1.7: Decomposition of 2,2'-azodiisobutyronitrile under heat or UV light

The functional monomers enable the formation of a complex with the target molecule (template) during the polymerization. The most commonly used acidic, basic and neutral functional monomers in MIP synthesis are shown in Figure 1.8

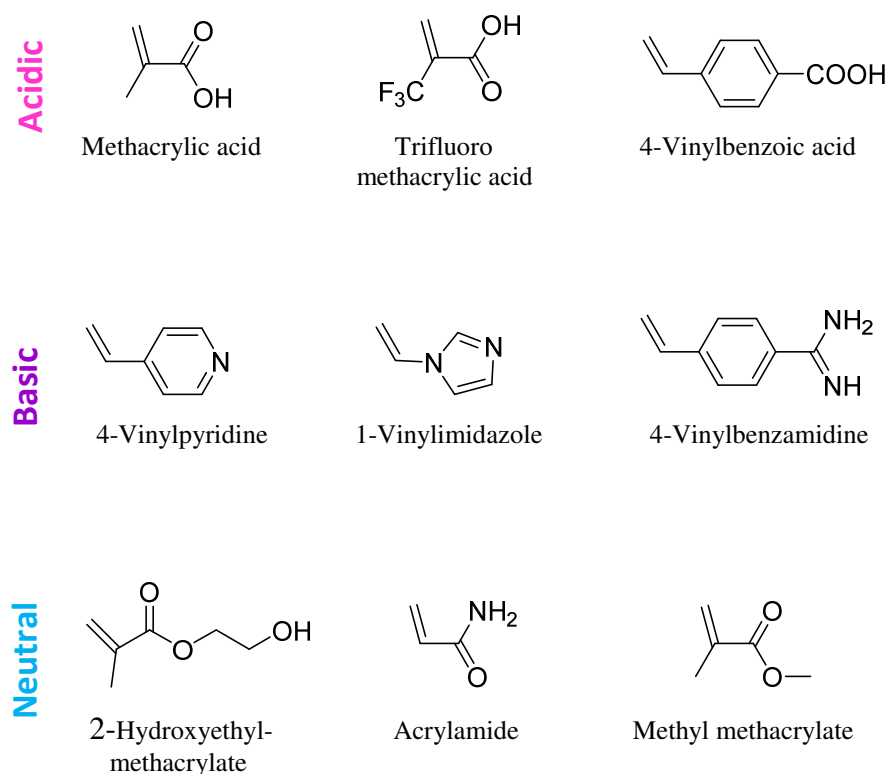


Figure 1.8: Examples of functional monomers used in MIP synthesis

Cross-linkers are crucial in the polymerization process. They have the largest proportion in the imprinting mixture and lead to the rigidity of the polymer

network formed during the polymerization. In Figure 1.9, the most commonly used cross-linkers in MIP synthesis are shown.

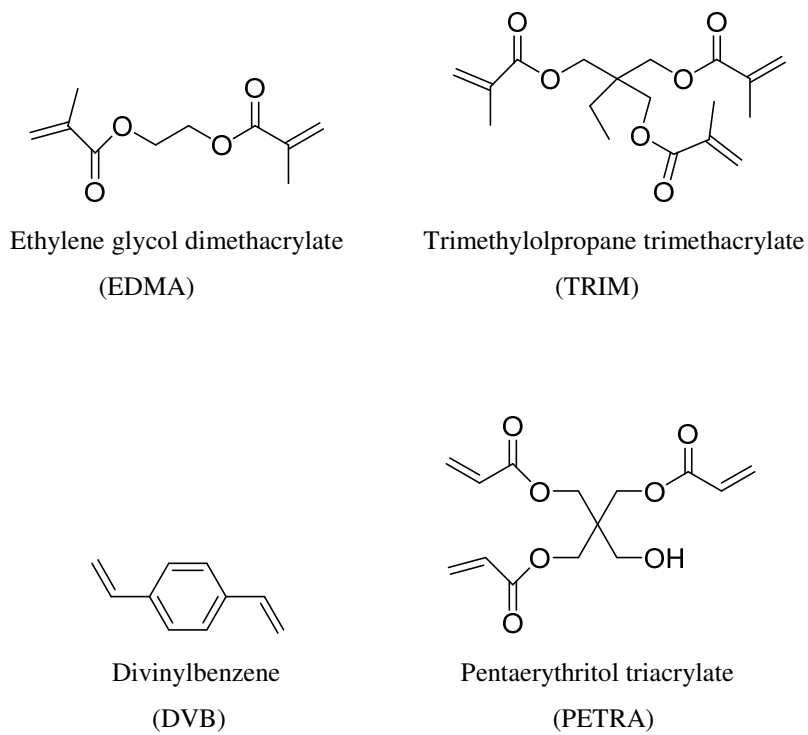


Figure 1.9: Most commonly used cross-linkers in MIP synthesis

1.3.1 Approaches for the preparation of MIPs

Three distinctly different approaches for the preparation of MIPs have been reported: covalent, non-covalent and semi-covalent approaches.

1.3.1.1 The covalent approach

In 1972, Günter Wulff and Ali Sarhan reported the first example of molecular imprinting introducing the covalent imprinting approach.^[74] The covalent approach involves coupling the template molecule to the functional monomer through a reversible covalent bond.^[75-79] The template-monomer is copolymerized with a cross-linking monomer and thus the template is initially incorporated into the MIP structure. Then, the template is removed from the

polymer structure using appropriate chemical methods to create cavities which are complementary in size and functional group orientation to the target compound.

The group of Wulff for example has investigated 4-nitrophenyl- α -D-mannopyranose imprinted polymers.^[80] The schematic depiction of the polymer is shown in Figure 1.10. As can be seen from the Figure 1.10, 4-vinylphenylboronic acid was used as a functional monomer and was covalently bound to the 4-nitrophenyl- α -D-mannopyranose via esterification with the hydroxyl groups.

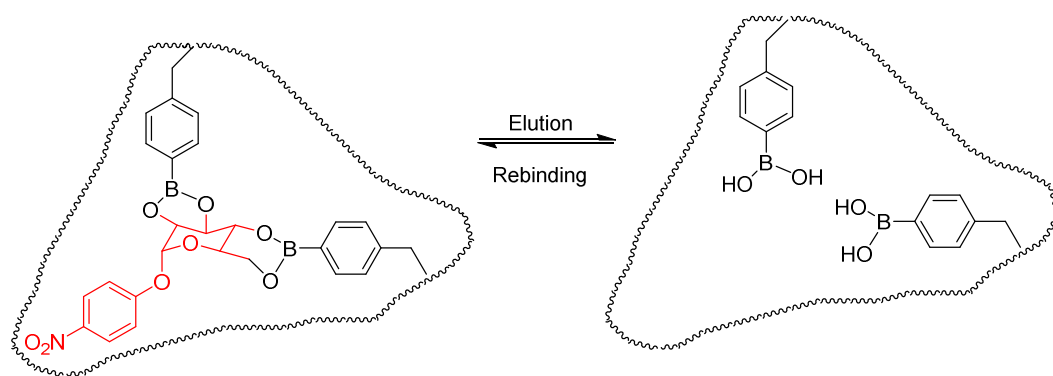


Figure 1.10: Schematic depiction of the covalently imprinted polymers towards 4-nitrophenyl- α -D-mannopyranose^[80]

The advantage of covalent interaction during the imprinting procedure is the exact control during the introduction of the functional groups in a certain vicinity of each other. Thus, the amount of non-specific binding should theoretically be low because there is no excess of reactive functional groups incorporated into the polymer. Despite the elegance of the approach, the range of templates and monomer pairs that are amenable to reversible covalent imprinting is very limited. The utility of the method is hampered by this limitation and the method is not very wide-spread.

1.3.1.2 The semi-covalent approach

Another approach for the synthesis of MIPs is known as the semi-covalent approach. This approach was introduced by Whitcombe et al.^[81] In this case, the interaction between the functional monomer and the template molecule before the polymerization process is covalent, whereas the interaction of the target analyte

and the MIP when the polymer is used is through non-covalent interactions. Whitcombe et al. have prepared cholesterol imprinted polymers using the semi-covalent approach. In their work, cholesteryl chloroformate was reacted with 4-vinylphenol to give cholesteryl (4-vinyl)phenyl carbonate. Then, this carbonate as a template was polymerized in the presence of a cross-linker. The template was removed from the polymeric structure via hydrolysis of the carbonate bond. The remaining phenolic functional group of the synthesized MIP selectively interacted with the cholesterol via non-covalent interactions (Figure 1.11).

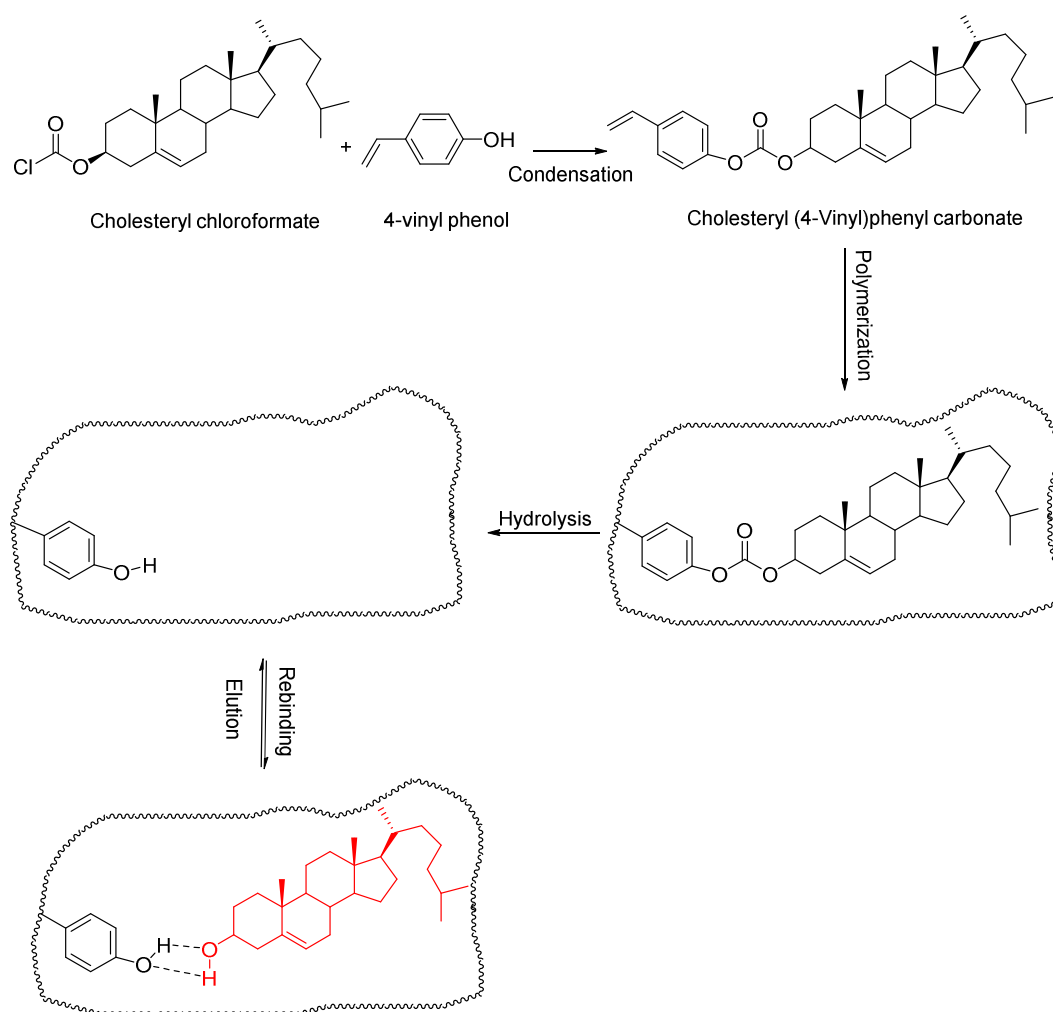


Figure 1.11: Schematic depiction of the semi-covalently imprinted polymers towards cholesterol [81]

In recent years, several studies using semi-covalent approach have been reported. [82, 83]

1.3.1.3 The non-covalent approach

Another approach of molecular imprinting is non-covalent imprinting which was first introduced Arshady and Mosbach^[84] and which is the most straight-forward method. In this approach, the functional monomers assemble around the template by non-covalent interactions (ionic, polar, hydrophobic interactions, hydrogen bonds, van der Waals forces) to form the recognition site after co-polymerization with cross-linking monomers.

For example, Yilmaz et al.^[85] investigated the chiral recognition behavior of (-)-isoproterenol imprinted polymers synthesized by the non-covalent approach as schematically depicted in Figure 1.12. The functional monomer used was trifluoromethacrylic acid (TFMAA) which has hydrogen bonding capability with (-)-isoproterenol. The imprinted polymer was found to be highly selective for the enantioselective recognition of (-)-isoproterenol.

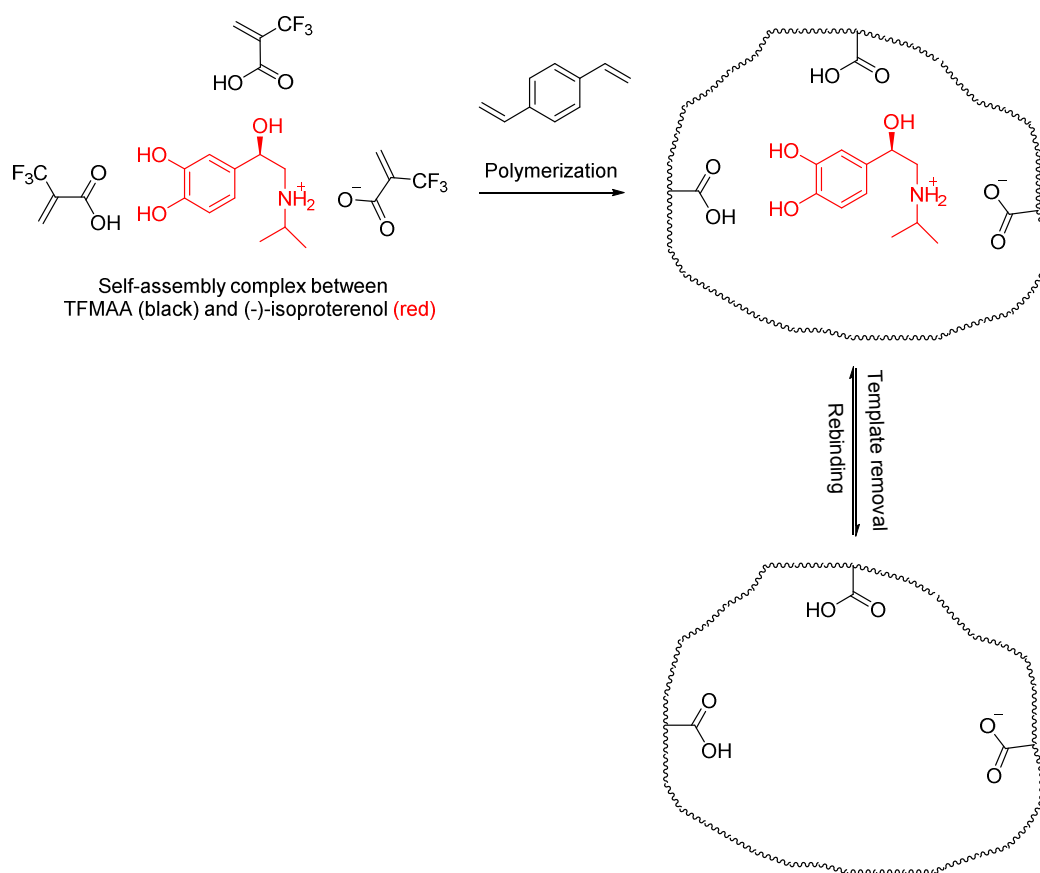


Figure 1.12: Schematic depiction of the non-covalently imprinted polymers towards (-)-isoproterenol^[85]

This method is the simplest to perform due to the availability of a much wider range of monomers and their facile applicability to a broad array of template molecules. The non-covalent nature of the interaction facilitates the removal of the template from the polymer network. The disadvantages of the MIPs prepared by this approach are the low capacity and heterogeneous binding sites of the materials.

1.3.2 MIPs for solid phase extraction (SPE)

Sample preparation is a crucial step of a variety of analytical techniques and often the most time consuming work step in an analytical task. Sample preparation is required for the removal of potential interference compounds, to increase the concentration of an analyte and to convert the analyte into a convenient form for separation and detection. Improving the sample preparation step is often desirable in order to optimize and to speed up analytical techniques.

SPE is today the most common technique for sample clean-up and enrichment. Compared to traditional liquid-liquid extraction, SPE has a lot of advantages such as lower solvent consumption, smaller sample volumes and less exposure to organic solvents. Furthermore, SPE materials provide more reproducible results and give cleaner analyte extracts prior to analysis. Currently, there are a large number of SPE materials commercially available. However, the selectivity of traditional SPE sorbents is often not very high, and moreover, low recoveries are often obtained. These problems can be overcome by using selective separation resins such as molecularly imprinted polymers (MIPs).

MIPs function as a novel type of SPE sorbents with improved selectivity and efficiency compared to traditional SPE materials such as silica or non-imprinted polymers. MIPs can be selective for a specific analyte and allow pre-concentration of this analyte in complex matrices. Compared to many other selective separation materials, MIPs are mechanically and chemically stable under harsh conditions such as extreme pHs, high temperatures and organic solvents. Consequently, a selective wash removing interfering compounds from the biological sample, is generally possible when the analytical method involves a MIP.

A general SPE procedure for aqueous samples using MIPs is shown in Figure 1.13.

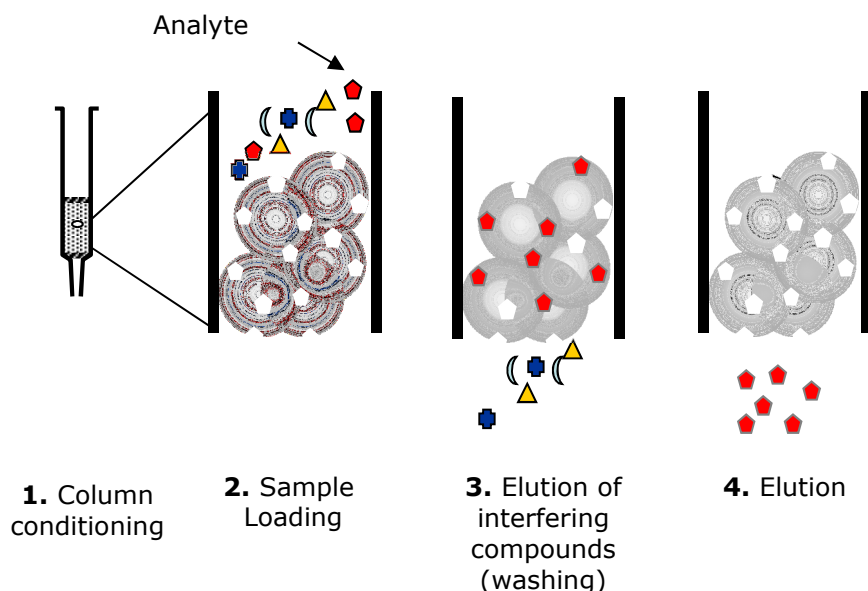


Figure 1.13: Principle of solid phase extraction

In a first step called the conditioning step, the MIP is conditioned with a solvent to swell and to wet the polymer. After the solvent conditioning, the analyte is loaded under aqueous conditions and the analyte and other interfering compounds present in the sample are generally retained on the MIP mainly due to non-selective hydrophobic interactions with the polymer backbone.

After sample loading, the next step of the SPE procedure is one or more washing step. The purpose of the washing step is to remove undesired interfering compounds that are not selectively bound to the MIP without eluting the analytes under conditions that maximize the selective interactions between the analyte and the MIP. Water or buffer is usually used as the first wash to remove hydrophilic interferences such as salts. In order to remove non-selectively bound compounds from the MIP, a second washing step with an organic solvent may be needed. As a general point, analytes exhibit the highest selectivity and binding towards the MIPs in an environment that corresponds to the solvent that was used as a porogen during the polymerization.

The washing step is followed by one or more elution steps, where the interactions between analyte and MIP are disrupted. Polar organic solvents e.g. methanol or acetonitrile, or an organic solvent with water or a so called modifier, e.g. acetic acid, formic acid, pyridine etc. are commonly used as elution solutions depending on the chemistry of the MIP and the bound analyte.

The samples obtained from the elution step are collected, the solvent evaporated and the dry residue re-dissolved and analyzed by HPLC, LC-MS, GC or other HPLC or GC techniques.

In 1994, Sellergren reported the first example of SPE using MIPs. In his work, extraction of pentamidine, used for treatment of HIV/AIDS related infection, from urine was successfully achieved.^[86]

Since then, several reviews^[87-92] and studies^[93-98] have been reported on the application of SPE using MIPs.

SPE using MIPs are currently being successfully employed in bioanalysis^[99-105], environmental analysis^[106-114] and food analysis^[115-120]

MIPs for SPE are marketed today by Biotage (Table 1.2), Sigma-Aldrich and Polyintell.^[72,121,122] Thus, over the last 10 years, MIPs have found their way into various markets and have now matured to commercial products.

Table 1.2: Examples of commercial MIPs for SPE from the Biotage product line^[72]

Product	Application
AFFINILUTE MIP- Clenbuterol	Clenbuterol extraction from biological samples
AFFINILUTE MIP-β- Agonist	β -Agonists extraction from urine and tissue samples
AFFINILUTE MIP-Triazine	Removal of triazines from water and soil
AFFINILUTE MIP- Chloramphenicol	Chloramphenicol extraction from biological samples
AFFINILUTE MIP-β Blocker	β-blockers extraction from biological samples
AFFINILUTE MIP-TSNAs	Tobacco specific nitrosamines extraction

Table 1.2 continues on the next page

Continuation of Table 1.2 from the previous page

AFFINILUTE MIP- Amphetamines	Amphetamine extraction from biological samples
AFFINILUTE MIP- Fluoroquinolones	Fluoroquinolones extraction from food samples
AFFINILUTE MIP- Nitroimidazoles	Nitroimidazoles extraction from food samples
AFFINILUTE MIP- NSAIDs	Non-steroidal anti-inflammatory drugs (NSAIDs) extraction from biological samples
AFFINILUTE MIP-PAH	Polyaromatic hydrocarbons extraction from organic matrices

1.3.3 Previous examples of MIPs for genotoxic impurity removal

Szekely et al. ^[25] prepared molecularly imprinted polymers using methacrylic acid (MAA) as the functional monomer and ethylene glycol dimethacrylate (EDMA), as the cross-linker towards the genotoxic impurity 1,3-diisopropylurea (IPU) for selective removal of IPU from the model APIs keppra (KP), mometasone furoate (Meta) and roxithromycin (Roxi). The synthesized polymers displayed 80 % binding of IPU with 15 % of undesired API binding.

In another study, the same authors have reported ^[26] the use of an OSN and MIP hybrid approach for the removal of IPU from model the API Meta. An initial OSN step was applied for the removal of IPU and after that the low amount of IPU retained in the solution was removed by MIPs. 90 % IPU was removed using OSN and 83 % of the remaining IPU was removed by MIPs with the loss of 2.5 % of API.

Del Blanco et al. ^[28] reported the use of molecularly imprinted membranes for selective removal of the genotoxic impurity 4,4'-methylenedianiline. In their work, poly(acrylonitrile-co-acrylic acid), poly(acrylonitrile-co-methacrylic acid) and poly(acrylonitrile-co-itaconic acid) imprinted membranes were prepared. The recognition properties of the prepared membranes towards 4,4'-methylenedianiline were evaluated.

4,4'-Methylenedianiline imprinted poly(acrylonitrile-co-acrylic acid) membranes displayed the highest binding with $2.6 \mu\text{mol/g}_{\text{memb}}$ in isopropanol and also showed cross-reactivity towards the analogues aniline and 4,4'-ethylenedianiline.

1.3.4 Screening of MIP libraries

The commonly used statement in the scientific literature is that MIPs are very selective towards the analytes of interest. However, in some cases as discussed below, MIPs also display selectivity towards molecules that are not obviously related to the template molecule.

As MIPs are synthesized using the target compound as template, leakage of trace amount of template (bleeding) from the MIP may occur at very low levels under harsh conditions, which can falsify the analytical result. Thus, it was often not desirable to use the target molecule as the template and instead a similar molecule was proposed to be used as a 'dummy template'.

A study was presented by Andersson et al ^[123] in which the dummy template provided exquisite binding site cavities for the target pharmaceutical compound, sameridine (Figure 1.14).

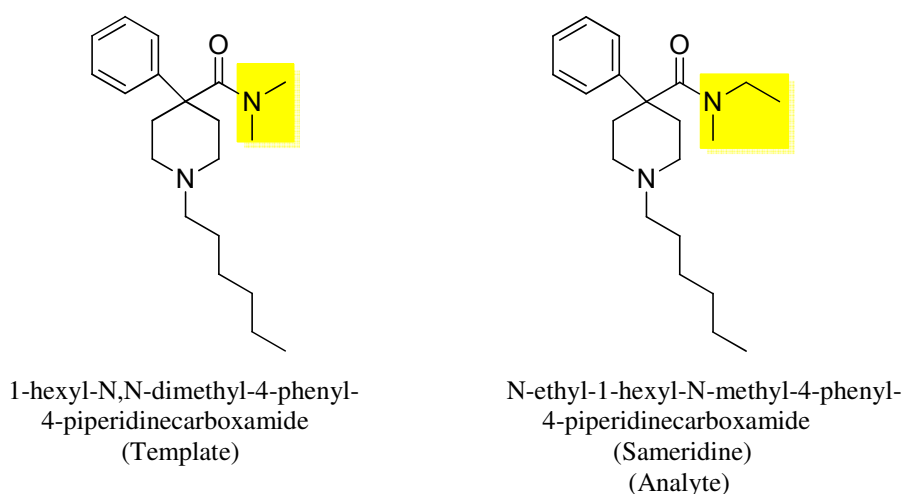


Figure 1.14: Template and bound molecule in the work of Andersson et al. ^[123]

In an extension of this approach, Takeuchi and his co-workers prepared synthetic polymer receptors selective for triazine pesticides using trialkylmelamines as template.^[124]

In another work, the group of Haupt^[125] have presented 2,4-dichlorophenoxyacetic acid imprinted polymer that displays an extended cross-reactivity profile. The group showed that other compounds with the phenoxyacetic acid moiety, such as 7-carboxymethoxy-4-methylcoumarine, could compete with the binding (Figure 1.15).

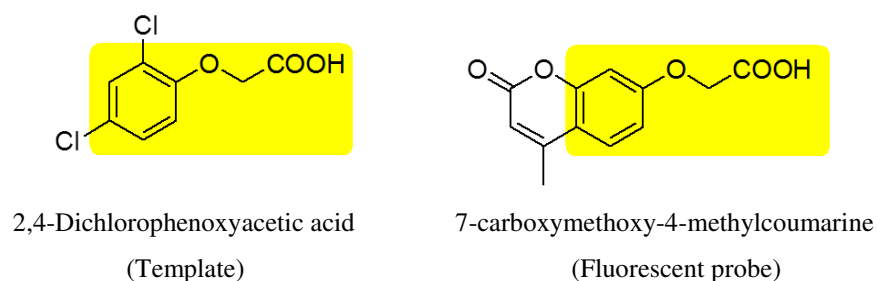


Figure 1.15: Template and bound molecule in the work of Haupt et al.^[125]

Martin et al^[126] prepared polymers towards tamoxifen and propranolol. In their study, the tamoxifen imprinted polymer was compared to the non-related compound propranolol as a control experiment. Interestingly, only the propranolol imprinted polymer displayed an imprinting effect towards tamoxifen, whereas the tamoxifen-imprinted polymers did not show any imprinting effect. Figure 1.16 depicts the common molecular feature in both molecules that may explain the imprinting effect, an ionizable aliphatic amine in the same proximity to an oxygen atom.

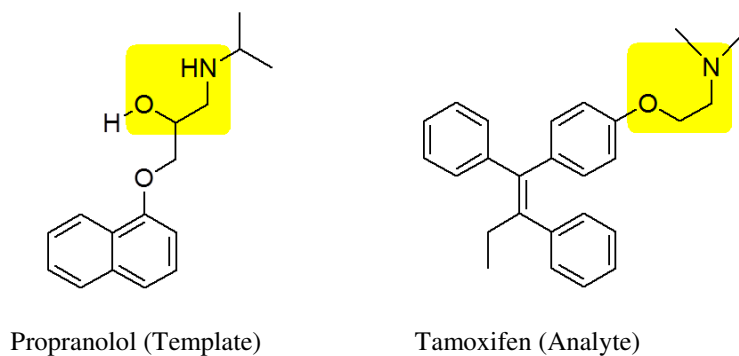


Figure 1.16: Template and bound molecule in the work of Martin et al. ^[126]

Even though the recognized molecule is different from the template in these cases, the template and the analyte have common features (marked in yellow in the figures) which are the basis for cross-reactivity and thus binding to the respective binding sites.

As shown by Martin et al, some compounds such as tamoxifen are difficult to use as templates.

Wulff et al. ^[127] prepared a D-fructopyranose MIP which has chiral selectivity and recognized D-galactopyranose over L-galactopyranose (Figure 1.17). This work was the first example illustrating a racemic resolution of free sugars using MIPs. This MIP could distinguish between D and L-fructopyranose with a binding preference to the D-fructopyranose. In comparative studies, the same MIP could also distinguish between galactopyranose enantiomers.

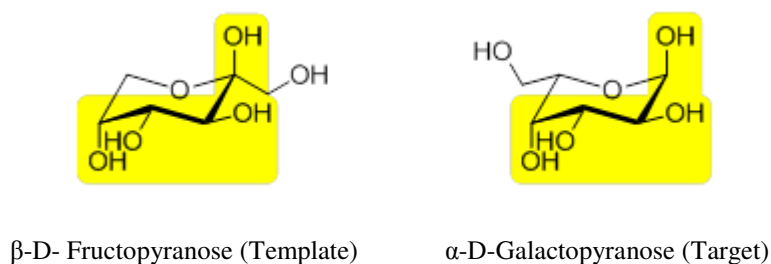


Figure 1.17: Template and bound molecule in the work of Wulff et al. ^[127]

Finally, Turiel and co-workers ^[128] reported the use of propazine (2-chloro-4,6-diisopropylamino-triazine) as a dummy template for the synthesis of MIPs. The prepared MIPs displayed cross-reactivity towards various 2-chloro-4,6-dialkylamino-triazines (Figure 1.18)

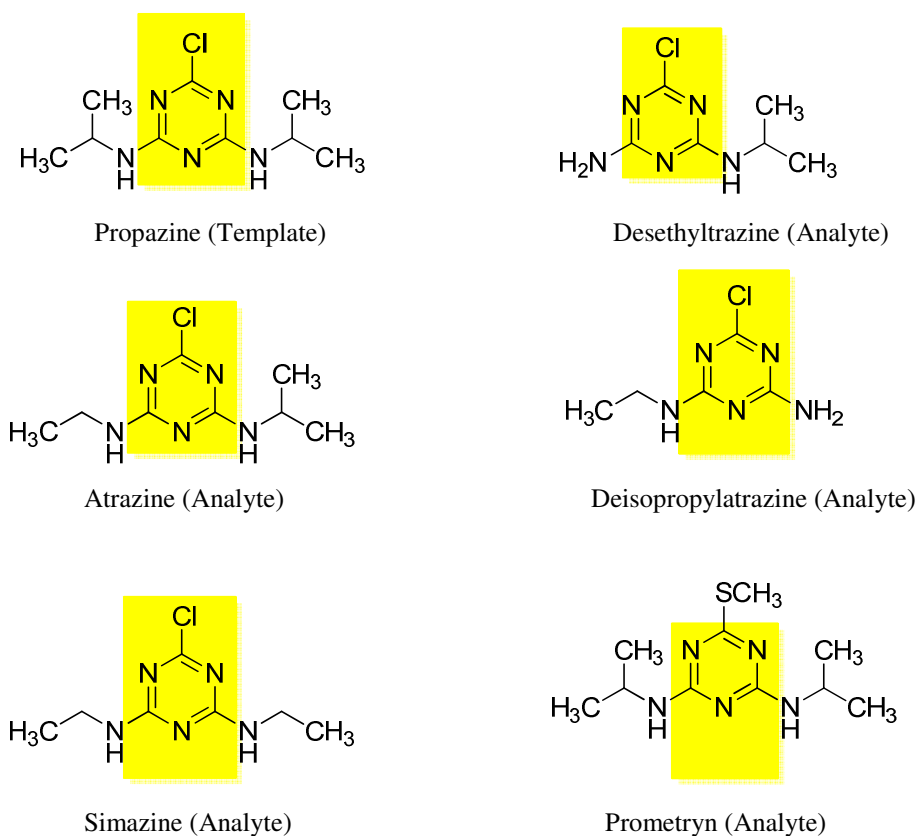


Figure 1.18: Template and bound molecules in the work of Turiel et al. ^[128]

As Biotage AB has over the years synthesized a large number of imprinted polymers and their corresponding control (non-imprinted) counterparts, it was believed that one could find interesting and useful cross-reactivities by screening those existing in-house polymers with new compounds. Therefore, libraries of polymers were compiled based on four different MIP library chemistries. Those MIP libraries are collected on 96-well plates.

Scanning electron microscope images of a resin from the library is shown in Figure 1.19. As can be seen from the picture, particles are spherical beads ca. 50 μm in size made by scalable (proprietary) methods.

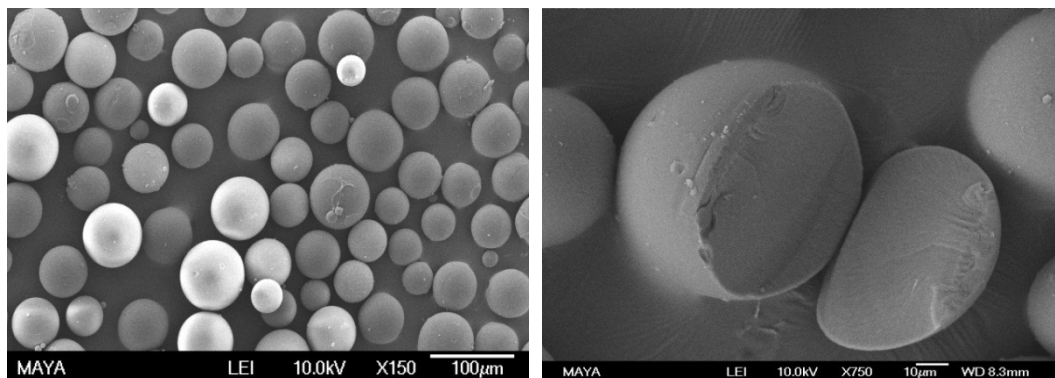


Figure 1.19: SEM images of a resin from MIP library

Table 1.3 shows BET results for some of the resins from the plates. As can be seen from the table, the resins have large surface area.

Table 1.3: Example BET results for the resins from different plates

Polymer	Surface Area (m ² /g)	Pore Volume (ml/g)	Pore Diameter (nm)
Resin from U Plate	178	0.2	3
Resin from C Plate	156	0.4	10

The composition of the materials in the screening plates is approximately 55 % DVB, 40 % EDMA and ~ 5 % monomer (Figure 1.20)

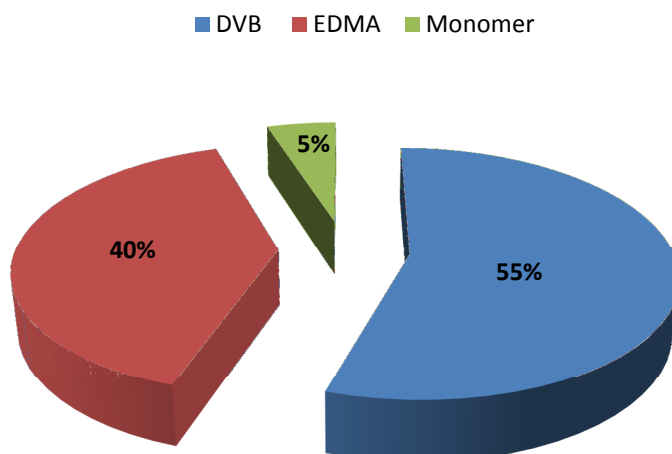


Figure 1.20: Typical composition of a MIP for screening

Full details of the resins product cannot be revealed due to company confidentiality restrictions. However, the performance of these MIP libraries is intriguing as all polymers on a given plate have essentially identical compositions. Differences in retentivity or selectivity are thus predominantly governed by the imprinting effect. It is an interesting fact that resins with virtually or even identical compositions, morphology and surface area can differ so markedly in binding of chemical compounds. Again, the imprinting process that organizes the positions of the functionalities is the basis for this recognition.

The resins are categorized in plates according to the chemical families.

Carboxylic acid plate (A Plate): The polymers in this plate are based on a hydrophobic backbone and have carboxylic acid groups as functional moieties and can be used for the screening of polar, basic (e.g. amines), neutral (e.g. amides or esters), and acidic (e.g. carboxylic acid) compounds. The carboxylic acid functionality constitutes a weak cation exchanger and has the ability to bind via ionic interaction with appropriate basic groups. Its hydrogen bonding capability also allows it to interact with e.g. amides and other compounds with hydrogen bonding ability (Figure 1.21).

Carboxylic acid based MIPs are the most prevalent and most published MIPs in the literature. It is estimated that in the vast majority (over 80 %) of the MIP publications, methacrylic acid is used as the functional monomer.

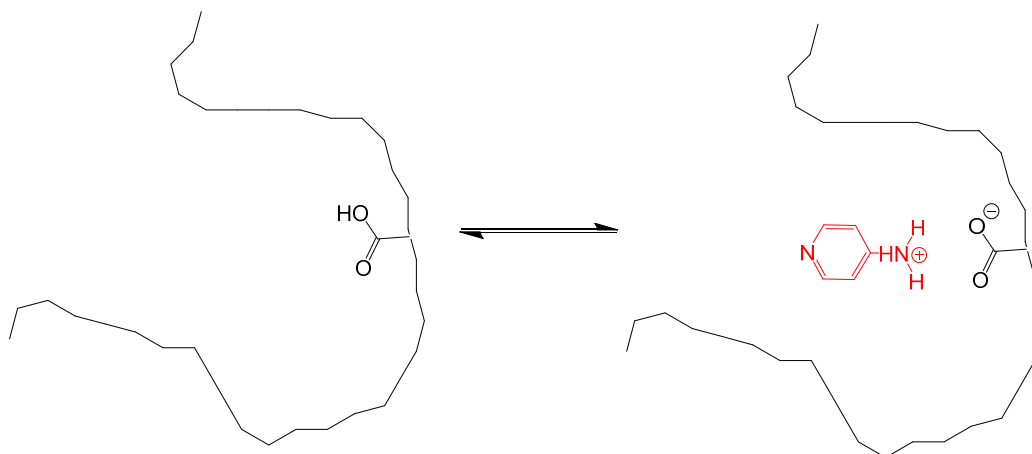


Figure 1.21: Schematic depiction of the binding site of the materials in for carboxylic acid plate; to the right an example of a molecule able to bind to the cavity is presented

Urea plate (U Plate): The polymers in this plate are based on a hydrophobic backbone and have urea groups as functional moieties and are used for screening of compounds that contain phosphates, phosphonates, sulphates and sulphonates as well as anions of carboxylic acids and also lactones.

The interaction chemistry expected in this plate is hydrogen bonding between the urea functional monomer and the hydrogen-bond acceptor sites of the target molecules.

A schematic depiction of the binding site of the materials in the urea plate is shown in Figure 1.22.

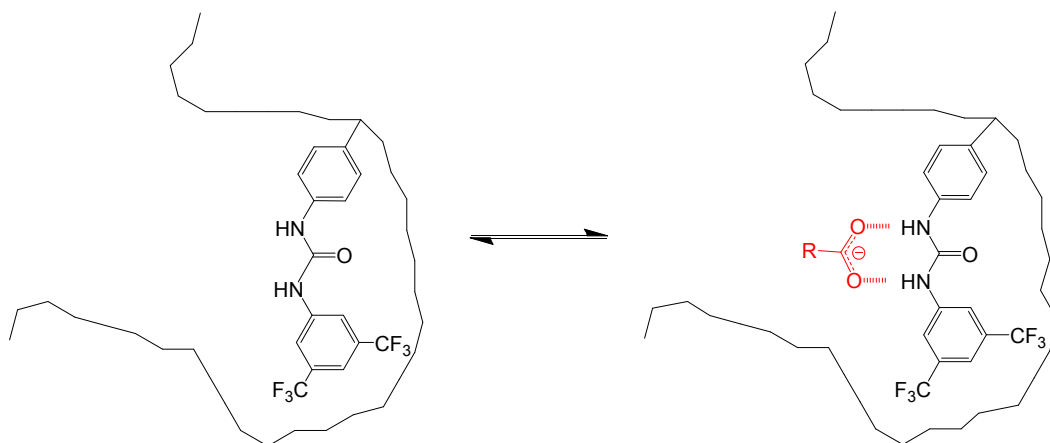
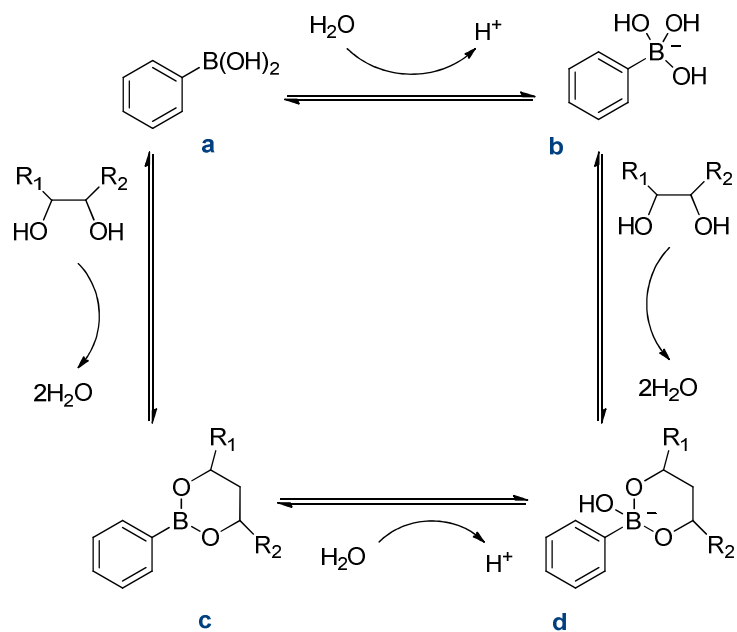


Figure 1.22: Schematic depiction of the binding site of the materials in the urea plate; to the right a carboxylate moiety able to bind to the cavity is presented

Sellergren et al. have investigated MIPs using urea-based functional monomers for recognition of triphenyl phosphate and diethylphenyl phosphate.^[129]

Boronic acid plate (C Plate): The polymers in this plate are based on a hydrophobic backbone with boronic acid groups as the functional moieties. Boronic acids can form reversible covalent complexes with diols, α -hydroxyacids and α -amino alcohols.^[130] This high affinity binding allows boronic acid to be used as a recognition element in sensors for carbohydrates^[131-137], α -hydroxyacids,^[138-140] α -amino alcohols^[141,142] and as an affinity ligand for separation of glycoproteins, carbohydrates, nucleosides and nucleic acids^[143-146] A comprehensive review on boronic acid and its use in biological applications has been published.^[147]

Boronic acid such as phenyl boronic acid (PBA) are weak acids and can react with water at alkaline pHs to go from the trigonal configuration (**a**) to the anionic tetrahedral form (**b**) via an acid-base reaction. PBA and the phenyl boronate anion can react with diol groups with releasing of two water molecules and trigonalboronic acid is converted to the trigonal ester (**c**), anionic tetrahedral boronate is converted to the its tetragonal ester (**d**) (Scheme 1.4).



Scheme 1.4: Phenylboronic acid-diol interaction ^[148]

In Figure 1.23, a schematic depiction of the binding site of the materials in boronic acid plate is shown

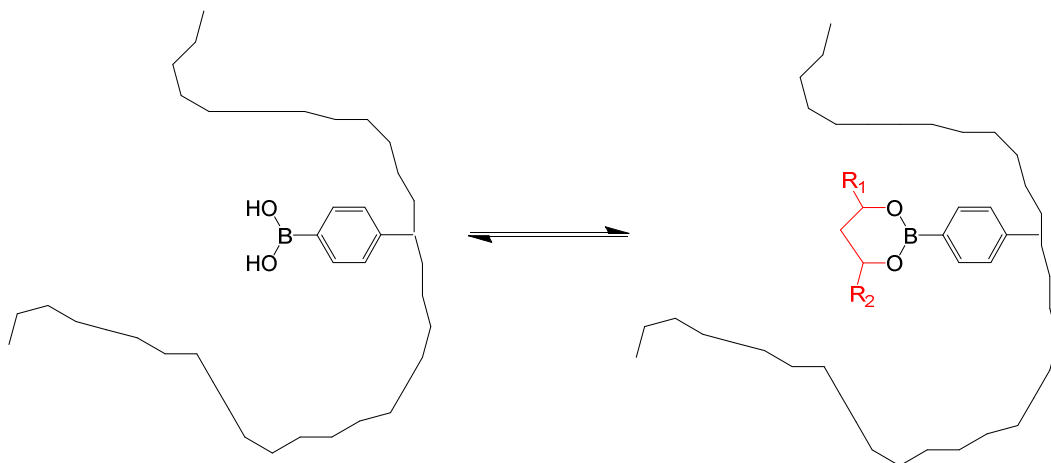


Figure 1.23: Schematic depiction of the binding site of the materials in boronic acid plate; to the right a diol moiety able to bind to the cavity is presented

Hydrophobic plate (H Plate): The polymers in this plate have phenyl or pyridine moieties that can interact through hydrophobic interactions and that can also form π - π interactions and charge transfer complexes (Figure 1.24).

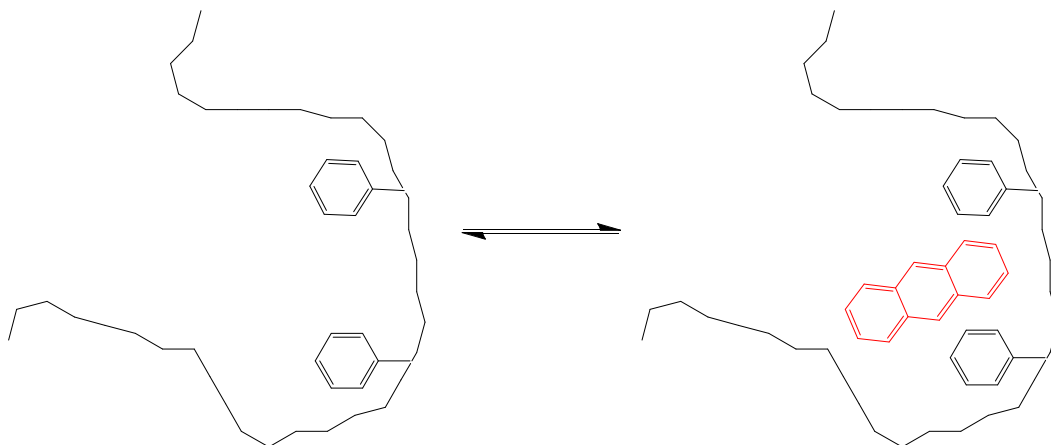


Figure 1.24: Schematic depiction of the binding site of the materials in the hydrophobic plate; to the right an example of a molecule able to bind to the cavity is presented

The resins in the library described above are packed into 96-well plates. Each resin is present in 40 mg quantities in duplicates. The plates include molecularly imprinted polymers (MIPs) and their corresponding non-imprinted polymers (NIPs).

The difference in retention of target compound on MIPs and their corresponding NIPs gives a measure of selectivity and is usually called “selectivity factor”.

The positions of the different MIPs and NIPs on a screening plate are shown in Table 1.4. All resins on the plates are re-usable when clean solvents are used and can be regenerated.

Table 1.4: Positions for MIPs and NIPs on plate A

	1	2	3	4	5	6	7	8	9	10	11	12
A	EA 085	EA 089	EA 093	EA 097	EA 101	EA 107	EA 111	EA 115	A-MIP 4	A-MIP 22	Blank 1	Std 1
B	EA 085	EA 089	EA 093	EA 097	EA 101	EA 107	EA 111	EA 115	A-MIP 4	A-MIP 22	Blank 2	Std 2
C	EA 086	EA 090	EA 094	EA 098	EA 102	EA 108	EA 112	EA 116	A-NIP 4	A-NIP 22	-	Std 3
D	EA 086	EA 090	EA 094	EA 098	EA 102	EA 108	EA 112	EA 116	A-NIP 4	A-NIP 22	-	Std 4
E	EA 087	EA 091	EA 095	EA 099	EA 103	EA 109	EA 113	EA 117	A-MIP 8	A-MIP 24	-	Std 5
F	EA 087	EA 091	EA 095	EA 099	EA 103	EA 109	EA 113	EA 117	A-MIP 8	A-MIP 24	-	Std 6
G	EA 088	EA 092	EA 096	EA 100	EA 104	EA 110	EA 114	EA 118	A-NIP 8	A-NIP 24	-	Std 7
H	EA 088	EA 092	EA 096	EA 100	EA 104	EA 110	EA 114	EA 118	A-NIP 8	A-NIP 24	-	Std 8

A screen of the MIP resin library allows the identification of a selective resin, a “hit resin”, towards a target compound. When a hit resin has been identified, the application method for hit resin might require further optimization (Figure 1.25).

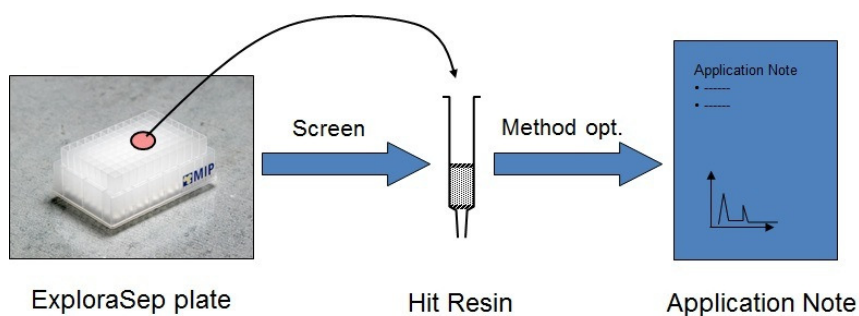


Figure 1.25: Screening approach

Some examples of the screening of the MIP libraries described above at Biotage AB are given below.

In the first example, screening experiments to identify a selective resin towards the antibiotic compound chloramphenicol were carried out (Figure 1.26).^[149]

A MIP library composed of resins with 4-vinylbenzeneboronic acid as the functional monomer was screened against chloramphenicol and it was identified that a resin imprinted with the unrelated molecule methyl- α -D-mannopyranoside displayed a high imprinting effect towards chloramphenicol compared to its corresponding non-imprinted polymer (NIP). The chromatographic evaluation of the MIP and NIP towards chloramphenicol is shown in Figure 1.27.

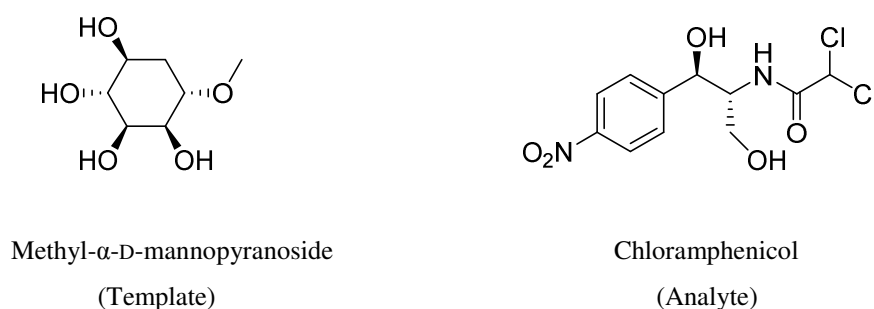


Figure 1.26: Structures of methyl- α -D-mannopyranoside (template) and chloramphenicol (target) ^[149]

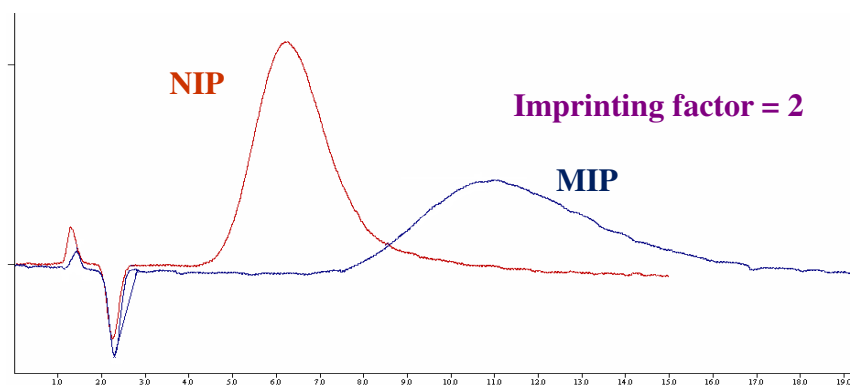


Figure 1.27: Imprinting effect for chloramphenicol on a MIP imprinted with methyl- α -D-mannopyranoside. MIP and NIP packed in 200×4.6 mm stainless steel columns, mobile phase 36 % acetonitrile in 1 % ammonium hydroxide, flow rate 1 mL/min, detection wavelength 215 nm ^[149]

In another study, various MIPs and their corresponding NIPs with methacrylic acid as functional monomer were screened towards the beta blocker metoprolol. A candidate MIP was identified for metoprolol which is imprinted with (-)-ephedrine (Figure 1.28). The identified MIP was prepared with a template which contains the aminoethanol moiety found in metoprolol (Figure 1.28).

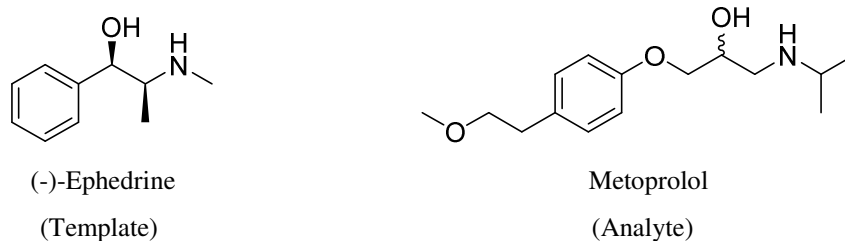


Figure 1.28: Structures of (-)-ephedrine (template) and metoprolol (target)^[149]

In a related work, the MIP library using methacrylic acid as functional monomer was screened for MIPs that selectively bind the antibiotic ciprofloxacin, a member of the fluoroquinolone class of antibiotics. A candidate polymer was found that was imprinted with tramadol, a template which is not related to ciprofloxacin (Figure 1.29).

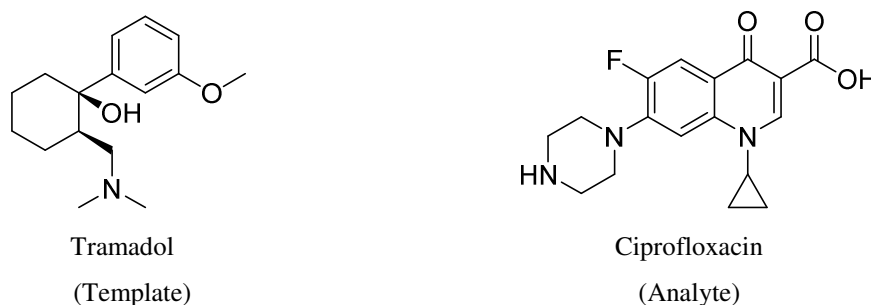


Figure 1.29: Structures of tramadol (template) and ciprofloxacin (target)^[149]

These examples show that MIPs often not only can bind the template molecule itself but also related compounds.

It should be noted that the MIPs towards chloramphenicol, metoprolol and fluoroquinolones are now commercially available products at Biotage AB (Sweden).

1.4 Reactive scavengers

Scavengers are resins equipped with reactive functional groups such as nucleophiles or electrophiles that can react with a range of compounds. In a pharmaceutical process chemistry set-up, typical target compounds could be for example by-products, impurities or excess reagents produced in an organic reaction. Appropriate reactive groups (e.g., amines, aldehydes, thiols, hydrazines, isocyanates, etc) may be attached to polymeric carriers such as poly(styrene-divinylbenzene) beads (typically 1 or 2 % cross-linked) or inorganic carriers such as silica beads. These scavenging resins are particularly useful in solution-phase combinatorial chemistry, where the purification of compounds using traditional purification methods such as chromatography, crystallization, liquid-liquid extraction and distillation would be very time-consuming.

In Figure 1.30, the principle of scavenging and removal of excess reagents and by-products using scavenger resins is demonstrated. The scavengers are designed to react and bind with undesired compounds, facilitating their removal by simple filtration. The desired product remains in solution.

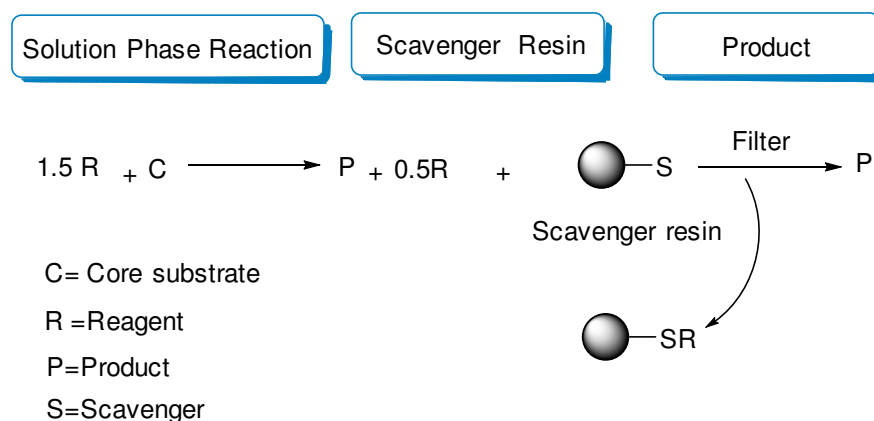


Figure 1.30: Scavenging of excess reagents using scavenger resins ^[72]

Polymer-supported scavengers as a concept was already utilized in 1980 by Cheminat et al ^[150] who used polymer-bound primary amines for selective removal of allergens from complex mixtures.

Later, Flynn et al. reported the use of reactive resins as a purification method for solution-phase combinatorial libraries. ^[151] In their work, the reactive resins were used to remove excess of reactants, reagents, and by-products generated after a chemical reaction. They demonstrated amine acylations, the reaction of organometallics and carbonyl compounds using primary and tertiary amine and sulphonic acid bound polystyrene resins and commercial Amberlyst 15, Amberlyst A-21 and Amberlite (IRC-50 S). They pointed out that these resins are applicable to a broad spectrum of organic reactions.

Kaldor et al. ^[152] synthesized various polymeric scavengers modified with nucleophilic and electrophilic ligands for selective removal of impurities from reaction mixtures. The scavengers were employed successfully for removal of primary and tertiary amines in amine acylation and alkylation reactions.

Lin and co-workers have described the synthesis of polymeric microspheres modified with acrolein groups for removal of aniline and various primary amines. ^[153] In their work, they used three and five equivalents of the polymeric resin for selective removal of primary amines and aniline in DCM. 96 % of the aniline and 82 % of the amines were removed from the solutions.

In another work, Siegel et al. ^[154] demonstrated the utility of cation exchanger resins functionalized with amines for rapid removal of excess of aldehydes in amination reaction mixtures. Purification of the amines with 86 % purity was achieved.

In 1998, Coppala reported the use of polystyrene supports functionalized with isatoic anhydride for the selective removal of amines from organic reactions. In this work, various amines were reacted with phenyl isothiocyanate and N-methylisatoic anhydride to give thiourea and anthranilamides as products, respectively. ^[155] After completion of the reaction, the isatoic anhydride reactive resin was added to reaction media and within 30-90 min complete removal of the excess of the amines was obtained.

Today, a considerable number of this type of resins are commercially available for these applications. Some examples can be found at web pages of Biotage ^[72] and Sigma Aldrich ^[121] and many others.

Biotage AB (Sweden) provides 3 different base resin types for scavengers, 1 % cross-linked poly(styrene-co-divinylbenzene) (PS) and highly cross-linked macroporous poly(styrene-co-divinylbenzene) (MP) and also silica. Lightly cross-linked polystyrenes typically require the use of solvents to swell the resin to allow reagents access to the reactive functional groups within the scavenger. In some cases where the solvent does not swell the resin, it may be necessary to add a co-solvent such as THF that promotes the swelling of the resin. Highly cross-linked macroporous polystyrene resins are robust and low-swelling materials. This makes them ideal resins in restricted volumes (eg, microwave vials, columns, 96-well plates, etc). Due to the macroporosity, target compounds can easily access the reactive groups present on the scavenger. This leads to faster scavenging reaction and higher recoveries.

There is also a range of silica- based scavengers available that are functionalized silica gels with reactive groups designed to react with excess of substrates, reagents or by-products in reaction mixtures. The silica based scavengers have some advantages compared to polymer based scavengers while the scavenging reaction principles are the same. The functional reactive groups of the silica based scavengers are on the surface which leads to faster scavenging kinetics and better efficiency while the reactive groups of the polymer based scavengers are inside so that the scavenging kinetics are dependent on the rate of diffusion of the target compound through the polymer.

Furthermore, the morphology of silica gel is not affected by any organic solvent since its pore structure is rigid and permanent and also mechanically and thermally stable. A disadvantage of silica is the lower chemical stability, e.g. towards bases, whereas polymeric PS-based resins generally display a high chemical stability.

2 OBJECTIVES OF THE THESIS

The objectives of this thesis are as follows:

- 1) To identify and characterize polymers for selective removal of the genotoxic impurities methyl p-toluenesulfonate and aminopyridines from their corresponding APIs by screening of molecularly imprinted polymer libraries.
- 2) To identify and characterize reactive resins for selective removal of the genotoxic impurities methyl p-toluenesulfonate and acrolein from their corresponding APIs by screening of polystyrene and silica supported reactive scavenger libraries.
- 3) To design and characterize MIP materials for removal of methyl p-toluenesulfonate and acrolein from their model APIs.
- 4) To compare MIPs and reactive scavengers under the comparable conditions.

An overview of the main contributions of this thesis and their connection is given in Figure 2.1.

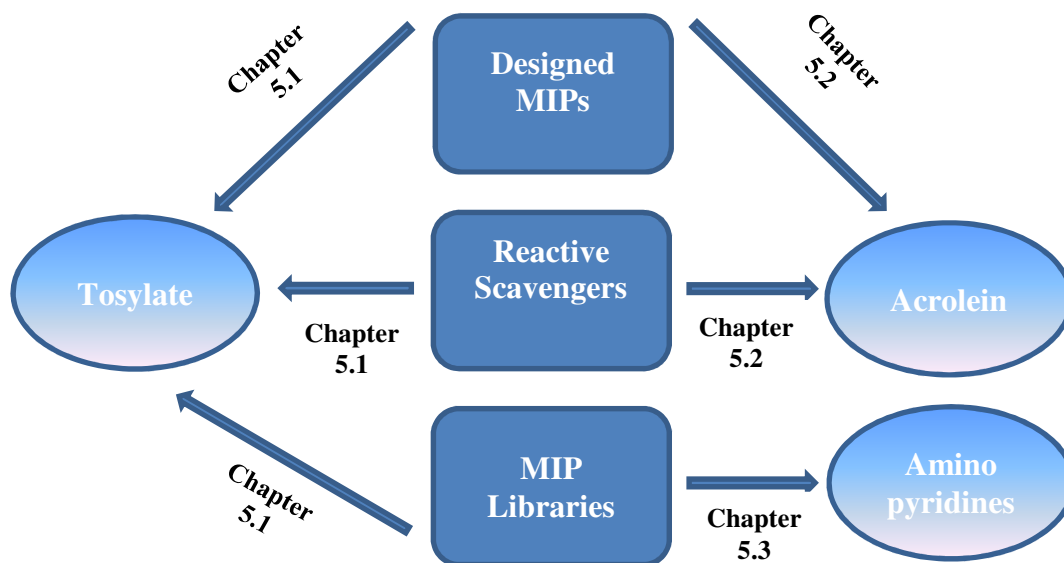


Figure 2.1: Overview of the main contributions of this thesis and their connection

3 MATERIALS

Acrolein, 2,4-dinitrophenylhydrazine (DNPH), formic acid, iodixanol, ethylene glycol dimethacrylate (EDMA), azo-bis-dimethylvaleronitrile (ABDV), methyl p-toluenesulfonate, hydrazine monohydrate, vinylbenzyl chloride, phenyl acetaldehyde, 4-vinylaniline, 3,5-bis(trifluoromethyl)phenyl isothiocyanate, 3,5-bis(trifluoromethyl)phenyl isocyanate, 2-aminopyridine, 3-aminopyridine, 4-aminopyridine, 5-amino-2-methylpyridine, 5-amino-2-chloropyridine, piroxicam, tenoxicam, Amberlite CG-50 and HPLC-grade solvents were purchased from Sigma-Aldrich (Steinheim, Germany). Scavenging resins were from Biotage GB Limited (Cardiff, UK). 21-Chlorodiflorasone was a gift from Hovione FarmaCiencia SA (Lisbon, Portugal). All distilled water used was purified using an ultra-pure water system from Elga (High Wycombe, UK).

HPLC-UV experiments were carried out on a Shimadzu LC10 AD equipped with a PDA detector (SPD –M10A) and an autosampler (SIL-HT_A). The reversed phase analytical column was a Supelco Discovery C₁₈ (5.0 μm, 50x4.6 mm).

LC-MS/MS experiments were performed on a Shimadzu HPLC instrument consisting of two HPLC pumps (LC-20AD), a vacuum degasser (DGU-20A₃), and an autosampler (SIL-20AC) connected to an Applied Biosystems mass spectrometer (API3200) with an electrospray ionization interface. The analytical column was a Supelco Discovery HSF5 (5.0 μm , 150x4.0 mm).

FT-IR experiments were performed on a Perkin Elmer Spectrum 100 FT-IR spectrometer.

A Nikon ECLIPSE ME600 microscope was used to measure the particle size of the polymers.

Scanning electron microscope (SEM) was provided at the Department of Chemistry, Lund University (Lund, Sweden). The SEM pictures were recorded on a JEOL JSM-6700 F scanning electron microscope.

All nuclear magnetic resonance spectra (NMR) were acquired on a Bruker Avance spectrometer at 500 MHz at the Faculty of Chemistry, Technical University of Dortmund (Dortmund, Germany).

Surface area, pore volume and pore diameter of synthesized polymers were determined at the Department of Chemistry, Lund University (Lund, Sweden) using an ASAP 2400, Micromeritics (Norcross, Georgia) analyser.

Elemental analysis was performed at the Department of Organic Chemistry, Johannes Gutenberg Universität Mainz using a Heraeus CHN-rapid analyzer (Hanau, Germany).

4 METHODS

4.1 Analysis of target GTIs and APIs

4.1.1 HPLC analysis

Derivatization of acrolein with DNPH before HPLC analysis was adapted from a published procedure ^[156] Briefly, 50 mg of DNPH was dissolved in 20 mL of acetonitrile and acidified by adding 0.4 mL of formic acid. Derivatization of acrolein was carried out prior to analysis by mixing 100 μ L of sample with 100 μ L of DNPH and stirring at room temperature for 1h.

HPLC analysis of acrolein and its corresponding API iodixanol was carried out on a Shimadzu LC10 AD (Figure 4.1). The column was Supelco Ascentis Express C18 (2.7 μ m, 50x4.6 mm). Gradient elution was performed with ultra-pure water (mobile phase A) and acetonitrile (mobile phase B). The gradient started with A:B 60:40 (v/v), then a linear gradient elution up to 55 % acetonitrile within 2 min and then raised to 100 % acetonitrile in another 2 min. The final composition was maintained for 3 min before re-equilibrating the column with the initial mobile phase. The flow rate was 0.6 mL/min, the detection wavelengths were 370 nm (for acrolein) and 254 nm (for iodixanol) and the injection volume was 10 μ L.



Figure 4.1: HPLC system used in this study

4.1.2 LC-MS/MS analysis

Quantification of methyl p-toluenesulfonate, aminopyridines and their corresponding APIs were done using a Shimadzu HPLC instrument consisting of two HPLC pumps (LC-20AD), a vacuum degasser (DGU-20A₃), and an autosampler (SIL-20AC) connected to an Applied Biosystems mass spectrometer (API3200) with an electro spray ionization interface (Figure 4.2). The analytical column was a Restek Ultra II PFP Propyl (3.0 μ m, 50x2.1 mm). Gradient elution was performed with 10 mM ammonium formate (NH₄Ac) pH 8.0 (mobile phase A) and acetonitrile (MeCN) (mobile phase B). The gradient started with A:B 20:80 (v/v), then a linear gradient elution down to 30 % B within 2 min was done, kept at that level for 2.5 min and then increased to 80 % B within 0.1 min. This composition was maintained for 1.5 min to re-equilibrate the column with the 80 % B initial mobile phase. The flow rate was 0.5 mL/min and the injection volume was 10 μ L.

The turbo ion-spray source was used in positive mode (ESI⁺) for methyl p-toluenesulfonate and 21-chlorodiflorasone with the following settings: electrospray capillary voltage, 5500 V; ion source temperature, 450 °C; curtain gas (N₂), 10 psi; collision gas (N₂), 6 psi. Data was acquired through multiple reactions monitoring mode (MRM), with the following transitions monitored: m/z 116.2 precursor ion to m/z 72.3 and m/z 86.1 product ions for methyl p-toluenesulfonate, m/z 429.2 precursor ion to m/z 253.2 and m/z 389.4 product ions for 21-chlorodiflorasone.

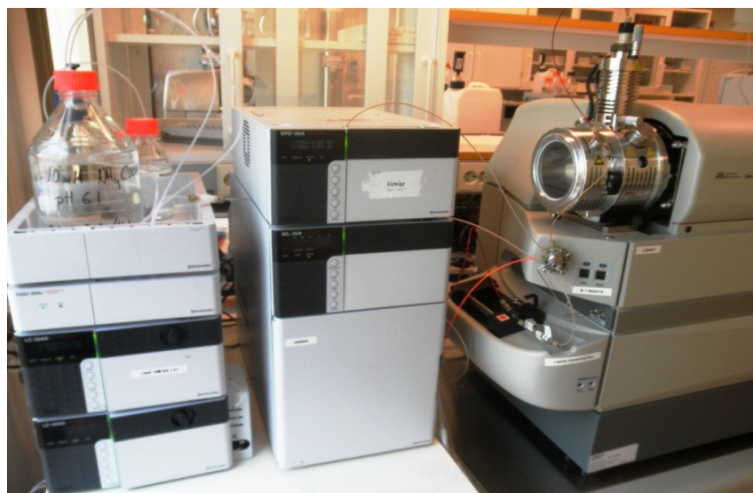


Figure 4.2: LC-MS/MS system used in this study

LC-MS/MS experiments for aminopyridines were performed on the same instrument described above. The analytical column was a Supelco Discovery HSF5 (5.0 μm , 150x4.0 mm). Gradient elution was performed with 10 mM ammonium formate (NH_4FA) pH 6.5 (mobile phase A) and acetonitrile (MeCN) (mobile phase B). The gradient started with A:B 85:15 (v/v) followed by a linear gradient up to 50 % B within 1 min, kept at that level for 3 min and then increased to 90 % B within 1 min and kept at that level for 1 min. Then, the composition was decreased to 15 % B within 0.1 min and maintained for 1.5 min to re-equilibrate the column with the initial mobile phase. The flow rate was 0.5 mL/min and the injection volume was 10 μL .

The turbo ion-spray source was used in positive mode (ESI^+) for all analytes with the following settings: electrospray capillary voltage, 4500 V; ion source temperature, 400 $^\circ\text{C}$; curtain gas (N_2), 15 psi; collision gas (N_2), 8 psi. Data was acquired through multiple reactions monitoring mode (MRM), with the following transitions monitored: m/z 95.1 precursor ion to m/z 77.9 product ion for 2-aminopyridine, m/z 95.5 precursor ion to m/z 68.1 product ion for 3-aminopyridine, m/z 94.7 precursor ion to m/z 78.0 product ion for 4-aminopyridine, m/z 129.1 precursor ion to m/z 98.0 product ion for 5-amino-2-chloropyridine, m/z 108.0 precursor ion to m/z 80.4 product ion for 5-amino-2-

methylpyridine, m/z 332.4 precursor ion to m/z 95.1 product ion for piroxicam and m/z 338.1 precursor ion to m/z 121.1 product ion for tenoxicam.

4.2 MIP library screening procedures

The methyl *p*-toluenesulfonate screening was carried out on urea MIPs. 32 different resins with urea functionality were packed with 40 mg into 1 mL polypropylene SPE cartridges fitted with 20 μ m pore-size polyethylene frits on both top and bottom of the resin bed inserted to a 96-well-plate (Figure 4.3). Methanol was used to rinse the walls of the column during packing. Each resin packed-column was prepared in duplicate. After loading, fractions were collected and analysed together with standards and blanks by LC-MS/MS.

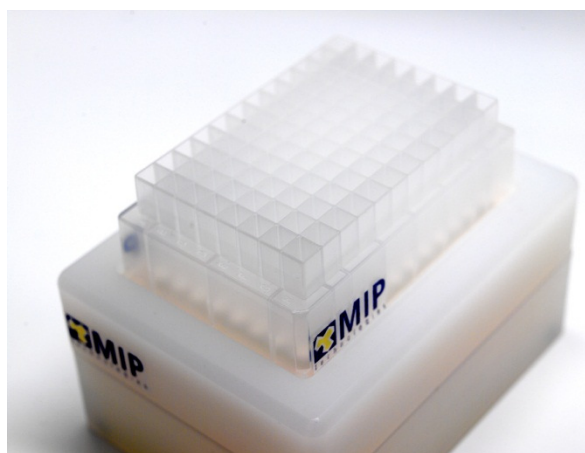


Figure 4.3: A 96-well-plate used for screening

Conditioning of the polymers was done with methanol and isopropanol to wet the packed resin bed in the columns and to facilitate interaction with the analytes.

In the screening experiments, a solution containing 1 μ g/mL of methyl *p*-toluenesulfonate and 100 μ g/mL 21-chlorodiflorasone was prepared as a mixture in isopropanol. 1 mL of this solution was passed through the pre-conditioned polymers and the analytes found in the eluate were quantified.

In the screening of resin chemistries experiments for aminopyridines, 32 resins with a large variety of chemistries (e.g. containing hydrophobic moieties, urea groups, carboxylic acid groups, boronate groups, imidazole groups, pyridine groups, amide groups, acrylate groups and strong and weak ion exchange moieties) were packed with 40 mg into 1 mL polypropylene SPE cartridges fitted with 20 μm pore-size frits on both top and bottom of the resin bed inserted into a 96-well modular plate in duplicates. Conditioning of the polymers was done with 1 mL of methanol and 1 mL of 10 mM NH_4FA buffer, pH 6.5 to wet the columns. A solution of 10 $\mu\text{g}/\text{mL}$ each of 2-aminopyridine, 3-aminopyridine, 4-aminopyridine, 5-amino-2-methylpyridine and 5-amino-2-chloropyridine was prepared in 10 mM NH_4FA buffer, pH 6.5. 1 mL of this solution passed through the polymers packed SPE columns. Eluate fractions were collected and analysed together with standards and blanks by the LC-MS/MS method described above.

In the screening experiments for aminopyridines on carboxylic acid MIPs, 32 different MIPs with methacrylic acid as the functional monomer and their corresponding non-imprinted polymers, NIPs, were packed with approximately 40 mg into small columns and inserted to a 96-well plate.

A solution of 10 $\mu\text{g}/\text{mL}$ each of aminopyridines as a loading solution was prepared in 10 mM NH_4FA buffer, pH 6.5. Screening experiments was carried out by the same procedure as for the screening of resin chemistries described above.

4.3 HPLC column packing

The packing method used in this work was done via the down-fill slurry packing technique. In this packing step, 2.1 g polymer was dispersed in 70 mL ethanol. and then poured into the slurry reservoir bomb (shown in Figure 4.4). An adaptor tube is attached to the bomb and the empty column is then connected to the adaptor. The bottom end of the LC-column is closed with a frit. The polymer slurry is then packed into the column with pressure from a pump which pumps liquid through the column, which pushes the slurry into the column with a certain pressure. Then the pressure is increased with time so that the whole column is filled and thoroughly packed. The dimension of the column was 50 mm x 4.6 mm.

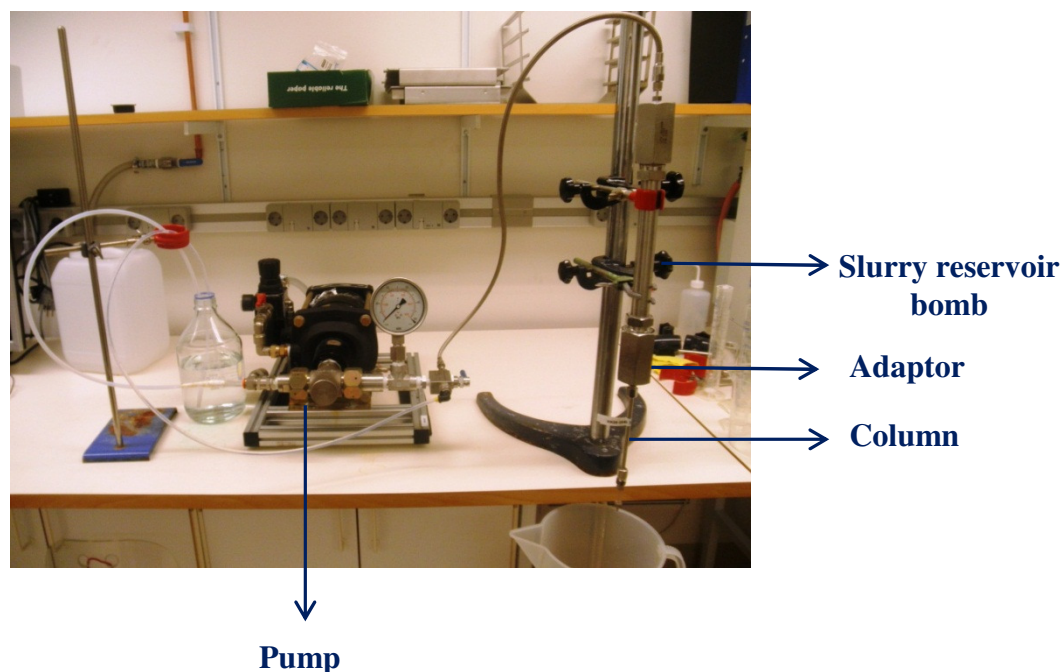


Figure 4.4: HPLC column packing setup

4.4 Flow through scavenging procedures for reactive scavengers

Flow-through scavenging experiments of methyl p-toluenesulfonate and its corresponding API 21-chlorodiflorasone were carried out using various scavenger resins packed in solid phase extraction (SPE) cartridges (Figure 4.5). The resins were manually packed as 150 mg amounts in 1 mL polypropylene SPE cartridges (55 mm height x 9 mm diameter) fitted with 20 μm pore-size polyethylene frits on both top and bottom of the resin bed. The cartridges were conditioned with 1 mL of methanol and then with 1 mL of 2-propanol. Samples of 1 mL of 5 $\mu\text{g}/\text{mL}$ methyl p-toluenesulfonate and 500 $\mu\text{g}/\text{mL}$ 21-chlorodiflorasone in 2-propanol were loaded onto the cartridges. 1 mL of each fraction was collected applying ~ 0.5 mL/min flow rate and analyzed by LC-MS/MS as described in 4.1.2.

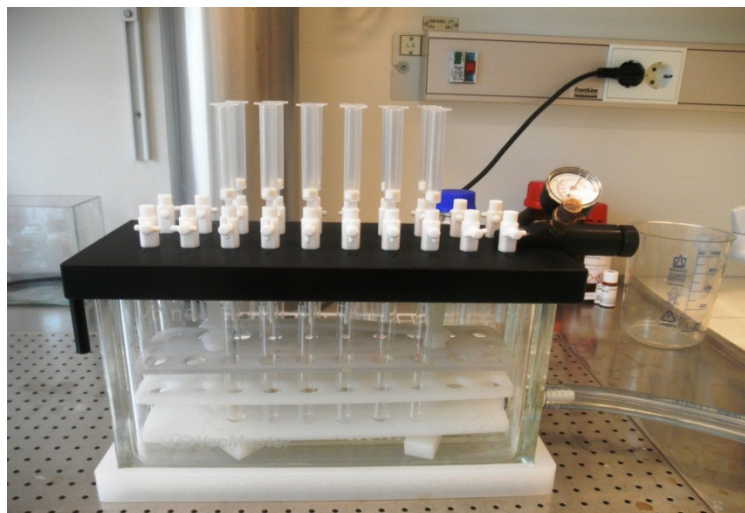


Figure 4.5: The setup for SPE flow-through experiments

Flow through scavenging experiments of acrolein in the presence of iodixanol was carried out using scavenger resin packed in SPE cartridges as described above. 75 mg of each scavenger was packed in 1mL SPE cartridges. The cartridges were conditioned with 1 mL of methanol and then 1 mL of ethanol. Samples of 1 mL of a solution of 5 $\mu\text{g}/\text{mL}$ acrolein and 2 mg/mL iodixanol in EtOH, 100 μL of the collected aliquots of the sample were derivatized by DNPH and assayed by HPLC as described in 4.1.1.

4.5 Batch scavenging procedures for reactive scavengers

Batch scavenging experiments for methyl p-toluenesulfonate were done with 150 mg of each scavenger placed in HPLC vials and addition of 1 mL of a solution of 5 $\mu\text{g}/\text{mL}$ methyl p-toluenesulfonate and 500 $\mu\text{g}/\text{mL}$ 21-chlorodiflorasone in 2-propanol. The relative concentrations of GTI and API (1:100) were aimed to reflect the industrial situation where the API is highly concentrated and the GTI is present at much lower concentration. The suspension mixtures were then stirred for 2 hours. The scavengers were allowed to settle briefly and aliquots of 100 μL were taken and assayed by HPLC.

In the batch scavenging experiments for acrolein, 75 mg of each scavenger was placed in HPLC vials and after the addition of 1 mL of a solution of 5 µg/mL acrolein and 2 mg/mL iodixanol in EtOH, the mixtures were shaken for 30 min and then the scavenger resin was allowed to settle for 2 min and aliquots of 100 µL were taken, derivatized by DNPH and assayed by HPLC.

4.6 Synthesis of urea based functional monomers

The polymerizable urea monomers (oxo-urea and thio-urea) were synthesized according to a published procedure^[157] which is also described below.

For the synthesis of 1-(4-vinylphenyl)-3-(3,5-bis(trifluoromethyl)phenyl)-urea, to a stirred solution of 10 mmol of 4-vinylaniline (1.19 g) in anhydrous THF (50 mL) under a N₂ atmosphere was added 3,5-bis(trifluoromethyl)phenyl isocyanate (10 mmol, 2.55 g). The solution was allowed to stir at room temperature overnight and then the solvent was evaporated under reduced pressure. The solid residue was recrystallized from chloroform and subsequently treated with activated charcoal.

¹H NMR (400 MHz, DMSO) δ 9.41 (s, 1H), 9.08 (s, 1H), 8.14 (s, 2H), 7.65 (s, 1H), 7.53 – 7.33 (m, 4H), 6.68 (dd, *J* = 17.7, 11.0 Hz, 1H), 5.73 (d, *J* = 17.7 Hz, 1H), 5.16 (d, *J* = 11.1 Hz, 1H)

¹³C NMR (101 MHz, DMSO) δ 153.16, 142.66, 139.63, 137.01, 132.36, 127.53, 119.60, 118.87, 113.29

For the synthesis of 1-(4-vinylphenyl)-3-(3,5-bis(trifluoromethyl)phenyl)thiourea, to a stirred solution of 3.5 mmol of 4-vinylaniline (0.42 g) in anhydrous THF (20 mL) under N₂ atmosphere was added 3,5-bis(trifluoromethyl)phenyl isothiocyanate (3.5 mmol, 0.95 g). The solution was refluxed overnight and then the solvent was evaporated under reduced pressure. The monomer was purified using silica gel column chromatography with dichloromethane.

^1H NMR (400 MHz, DMSO) δ 10.36 (s, 1H), 10.24 (s, 1H), 8.26 (s, 2H), 7.80 (s, 1H), 7.43 – 7.50 (m, 4H), 6.69-6.76 (m, 1H), 5.79, 5.83 (d, 1H), 5.26, 5.23 (d, 1H)

^{13}C NMR (101 MHz, DMSO) δ 179.71, 141.83, 138.21, 135.97, 134.02, 130.12, 129.80, 126.53, 125.41, 124.59, 123.89, 123.51

4.7 Preparation of methyl *p*-toluenesulfonate imprinted polymers

The imprinted polymers were prepared in the following manner. The template molecule, methyl *p*-toluenesulfonate (0.1 mmol, 0.019 g) and functional monomer (oxo-urea 0.1 mmol, 0.037 g or thio-urea 0.1 mmol, 0.039 g) were dissolved in toluene:acetonitrile mixtures (7.5 mL) and then DVB (2 mmol, 0.26 g) was added to the solution. Finally, the initiator ABDV (1% w/w of total monomers) was added.

The solution was transferred to a glass ampoule and purged with a flow of dry nitrogen for 5 min under cooling. The tubes were then flame-sealed and the polymerization initiated by placing the tubes in a thermostated water bath at 40 °C for 12 h. The temperature was then increased to 60 °C and was held constant for the next 12 h. After 24 h the tubes were broken and the polymers lightly crushed. Removal of the template molecule from the polymers was achieved by extraction with MeOH:0.1 N HCl (80:20) in a Soxhlet apparatus for 24 h. Thereafter, the polymers were crushed and sieved with a 25 μm and 36 μm sieve. A non-imprinted polymer was prepared in the same way as described above

The detailed compositions of the polymers are shown in Table 4.1.

Table 4.1: Polymer compositions

Polymer	Composition	Stoichiometry [mmol]	Porogen	Volume [ml]	Method
MIP I	Methyl p-toluenesulfonate /Oxo-urea /DVB	0.1/0.1/2	Toluene: MeCN (99:1)	7.5	ABDV 40/60 °C **
MIP II	Methyl p-toluenesulfonate /Thio-urea /DVB	0.1/0.1/2	Toluene: MeCN (94:6)	7.5	ABDV 40/60 °C **
NIP I	Oxo-urea /DVB	0.1/2	Toluene: MeCN (99:1)	7.5	ABDV 40/60 °C **
NIP II	Thio-urea /DVB	0.1/2	Toluene: MeCN (94:6)	7.5	ABDV 40/60 °C **

** The polymerization starts at lower temperature (40 °C) for 12 h to maximize the interaction between monomer and template and the temperature is then increased to 60 °C for complete polymerization (curing step).

4.8 Characterization of the polymers

The imprinted polymers were characterized by elemental analysis, FTIR and BET to gain information on polymer composition and to confirm removal of the target molecule. BET was carried out to estimate the pore size distribution of the prepared polymers, as well as their specific pore volume and surface area, whereas the polymer particle size and shape was characterized by microscopy and particle size distribution was measured by light scattering analysis.

4.8.1 Nitrogen adsorption

Nitrogen adsorption measurements were performed using an ASAP 2400, Micromeritics (Norcross, Georgia) analyzer. Before measurements, the samples were placed in a glass cell and degassed under vacuum over night at different temperatures depending on the nature of the sample.

In 1938, Brunauer, Emmett and Teller have first introduced the model for adsorption of gases onto a solid surface.^[158] According to the BET theory it is assumed that each unit of the solid surface consists of n sites, which can adsorb one molecule and that all of these sites are energetically same. The BET isotherm is the most commonly used isotherm type dealing with multilayer adsorption of molecules. The equation for the BET isotherm is shown below:

$$\frac{1}{v\left(\frac{P_0}{P}\right)-1} = \frac{(C-1).P}{Vm.c.P_0} + \frac{1}{Vm.c} \quad (2)$$

v is the amount of adsorbed gas, P is the partial vapour pressure of adsorbed gas in equilibrium with the surface at 77.4 K, P_0 is the saturated pressure of adsorbed gas, Vm is amount of adsorbed gas and c is the BET constant.

The pore size distribution can be evaluated by Barrett-Joyner-Halenda (BJH) method^[159] using the desorption steps.

The surface area covered by each adsorbed gas molecule, the total surface area A_{total} can be calculated using the following equation:

$$A_{total} = \frac{Vm.N.s}{V} \quad (3)$$

N is the Avogadro's number, s is the adsorption cross section of the adsorbing species and V is the molar volume of adsorbed gas

The specific surface area can be calculated using the following equation:

$$A_{\text{specific}} = \frac{A_{\text{total}}}{\alpha} \quad (4)$$

Where α is the mass of adsorbed gas on the solid surface.

4.8.2 Elemental analysis

Carbon, hydrogen, nitrogen and sulfur contents were determined at the Department of Organic Chemistry, Johannes Gutenberg University of Mainz using a Heraeus CHN-rapid analyzer (Hanau, Germany).

4.8.3 Particle size analysis

The particle size measurements were done according to the following procedure: First, ca. 0.1 g of the polymer material was dispersed in 3 mL ethanol and then 15 mL water was added. This solution was then put into an ultrasonic bath to disperse all the material in order to avoid agglomeration and to avoid false results in the particle size measurement. Then, this solution was measured in a Malvern Mastersizer 2000 particle size analyzer. Experiments were done in triplicates.

4.8.4 Optical microscopy

To measure the particle size of the polymers in the microscope, a small amount of dry sample of the polymer beads was put on to a slide glass and then a cover slip was put over the sample. The microscope was a Nikon ECLIPSE ME600 with Infinity Analyse 5.0.3 software calibrated with a ruler to measure the size of the polymer beads.

4.8.5 Swelling experiments

NMR tubes were filled with dry polymer up to 1 cm in order to evaluate the swelling behavior of the polymers. The polymer particles were allowed to equilibrate in the solvent for 2 h. Afterwards, the volume of the swollen polymer particles was measured.

The swelling ratio was calculated according to the following equation:

Swelling ratio = bed volume of swollen particles / bed volume of dry particles (5)

4.8.6 Infrared spectroscopy

FT-IR spectra of the polymers were recorded on a Perkin Elmer Spectrum 100 FT-IR spectrometer using a ZnSe ATR crystal.

4.9 *Batch rebinding procedure for the polymers*

To evaluate the binding properties of the various scavengers, 50 mg of each polymer, MIP1, MIP2, NIP1 and NIP2 were placed in HPLC vials and 1 ml of 5 µg/ml methyl p-toluenesulfonate and 500 µg/ml 21-chlorodiflorasone in isopropanol was added to each MIP scavenger respectively. The vials were sealed and the rebinding mixtures were shaken for 24 hours. After sedimentation the supernatants were filtered with Millipore syringe filters in order to remove any particles before analysis. The samples were then analyzed by HPLC.

4.10 *Comparison experiments of the binding behavior of the polymers and reactive scavengers*

Comparison experiments of the binding of methyl p-toluenesulfonate using MIPs and reactive scavengers in different solvents were carried out in batch mode.

Experiments were carried out in small HPLC vials contain 50 mg polymer or reactive scavenger, and 1 mL of 5 µg/ml methyl p-toluenesulfonate and 500 µg/ml 21-chlorodiflorasone dissolved in IPA, MeCN and DCM, separately. These suspensions were stirred for 30 min, then they were allowed to settle for 2 min and aliquots of 100 µL were taken and analyzed by HPLC.

4.11 *Synthesis of functional monomers for acrolein MIPs*

Synthesis of vinylbenzyl hydrazine monomer

The polymerizable vinylbenzyl hydrazine monomer was synthesized according to a published procedure ^[160] also described below.

0.034 mol (5.16 g) of 4-vinylbenzyl chloride and 0.034 mol (4.8 g) of potassium carbonate were added to a solution of 0.076 mol (3.8 g) of hydrazine monohydrate in 34 g of acetonitrile in a 100 mL round-bottom flask. The solution was stirred at room temperature for 4 h and was then distilled under reduced pressure. The obtained orange oily product was purified by silica gel column chromatography with dichloromethane.

The purity of the vinylbenzyl hydrazine monomer was confirmed by ¹H-NMR.

¹H NMR (CDCl₃) (400 MHz); δ : 7.23-7.44 (m, 4H, aromatic), 6.20-6.78 (m, 1H, vinylic), 5.75-5.82 (m, 1H, vinylic), 5.24-5.30 (m, 1H, vinylic), 3.75-3.94 (m, 2H, -CH₂), 2.97 (s, 3H, NH₂-NH)

Synthesis of Schiff base using vinylbenzyl hydrazine and phenyl acetaldehyde

Phenyl acetaldehyde (2.5 mmol, 0.3 g) is dissolved in absolute methanol (20 mL) and the equimolar amount of vinylbenzyl hydrazine (2.5 mmol, 0.34 g) in a minimum volume of absolute methanol is added. The resulting yellow reaction mixture was heated and refluxed overnight. The color gradually turned deep yellow. The solvent was evaporated and the oily product was purified by silica gel column chromatography with dichloromethane.

The purity of the Schiff base was confirmed by ¹H-NMR spectroscopy and mass spectrometry.

¹H NMR (CDCl₃) (400 MHz); δ: 6.59 -7.58 (m, 11H), 6.7 (m, 1H, vinylic), 5.8 (m, 1H, vinylic), 5.3 (m, 1H, vinylic), 4.4 (m, 2H, CH₂)

MS (FAB) *m/z* (M⁺) 250.1, ([M + H]⁺) 251.1

4.12 Preparation of MIPs for acrolein

Imprinted polymers were prepared according to the following procedure:

The synthesized Schiff base as a functional monomer (1 mmol) was dissolved in chloroform (7.5 mL). Then, DVB or EDMA (20 mmol) was added to the solution. Finally, the initiator ABDV (1% w/w of total monomers) was added.

The solution was transferred to a glass ampule, and purged with a stream of dry nitrogen for 5 min. The tubes were then flame-sealed while still under cooling and the polymerization initiated by placing the tubes in a thermostated water bath at 40 °C for 12 h. The temperature was increased to 60 °C and held for the next 12 h. After 24 h the tubes were broken and the polymers lightly crushed. Hydrolysis of the Schiff base in the polymers was achieved by extraction with MeOH:0.1 N HCl (50:50) in a Soxhlet apparatus for 24 h. A non-imprinted polymer was prepared in the same way as described above, but instead using vinylbenzyl hydrazine as a functional monomer.

Note: Acidic methanol was chosen as a solvent for hydrolysis of the Schiff base based on a publication by Sasaki et al. ^[161]

The composition of the prepared polymers towards acrolein is given in Table 4.2.

Table 4.2: Composition of the prepared polymers towards acrolein

MIP 1

	Functional monomer (Schiff Base)	Cross-linker (DVB)	Initiator (ABDV)	Porogen (Chloroform)
Molar ratio [mmol]	0.10	2.0	-	-
Mass [mg]	250.3	2603.8	10	-
Density [g/ml]	-	0.91	-	-
Volume [ml]	-	2.85	-	7.5

NIP 1

	Functional monomer (Vinylbenzyl hydrazine)	Cross-linker (DVB)	Initiator (ABDV)	Porogen (Chloroform)
Molar ratio [mmol]	0.10	2.0	-	-
Mass [mg]	148	2603.8	10	-
Density [g/ml]	-	0.91	-	-
Volume [ml]	-	2.85	-	7.5

MIP 2

	Functional monomer (Schiff Base)	Cross-linker (EDMA)	Initiator (ABDV)	Porogen (Chloroform)
Molar ratio [mmol]	0.10	2.0	-	-
Mass [mg]	250.3	2603.8	10	-
Density [g/ml]	-	0.91	-	-
Volume [ml]	-	2.85	-	7.5

Table 4.2 continues on the next page

Continuation of Table 4.2 from the previous page

NIP 2

	Functional monomer (Vinylbenzyl hydrazine)	Cross-linker (EDMA)	Initiator (ABDV)	Porogen (Chloroform)
Molar ratio [mmol]	0.10	2.0	-	-
Mass [mg]	148	2603.8	10	-
Density [g/ml]	-	0.91	-	-
Volume [ml]	-	2.85	-	7.5

5 RESULTS AND DISCUSSION

5.1 *MIP resins and reactive scavengers towards methyl p-toluenesulfonate*

5.1.1 Screening of urea MIPs

As discussed in Section 1.3.4, in the extensive work conducted by Sellergren and his co-workers ^[129], the urea group is described to interact well with sulphates, sulphonates, phosphates and phosphonates via hydrogen bonding. They have investigated MIPs using urea-based functional monomers for recognition of triphenyl phosphate and diethylphenyl phosphate. ^[129] Etter et al. ^[162] have reported similar diarylureas to co-crystallize with weak hydrogen-bond acceptors such as cyclic ethers and ketones. In another study ^[163] they concluded that diaryl ureas ortho- or para-substituted with strong electron-withdrawing groups such as -NO₂ or -CF₃ do not form co-crystals through hydrogen bonding even with strong hydrogen acceptors. However, the hydrogen bond is stronger if there is meta substituted strong electron-withdrawing groups such as -CF₃ on the ring of the diaryl urea monomer.

It was the intention to utilize the same binding principle for this study, therefore the screening experiments for methyl p-toluenesulfonate were carried out using the collection of MIPs and NIPs with urea moieties described in Section 1.3.4. The methyl p-toluenesulfonate is known to have moderate hydrogen bonding ability in its sulfonate moiety ^[164-166] and the interaction chemistry expected in these experiments is hydrogen bonding between the urea moiety which can act as a strong hydrogen bond donor in the polymer and the hydrogen-bond acceptor site of the methyl p-toluenesulfonate as depicted in Figure 5.1.

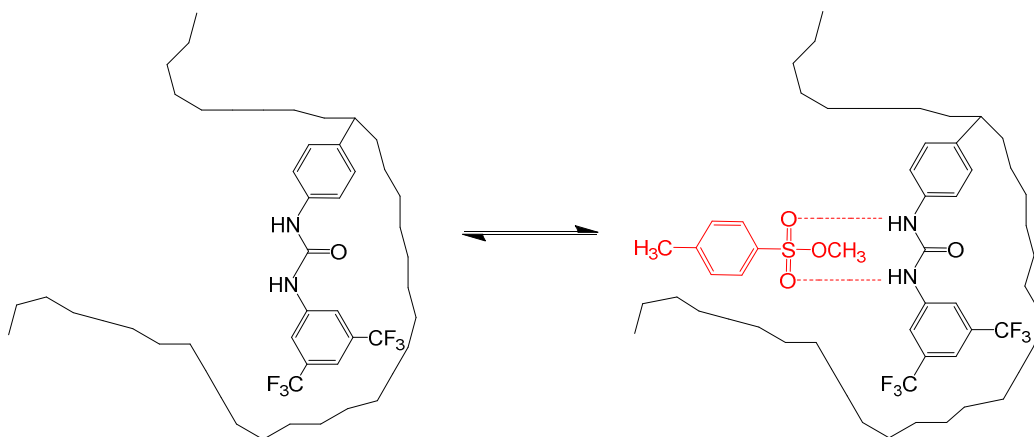


Figure 5.1: Schematic representation of the expected interaction between the urea functionality and methyl p-toluenesulfonate

The MIPs and NIPs are chemically related and have a hydrophobic backbone and urea groups as functional moieties. This plate was chosen because it was assumed that the urea group would be the most promising interaction chemistry available. Neither resins with carboxylic acid, boronic acids, or styrenes or pyridines were expected to be able to form specific interactions with the GTI while the CF_3 groups on the phenyl-group of the phenyl urea have a strong electron-withdrawing effect that makes the urea moiety potent in its hydrogen-bonding ability.

Prior to screening of methyl p-toluenesulfonate on the urea plate, preliminary experiments were carried out on a subset of the resins using MeCN, DCM, EtOH and IPA as loading solvents, all of them typical solvents used in process chemistry. In these preliminary experiments, a solution of methyl p-toluenesulfonate and 21-chlorodiflorasone was prepared as a mixture in the loading solvent. 1 mL SPE columns were packed with the various MIPs and their corresponding NIPs. This solution was passed through the SPE columns after conditioning and the analytes found in the eluate were analyzed by LC-MS/MS.

The results from this experiment are shown in Figure 5.2.

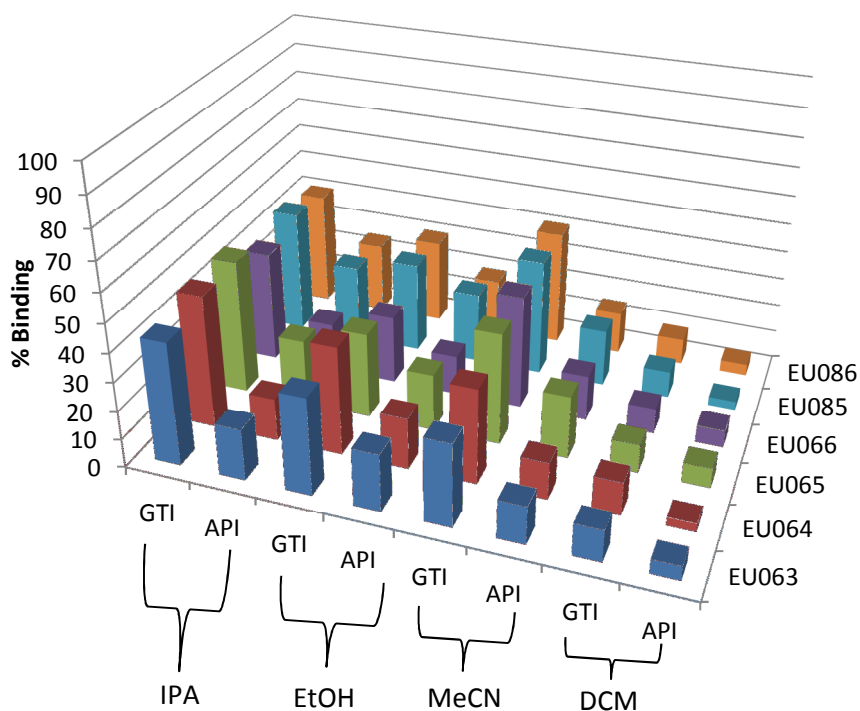


Figure 5.2: Pre-screening of 1 $\mu\text{g/mL}$ methyl-p-toluenesulfonate and 100 $\mu\text{g/mL}$ 21-chlorodiflorasone in various solvents. Odd numbered resins are MIPs, the resin with the following even number is the corresponding NIP.

A summary of the results is shown in Table 5.1. The binding of compounds in DCM was generally low, although one should expect a high binding, if expecting hydrogen bonding to be the dominating binding mechanism between the tosylate and the urea functionality. Perhaps solubility of GTI and API and competitor effects play a role here. In MeCN, binding of both GTI and API was higher than in DCM. In EtOH, one resin EU086 displayed a reasonable selectivity with high GTI retention although the selectivity for GTI over API was lower than in IPA. Based on these results, isopropanol was chosen as the loading solvent for the screening of methyl p-toluenesulfonate on the urea plate.

Table 5.1: Summary of pre-screening results for 1 $\mu\text{g/mL}$ methyl-p-toluenesulfonate and 100 $\mu\text{g/mL}$ 21-chlorodiflorasone in various solvents

Loading Solvent	Binding (GTI)	Selectivity (GTI/API)	Imprinting Effect (MIP/NIP)
Acetonitrile	~ 40 %	Medium	-
Dichloromethane	Very Low (10 %)	Medium	-
Isopropanol	~ 50 %	High	-
Ethanol	~ 40 %	Medium	-

In the screening experiment on the full urea plate, a solution of methyl p-toluenesulfonate and 21-chlorodiflorasone was prepared as a mixture in isopropanol. 1 ml SPE columns were packed with the MIPs and NIPs. The solution was passed through the SPE columns after conditioning and the analytes found in the eluate were analyzed by LC-MS/MS.

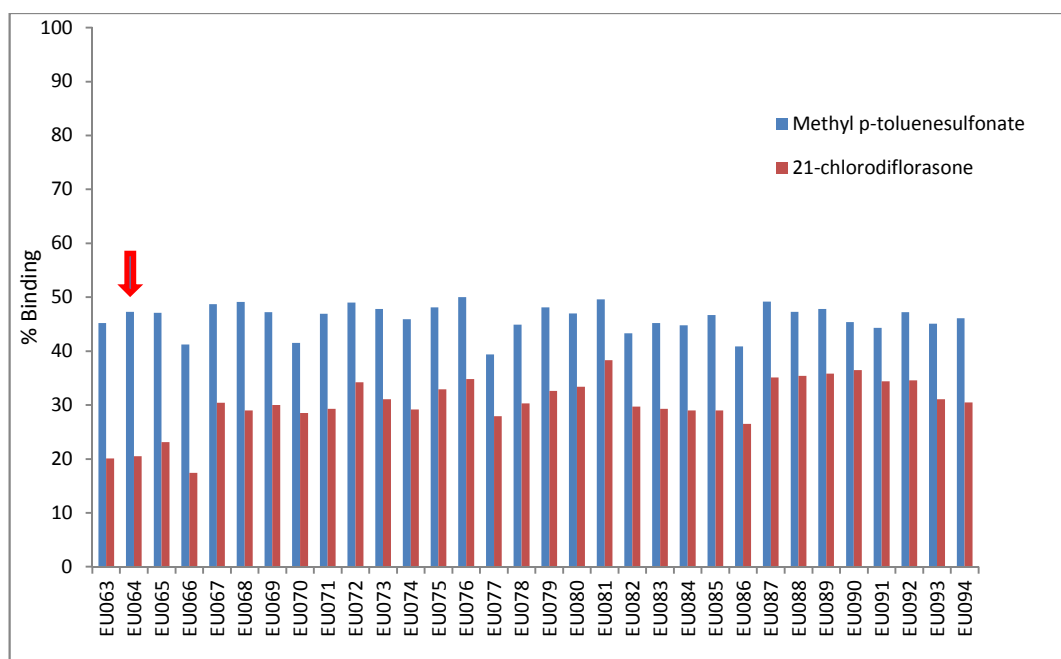


Figure 5.3: Binding of 1 $\mu\text{g/mL}$ methyl-p-toluenesulfonate and 100 $\mu\text{g/mL}$ 21-chlorodiflorasone on the urea plate loaded in IPA

The results from the screening of methyl p-toluenesulfonate in the presence of 21-chlorodiflorasone are shown in Figure 5.3 in the form of % binding of GTI and API. As can be seen in the figure, the majority of the urea-resins display selectivity towards the GTI over the API.

Most resins retained around 45 % of the GTI present in the IPA solution and some of the resins were close to 50 % retention (e.g EU064, EU067, EU068, EU075, and EU076). Only a few resins have a relatively low retention for the API, namely EU063, EU064, EU065 and EU066. All other resins retain close to 30 % or even more of the API. EU081 and EU090 are for example the materials with the least appropriate selectivity profile in the screening outcome. The difference in retention and selectivity is predominantly governed by the imprinting process and by the use of various porogens processes.

Of all materials, resins EU063-EU066 displayed the most advantageous selectivity of all EU polymers. Of those, EU063 and EU065 are imprinted polymers and EU064 and EU066 are non-imprinted polymers. Under these conditions, there is no imprinting effect between these resins and the non-imprinted resins EU064 and EU066 were able to conduct the same separation. Of those two, EU064 displayed a slightly higher retention towards the GTI. Although the differences between EU064 and EU066 were small, EU064 was chosen for further investigation.

5.1.2 Selectivity tests

In the preliminary experiment, IPA was identified to be a solvent where the resins show a good selectivity on the urea resin library.

EU064 was further investigated and selectivity experiments for methyl p-toluenesulfonate (GTI) and its corresponding API 21-chlorodiflorasone were carried out in different solvent mixtures based on IPA with varying additives. Adding these acidic, basic or neutral additives is common practice in MIP methodology.

In the experiments, methyl p-toluenesulfonate and 21-chlorodiflorasone were prepared as a mixture in IPA with different solvent additives (see Figure 5.4). Each of these solutions was passed through the pre-conditioned polymers packed SPE columns and the analytes found in the eluate were analyzed by LC-MS/MS.

The results from the loading experiments in the different solvents are shown in Figure 5.4. As can be seen from the figure, EU064 displayed the same binding behavior for GTI in IPA, 1 % HAc in IPA and 2 % HAc in IPA, 1% triethyl amine

in IPA and 2 % triethyl amine in IPA but the best binding was obtained in clean IPA with good selectivity for the GTI with 46% binding over the API with only 4 % binding. Any additive in the IPA solutions worsens the selectivity for GTI over API and the addition of 10 % or 20 % acetone almost eliminates the selectivity completely and the resin can only barely distinguish between GTI and API.

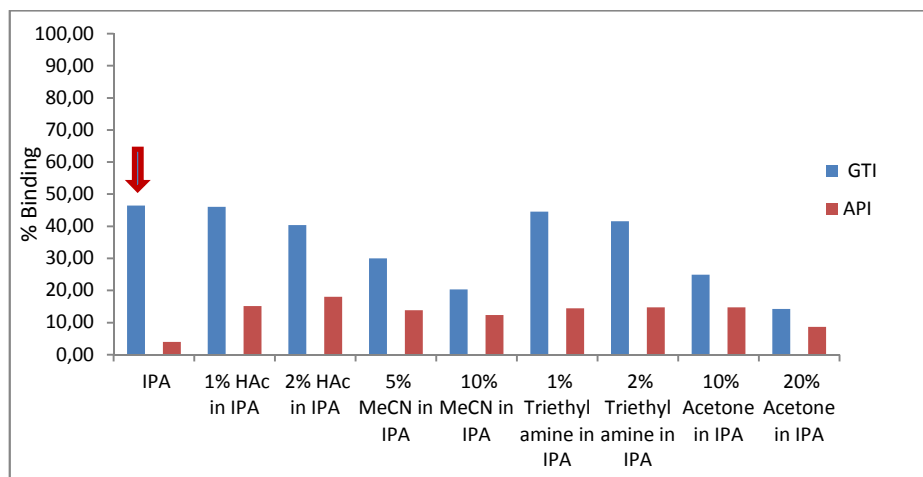


Figure 5.4: Selectivity between 1 µg/mL GTI and 100 µg/mL API in different loading solutions

Hence, among the loading solvents examined, IPA provides the most favorable difference of adsorption between API and GTI.

In a further experiment, the chromatographic separation of 10 µg/mL methyl p-toluenesulfonate (GTI) and 100 µg/mL 21-chlorodiflorasone (API) was evaluated using EU064 packed in an HPLC column. In Figure 5.5, an HPLC chromatogram for separation of the GTI and API mixture is shown. As can be seen in the chromatogram, the retention of the GTI in the column is stronger than for the API and the GTI is therefore eluted later.

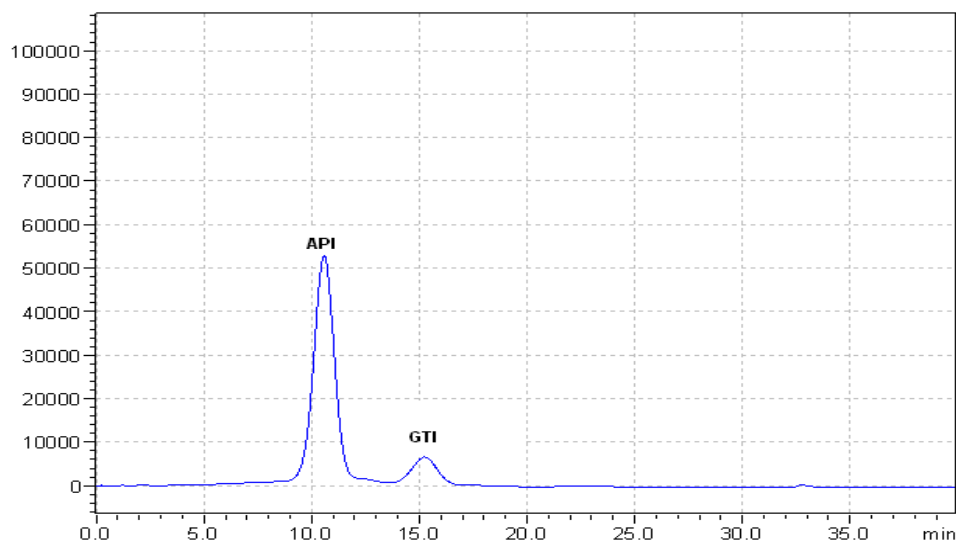


Figure 5.5: HPLC chromatogram of the separation of the GTI (10 $\mu\text{g/mL}$) and API (100 $\mu\text{g/mL}$) on a column packed with EU064; Gradient elution was performed with 10 mM NH_4Ac buffer pH 8.0 (mobile phase A) and MeCN (mobile phase B).The gradient started from 30 % B to 70 % B over 20 min, then kept at 70 % B for 10 min, then back to 30 % B over 1 min and kept at 30 % B for 9 min ; injection volume: 10 μL ; flow rate: 0.5 mL/min

The chromatographic separation of GTI and API is quite satisfactory with baseline separation between the peaks. The difference of retention time correlates to the screening outcome in Figure 5.3 where the resin displays a stronger retention of the GTI over the API. The resolution factor (R_s) of the separation between GTI and API is 2.38. From a practical and thus industrial point of view it is highly desirable that the impurity, here the genotoxic contaminant, is retarded longer in the column system. By this, a separation mode can be envisaged, where the pharmaceutical reaction mixture is loaded on a column, the desired product is passing through, while the undesired contaminant is retarded in the packed bed. In this or other process modes, a preparative separation in an industrial setting of this API and GTI using this resin could be foreseen.

The separation of GTI and API was also evaluated on a silica-based reversed phase C18 column for comparison. As can be seen from the Figure 5.6, the column also affords the separation of GTI and API. In this particular chromatogram the peaks are sharper due to the very small particle size (5.0 μm) of the packed material in the C18 column and the resolution factor (R_s) of the separation between GTI and API is 10.1. However, compared to EU064, the

elution order is reversed here. Due to its hydrophobicity, the retention of the API on C18 column is higher than for the GTI.

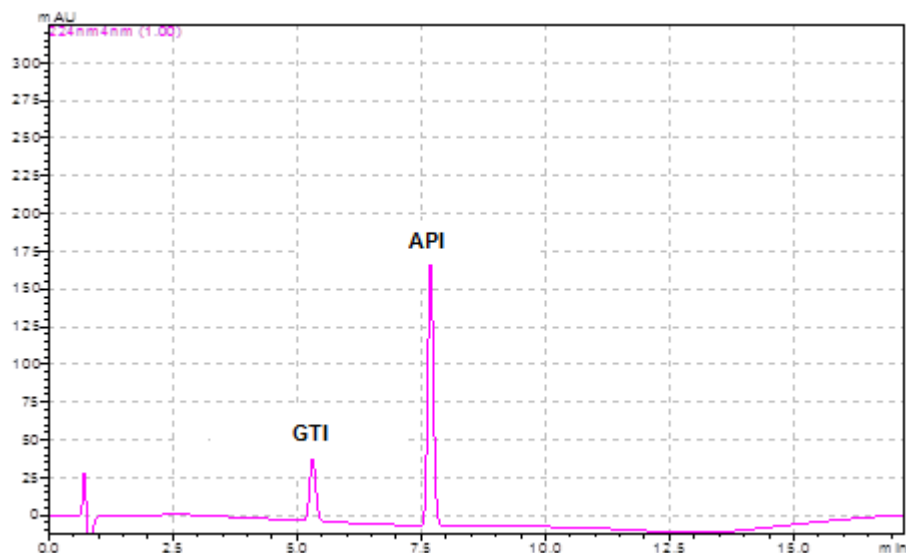


Figure 5.6: HPLC chromatogram of the separation of the 10 µg/mL GTI and 100 µg/mL API on C18 column; Gradient elution was performed with 10 mM NH₄Ac buffer pH 8.0 (mobile phase A) and MeCN (mobile phase B).The gradient started from 30 % B to 70 % B over 20 min, then kept at 70 % B for 10 min, then back to 30 % B over 1 min and kept at 30 % B for 9 min ; injection volume: 10 µL; flow rate: 0.5 mL/min

5.1.3 Binding isotherms

The amount of GTI bound to the polymer is a function of the concentration at a constant temperature and can be described in binding isotherms.

The Langmuir isotherm ^[167] model is probably the best known and most commonly used equation for binding isotherms. In the Langmuir binding model, binding data can be analyzed using the following equation:

$$\frac{1}{Q} = \left[\frac{1}{Q_{max} \times b} \right] \left[\frac{1}{C_{eq}} \right] + \frac{1}{Q_{max}} \quad (5)$$

Where **Q_{max}** represents the maximum binding capacity (mg analyte/g polymer), **C_{eq}** is the equilibrium concentration of analyte in the solution (mg/L) and measured experimentally, **Q** is the amount of analyte bound by the polymer (mg/g

polymer) and b is the Langmuir constant which reflects the affinity between analyte and polymer. Q can be calculated using the following equation:

$$Q = \left[\frac{C_0 - C_{eq}}{V} \right] \left[\frac{1}{m} \right] \quad (6)$$

V is the amount of solution (L) and m is the mass of polymer (g).

A binding curve was obtained for methyl-p-toluenesulfonate with resin EU064 using the optimized conditions and the results are given in Figure 5.7.

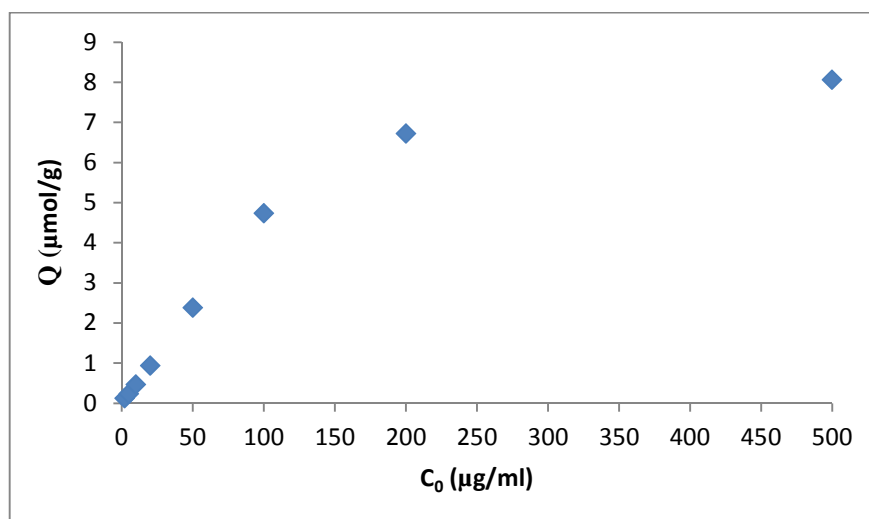


Figure 5.7: Methyl p-toluenesulfonate initial concentration effect on binding

The results were analyzed and the data was applied to the Langmuir isotherm.

From the graphs in Figure 5.7 and 5.8, the various binding parameters for methyl p-toluenesulfonate could be obtained. From the graph of Figure 5.7, it can be read that the maximum binding capacity is 8 μmol per gram, which is equal to 1.45 mg/g. Calculation of the Langmuir constant b is carried out using Equation 6, where the slope is $\left[\frac{1}{Q_{max} \times b} \right] = 12.396$ and thus b , the Langmuir constant towards methyl p-toluenesulfonate is 0.0103 mL/ μg .

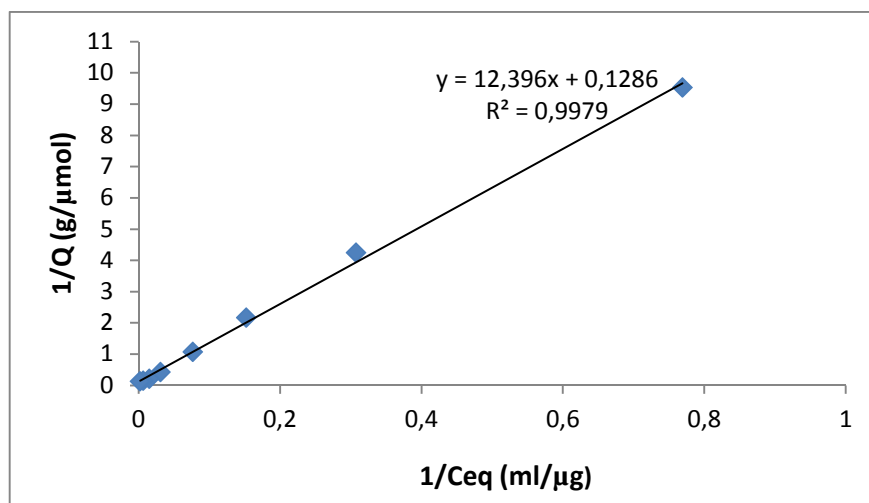


Figure 5.8: Linearized Langmuir binding isotherm for methyl p-toluenesulfonate

Another approach for the characterization of binding sites of the polymers is Freundlich binding model which is a generalized model from the Langmuir model.

The Freundlich isotherm described by the following equation:

$$Q = kF \times Ceq^{1/n} \quad (7)$$

Where **Q** represents the amount of analyte bound by the polymer (mg/g polymer), **Ceq** is the equilibrium concentration of analyte in the solution (mg/L), **kF** is the Freundlich constant and **n** is the Freundlich exponent. $1/n$ is a measure of heterogeneity of the binding sites of the polymer ranging between 0 and 1. When this value gets closer to zero heterogeneity increases.

The Freundlich isotherm equation can be linearized as:

$$\ln Q = \frac{1}{n} \ln Ceq + \ln kF \quad (8)$$

The linearized Freundlich binding isotherm for methyl p-toluenesulfonate is shown in Figure 5.9. The binding follows the equation up to 65 $\mu\text{g/mL}$ ($\ln C_{\text{eq}}$ is 4.1) methyl p-toluenesulfonate. It is an inherent characteristic of the Freundlich model that it has no upper limit whereas all real adsorbents get saturated at high concentrations.

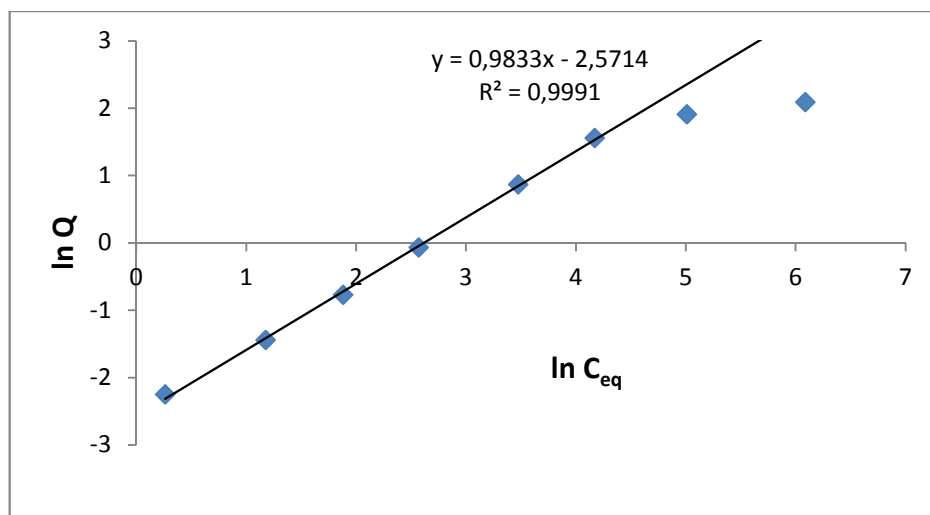


Figure 5.9: Freundlich binding isotherm for methyl p-toluenesulfonate

The parameters for the Langmuir and Freundlich equations for methyl p-toluenesulfonate binding to EU064 are shown in Table 5.2.

Methyl p-toluenesulfonate binding to the EU064 is well described by the Langmuir model at all concentrations while the Freundlich model can only be used up to 65 $\mu\text{g/mL}$ ($\ln C_{\text{eq}}$ is 4.1) methyl p-toluenesulfonate.

Table 5.2: Parameters for the Langmuir and Freundlich binding isotherms for methyl p-toluenesulfonate binding to EU064

Experimental	Langmuir				Freundlich		
	Q_{max} (mg/g)	Q_{max} (mg/g)	b (mL/ μg)	R^2	k_F (mL/mg)	n	R^2
EU064	1.45	1.45	0.0103	0.99	13.1	1.0	0.99

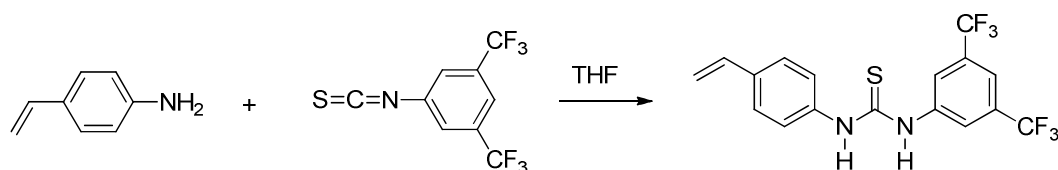
5.1.4 Synthesis of methyl p-toluenesulfonate imprinted polymers

As no selective imprinted polymers were discovered from the screening of the library, the subsequent approach was to design and synthesize novel imprinted polymers.

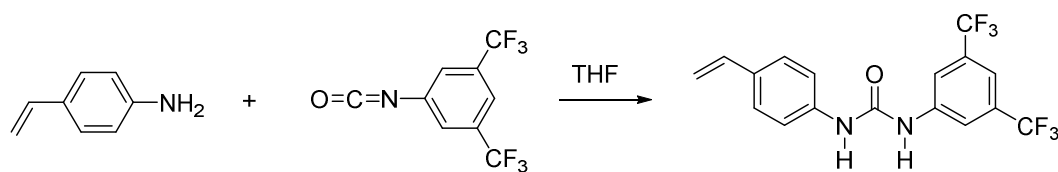
The urea monomers are currently not commercially available and have to be synthesized prior to polymer production. Therefore, polymerizable thio-urea and oxo-urea monomers were synthesized according to a published procedure.^[157]

To a stirred solution of the amine in THF was added the required isocyanate or isothiocyanate for the synthesis of oxo-urea and thio-urea monomer, respectively. After the reaction, the solid residue was recrystallized from chloroform and subsequently treated with activated charcoal.

Reaction schemes are given in Scheme 5.1 and 5.2.



Scheme 5.1: Synthesis of the thio-urea monomer



Scheme 5.2: Synthesis of the oxo-urea monomer

After the monomers had been prepared in sufficient quantities, a total of four different imprinted and non-imprinted polymers were prepared towards methyl p-toluenesulfonate. The two different functional monomers were used in combination with the cross-linker DVB. The polymers were prepared according to the following procedure. The template molecule methyl p-toluenesulfonate and

functional urea monomer were dissolved in toluene:acetonitrile mixtures and then DVB and initiator were added to the solution. After polymerization, the removal of template was carried out with acidified methanol mixture under reflux.

The imprinted polymers were characterized by elemental analysis to gain information on polymer composition and to confirm removal of the target molecule. In addition to that, BET was carried out to estimate the pore size distribution of the prepared polymers, as well as their specific pore volume and surface area, while the polymer particle size and shape were characterized by microscopy and light scattering.

High levels of residual template left in the polymer would be detrimental to the performance. Likewise, if the polymer composition would deviate from the expected elemental pattern or ratio, then the copolymerization would have been unsuccessful. If the MIP and the NIP would have very different pore structure such as very different areas, then a difference of capacity would not necessarily be based on an imprinting effect but could be related merely to the surface onto which molecules can bind.

BET results for the polymers are given in Table 5.3. As can be seen in the table, only a small difference between the surface area and pore volume of MIP and NIP was observed. For MIP 1 and NIP 1, the morphological properties are rather similar. However, the morphological difference of MIP 2 and NIP 2 is to a certain extent more pronounced and the surface area of the MIP is 20 % larger than the NIP. The reason for the varying pore morphologies lies in the initial composition of the polymer formulation. If the monomer and the growing polymer have a high solubility in the porogen then the pore size will be generally smaller. Likewise, a bad solubility of the monomer and the growing polymer will lead to an early precipitation and thus to larger pores in the particle.

The presence (or absence) of the template in the polymerization mixture of thio-urea-based materials has a stronger impact on the pore morphology than for the oxo-urea based materials.

Table 5.3: BET results for the oxo-urea based polymers RKM1 and RKN1, and the thio-urea based polymers RKM2 and RKN2

Polymer	Surface Area (m ² /g)	Pore Volume (ml/g)	Pore Diameter (nm)
RKM1	720	0.9	9
RKN1	695	0.8	10
RKM2	816	0.7	5
RKN2	680	0.6	6

The graphical pore size distributions of the polymers are shown in Figures 5.10 and 5.11. As can be seen in the figures as a primary observation, there is a significant difference in the pore size distribution curves between oxo-urea based materials and thio-urea based materials.

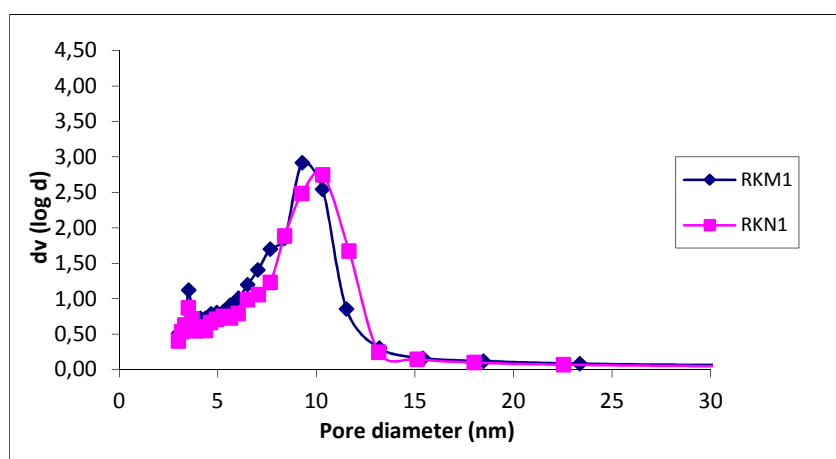


Figure 5.10: Pore size distribution of oxo-urea based polymers RKM1 and RKN1 obtained by BET analysis

From Figure 5.10, it can be seen that both RKM1 (MIP) and RKN1 (NIP) have rather similar pore size distributions. Hence there are no major morphological differences and the materials are very comparable in their porosity. This is in agreement with the data in Table 5.3. As for almost all porous polymeric materials, the pore size distribution is relatively broad and there is a considerable amount of smaller pores (pores below 5 nm).

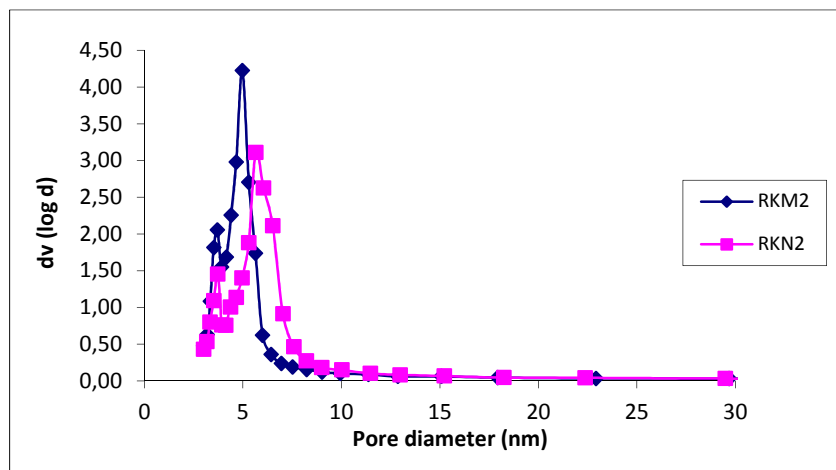


Figure 5.11: Pore size distribution of thio-urea based RKM2 and RKN2

The pore size analysis in Figure 5.11 shows a slight difference of main pore size of the thio-urea based RKM2 (MIP) and RKN2 (NIP). The pore size distribution is also here not uniform, but less broad than in the oxo-urea based materials. As a conclusion on the pore morphology of these urea-based polymers, it can be stated that the difference in pore properties between the imprinted and the non-imprinted materials is negligible.

The percentage by mass of carbon, hydrogen and nitrogen of the polymers determined by elemental analysis, as well as the expected values predicted from the feed ratio, are given in Table 5.4.

Table 5.4: Theoretical and experimental figures for the composition of the urea-based polymers

	Polymer	C %	H %	N %
Theoretical	RKM1	87.52	7.18	0.94
	RKN1	87.52	7.18	0.94
	RKM2	87.52	7.18	0.94
	RKN2	87.52	7.18	0.94
Experimental	RKM1	88.76	7.23	0.89
	RKN1	86.64	7.28	0.92
	RKM2	87.58	7.22	0.92
	RKN2	87.32	7.10	0.90

As seen from the table, the experimental results are compatible with the predicted values. From these findings, it can be concluded that conversion of monomers was essentially complete and the template quantitatively removed. As a side-note, the elemental analysis of sulfur was also conducted; however, the results were not conclusive. Due to the limited time-frame of the project, this elemental analysis was not repeated. However, if further studies are to be conducted, the elemental analysis of sulfur should be used for confirmation.

The FT-IR spectra of methyl p-toluenesulfonate imprinted polymers are shown in Figures 5.12 and 5.13. As seen from the spectra, all polymers have very similar FT-IR patterns indicating the similarity of the backbone structure. In the FT-IR spectra, absorption peaks due to aromatic C-H stretching ($\sim 3019\text{ cm}^{-1}$), carbonyl group stretch ($\sim 1705\text{ cm}^{-1}$) from the functional urea monomer and aliphatic C-H stretching ($\sim 2922\text{ cm}^{-1}$) and aromatic C=C ($\sim 1511\text{ cm}^{-1}$) from the cross-linker DVB were observed.

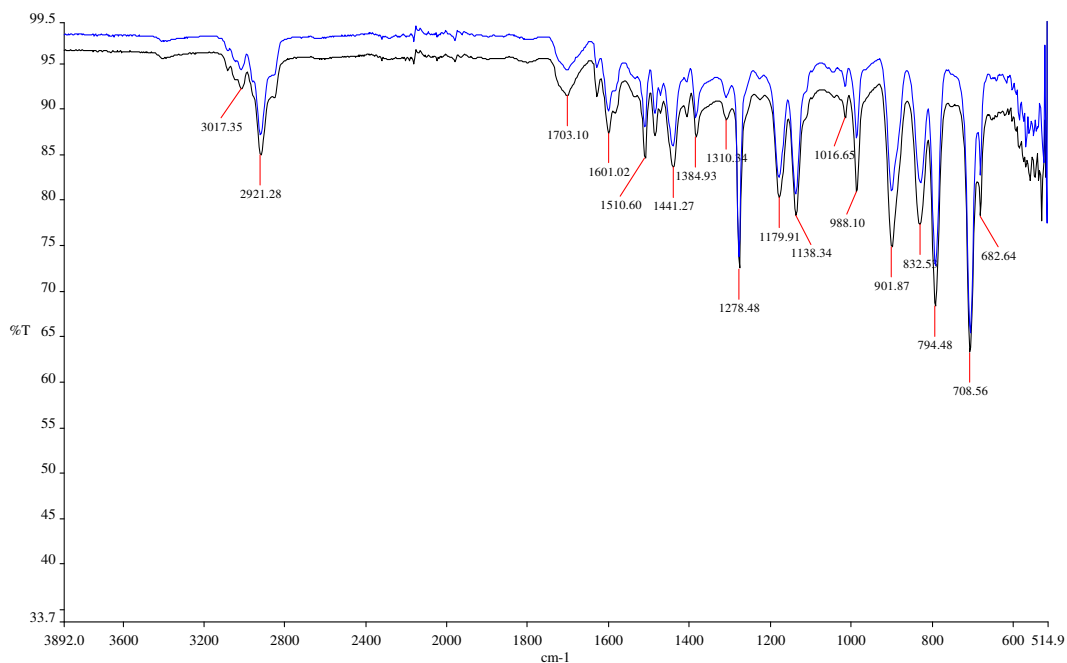


Figure 5.12: FT-IR spectra of oxo-urea based RKM1 (blue) and RKN1 (black)

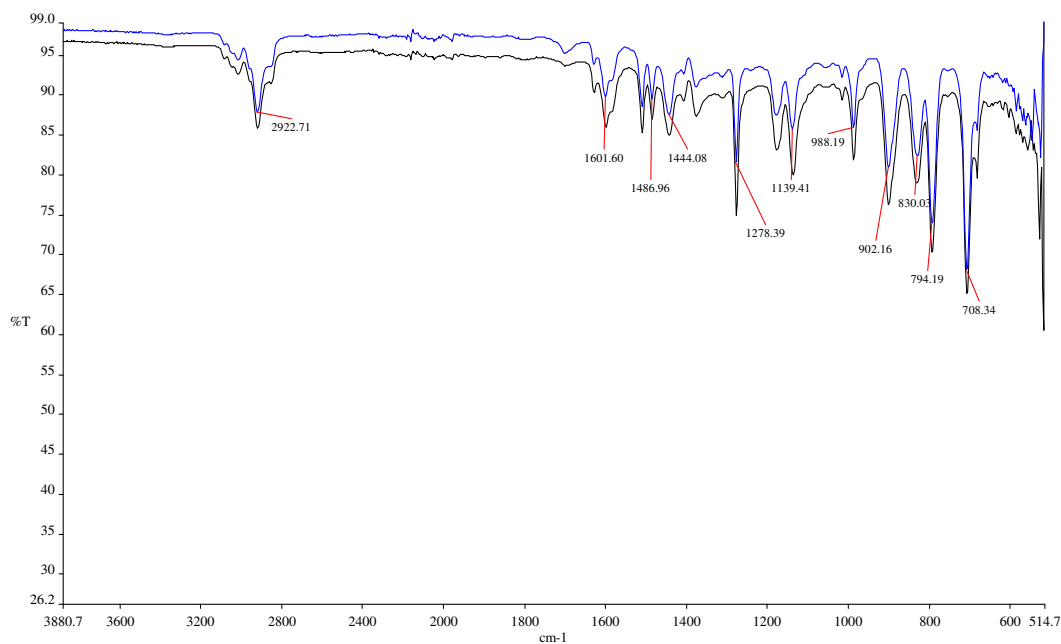


Figure 5.13: FT-IR spectra of thio-urea based RKM2 (blue) and RKN2 (black)

An optical microscope image of MIP 1 is shown in Figure 5.14. Being ground from a piece of polymer block, the imprinted polymer particles are irregular in the size range 25-36 μm .

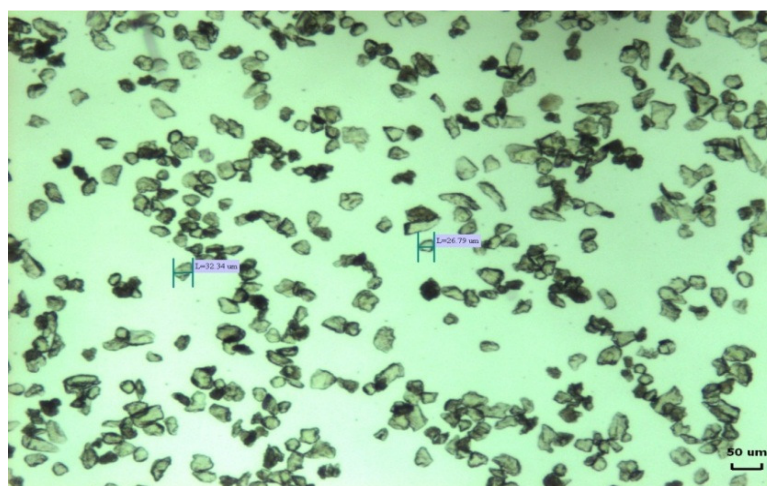


Figure 5.14: Optical microscope image of RKM1 (100 x total magnification)

In the light scattering measurement shown in Figure 5.15, the median of the particle size distribution is between 40-50 μm , whereas it should be between 25-36 μm as it was sieved to this particle size distribution. This slightly larger median of the particle size distribution may be caused by aggregation of the hydrophobic

particles in the water suspension in the measurement cell of the analytical light scattering device. The irregular nature of the particles contributes further to an alteration of the particle size read-out. Hence, light scattering produces less reliable results and has to be backed up with optical measurements.

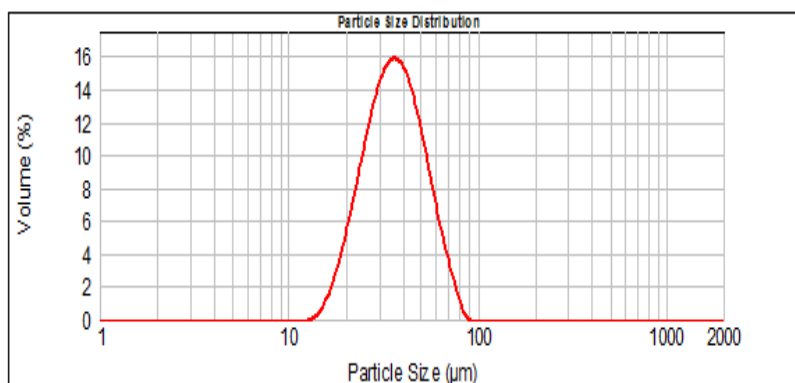


Figure 5.15: Particle size distribution of RKM1 by laser diffraction technology which is based on the fact that all polymer particles that pass through a laser beam will scatter the light, and the angle of the scattered light is directly related to the particle size of the polymer

The swelling behavior of the polymers is an important parameter for the binding performance and therefore the swelling behavior of the polymers was evaluated. Swelling tests were performed in the common solvents MeCN, THF and IPA. Swelling ratios of the MIPs and NIPs towards methyl p-toluenesulfonate are shown in Table 5.5. As can be seen from the table, the imprinted polymers RKM2 and RKM1 displayed higher swelling than their corresponding non-imprinted polymers RKN1 and RKN2 in most cases.

Table 5.5: Volume swelling ratios of the MIPs and NIPs

Solvent	RKM1 (MIP)	RKN1 (NIP)	RKM2 (MIP)	RKN2 (NIP)
MeCN	1.4	1.3	1.5	1.2
THF	1.3	1.4	1.4	1.2
IPA	1.5	1.4	1.6	1.4

5.1.5 Binding behavior of the new polymers for methyl p-toluenesulfonate

In this part of the study, experiments investigating the binding behavior of methyl p-toluenesulfonate imprinted polymers in batch mode were carried out.

Experiments were carried out in small HPLC vials containing polymer, GTI and API dissolved in IPA. This suspension was stirred for 24 h, then it was allowed to settle for 2 min and aliquots of 100 μ L were taken and analyzed by LC-MS/MS.

The results of batch binding of p-toluenesulfonate in acetonitrile: water mixtures are shown in Figure 5.16. As seen in the figure, increasing the water content led to higher binding, presumably because of the hydrophobic effect. In solvents with high water content, the most dominating binding effect was hydrophobic binding to the MIP or NIP polymer backbone.

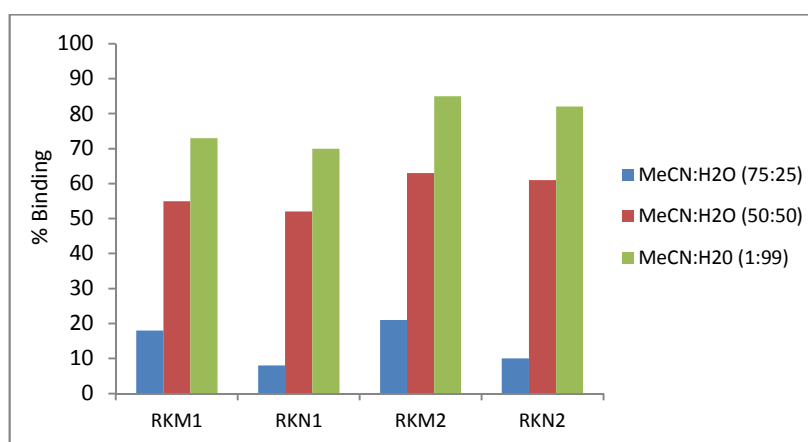


Figure 5.16: Binding of 5 μ g/mL methyl p-toluenesulfonate in acetonitrile:water mixtures to tosylate MIPs & NIPs

Because the materials appear to display a better selectivity in a water-free environment, further tests were done in organic solvent.

To evaluate the adsorption of methyl p-toluenesulfonate in the presence of model API 21-chlorodiflorasone in organic solvent, binding experiments were carried out in isopropanol. The outcomes of these experiments are shown in Figure 5.17. As shown in the figure, the MIPs (RKM1 and RKM2) showed selectivity towards

methyl p-toluenesulfonate over 21-chlorodiflorasone. For example, RKM2 displayed 44 % binding for methyl p-toluenesulfonate with imprinting effect.

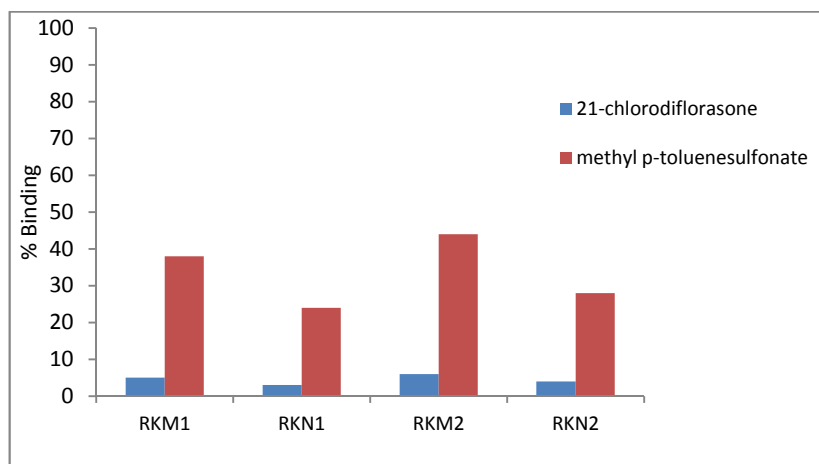


Figure 5.17: Binding of 5 µg/mL methyl p-toluenesulfonate in the presence of 500 µg/mL 21-chlorodiflorasone in isopropanol to tosylate MIPs & NIPs

After these results, commercially available reactive scavengers for the removal of methyl p-toluenesulfonate from pharmaceutical compounds were evaluated with the aim to achieve higher levels of impurity removal.

5.1.6 Properties of the studied reactive resins

The scavengers that were evaluated in this study were either based on cross-linked polystyrene-divinylbenzene or porous silica. The majority of the polymeric scavenger resins were low cross-linked, i.e, with a cross-linking degree of around 1-2 %. **PS** refers to these lightly cross-linked polystyrene resins. Lightly cross-linked polystyrene resins are gel-type and normally require the use of solvents that will swell the resin to allow the target compounds to access the reactive functional groups coupled to the resin.

Another type of resins referred to as **MP** are highly cross-linked, macroporous polystyrene resins. The swelling ratio of highly cross-linked macroporous resins is considerably lower than for PS-based resins and scavenging efficiency is not dependent on the swelling of the resins. Instead, target compounds diffuse through the macropores of the resin to reach the reactive functional groups coupled to the resin.

SEM images of PS based scavengers are shown in Figure 5.18. As can be seen from the figure gel-type PS scavengers are spherical particles in the size range 75-150 μm .

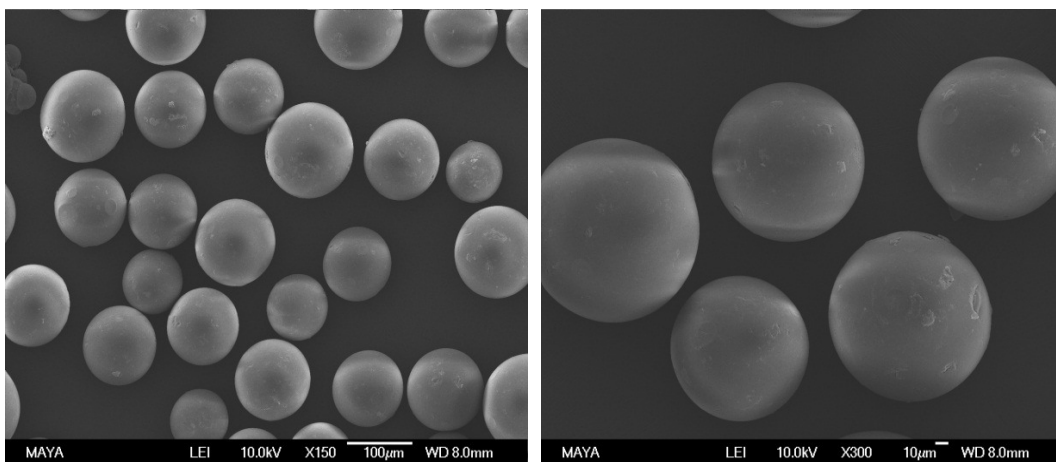


Figure 5.18: SEM images of gel-type polystyrene scavengers as used in this study

Figure 5.19 shows the SEM images of macro-porous polystyrene scavengers. The scavengers are spherical in the size range 150-250 μm . Although this material has relatively large pores, they are not visible under this magnification.

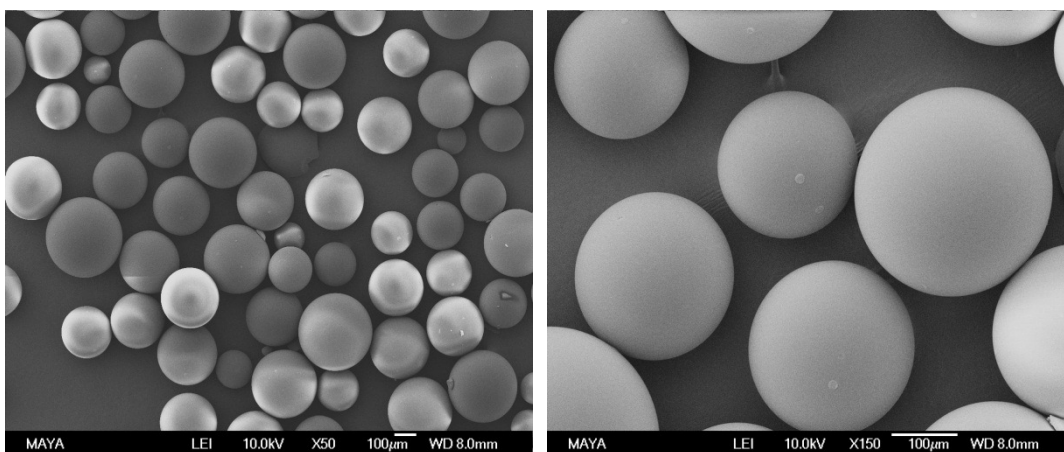


Figure 5.19: SEM images of macroporous polystyrene scavengers as used in this study

In Figure 5.20, SEM images of silica based scavengers are shown. As can be seen from the image, the silica particles are irregular in the size range 30-90 μm .

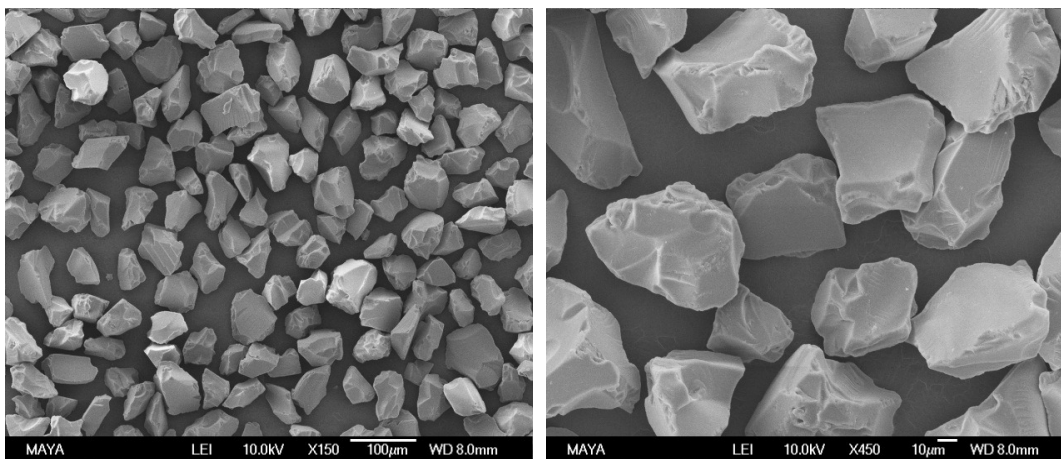


Figure 5.20: SEM images of silica based scavengers as used in this study

The properties of the reactive resins used in this study are as follows:

PS-Amine and PS-Trisamine functionalized with aminomethyl group and tris-(2-aminoethyl) amino groups, respectively, are typically used for scavenging of electrophiles such as acid chlorides, sulfonyl chlorides and isocyanates. Booth and Hodges prepared PS based resins functionalized with derivatives of tris(2-aminoethyl) amine and used them for the selective removal of excess reagents from reaction mixtures. ^[168]

PS-Tosylhydrazine functionalized with toluene sulfonyl hydrazine groups has the ability to react with aldehydes and ketones. Removal of these compounds from reaction mixtures generally requires an excess of the resin. Emerson et al. reported the use of this type of resin for scavenging of various aldehydes and ketones. ^[169]

PS-Thiophenol is equipped with thiophenol functionalities. The resin was developed for effective removal of alkylating agents such as alkyl halides.

MP-Trisamine and MP-TMT are porous scavenger resins with a high degree of cross-linking and have been functionalized with multifunctional amino and trimercaptotriazine groups, respectively.

MP-TMT is mainly intended for the scavenging of palladium from palladium catalyzed reactions. Metal catalyzed reactions are commonly used in the production of active pharmaceutical ingredients (APIs) and the removal of trace palladium impurities during the production process in the purification of final product is a crucial task in the pharmaceutical industry. Welch et al. ^[170] used various scavengers including MP-TMT for metal impurity removal from pharmaceutical compounds. In that work, MP-TMT displayed the highest selectivity for removal of palladium.

The following scavenging materials are based on silica: Si-Tosylhydrazine, a silica supported equivalent of p-toluenesulfonyl hydrazine, Si-Trisamine, a silica bound tris (2-aminoethyl) amine, Si-Thiol a silica bound 1-propanethiol and Si-Triamine, a silica bound diethylene triamine.

The structures and properties of the scavengers used in this part of this work are summarized in Table 5.6 and Table 5.7.

Table 5.6: Structures of the scavengers used in this study

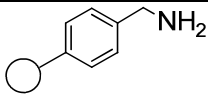
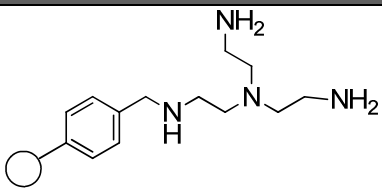
Scavenger	Schematic structure
PS-Amine	
PS-Trisamine MP-Trisamine	

Table 5.6 continues on the next page

Continuation of Table 5.6 from the previous page

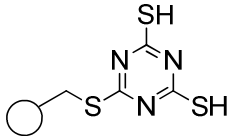
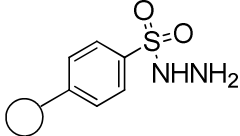
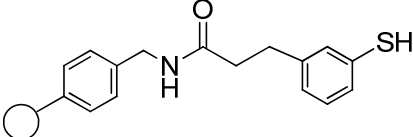
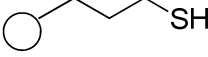
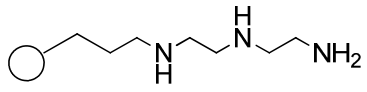
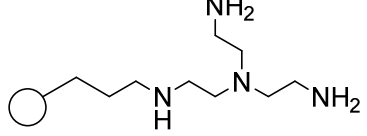
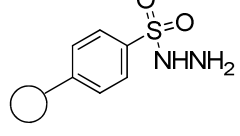
<p>MP-TMT</p>	
<p>PS-Tosylhydrazine</p>	
<p>PS-Thiophenol</p>	
<p>Si-Thiol</p>	
<p>Si-Triamine</p>	
<p>Si-Trisamine</p>	
<p>Si-Tosylhydrazine</p>	

Table 5.7: Properties of the scavengers used in this study

Scavenger	Bead size (μm)	Surface area (m ² /g)	Pore volume (ml/g)	Pore diameter (nm)	Typical capacity (mmol/g)
PS-Amine**	75-150	---	---	---	1.5
PS-Tosylhydrazine**		---	---	---	1.8 – 3.2
PS-Trisamine**		---	---	---	3-5
PS-Thiophenol**		---	---	---	1.5
MP-TMT	150-250	190	0.55	15	0.9
MP-Trisamine					2.13
Si-Trisamine	30-90	500	0.78	5.3	1.2 – 2.1
Si-Tosylhydrazine					0.6 – 1.1
Si-Triamine					2.2 – 2.4
Si-Thiol					1.3

** BET analyses are carried out at dry state. Low cross-linked polystyrene (PS) based resins are gel-type and virtually non-porous in the dry state.

As can be seen in the table, MP based scavengers are macroporous and the surface area is around 190 m²/g. PS scavengers are gel type materials and are virtually non-porous in the dry state. The silica particles have a surface area of around 500 m²/g.

5.1.7 Scavenging behavior of the reactive resins

In this Section, experiments evaluating the performance of modified polystyrene and silica based scavengers in organic media in the removal of methyl p-toluenesulfonate from API solutions were conducted. The removal was done in the presence of the API 21-chlorodiflorasone. It should be noted that 21-

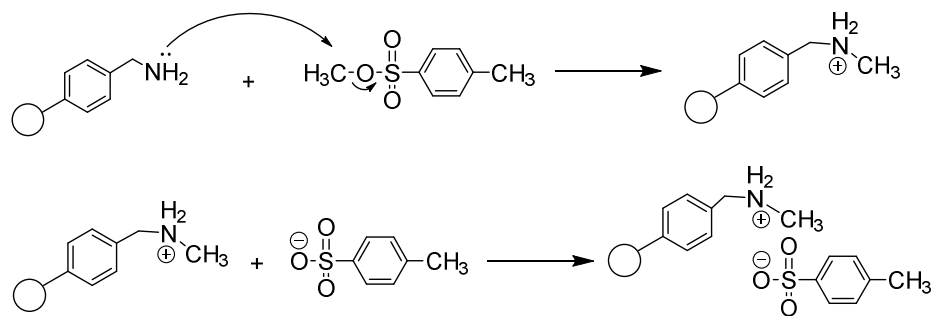
chlorodiflorasone is used here as a model compound and that there are no publications available that report contamination issues involving this API.

The use of reactive resins has recently been investigated by Lee et al. [23] for the removal of various sulfonate esters from model APIs using esters of methanesulfonic acid (MSA), benzenesulfonic acid (BSA) and *p*-toluenesulfonic acid (pTSA) as a model electrophilic GTIs. Several nucleophilic resins were used for removal of these GTIs from model APIs and polymer bound ethylenediamine resin displayed virtually complete removal of methyl *p*-toluenesulfonate in MeOH after 90 min at 40 °C. In contrast to the obtained results for methyl *p*-toluenesulfonate, the ethyl and isopropyl esters were only partially removed. Lee et al. noted that their protocol should not be used for APIs containing certain reactive groups which may interact with the reactive scavenging resins used in their study.

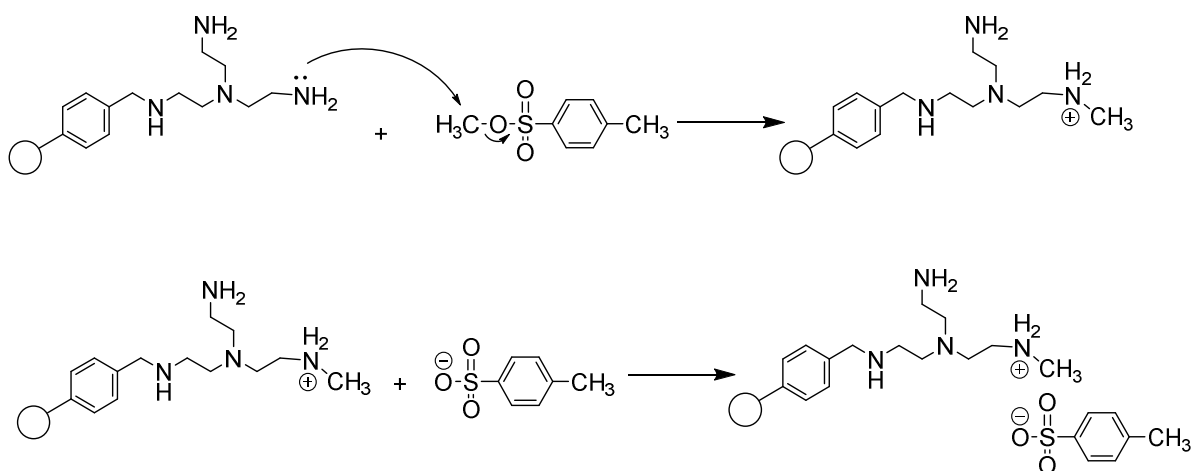
In the present work, a variety of silica and polystyrene based resins have been tested for the removal of methyl *p*-toluenesulfonate in the presence of a model API at room temperature.

The removal of methyl *p*-toluenesulfonate using the reactive scavengers is based on a chemical reaction between the nucleophilic group of the scavenger and the electrophilic group of methyl *p*-toluenesulfonate, as shown in Schemes 5.3 to 5.9. The amine or thiol group on the scavengers reacts first as a nucleophile, attacking the electrophilic center of methyl *p*-toluenesulfonate, CH₃. Cleavage of the C-O bond occurs and allows the departure of the tosylate anion, a good leaving group.

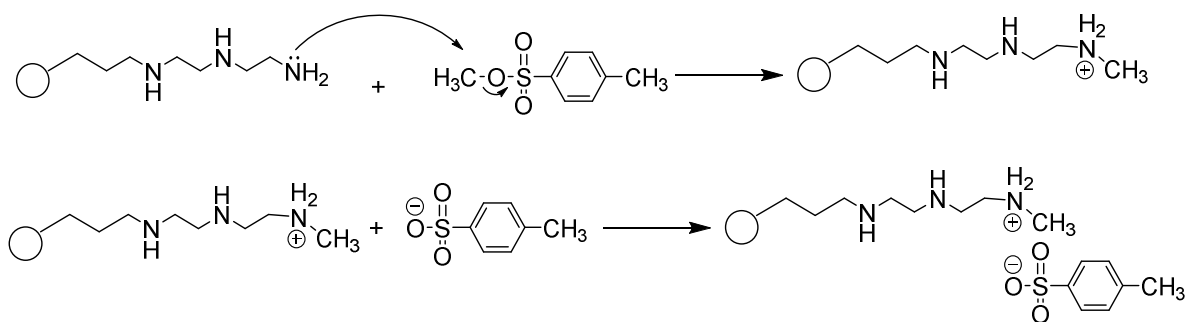
After the scavenging reaction, amine-based scavengers are able to also act as an ion-exchanger and bind the *p*-toluenesulfonic acid generated in the reaction. However, the *p*-toluenesulfonic acid generated in the scavenging reaction remains in the reaction media when thiol-based scavengers are used.



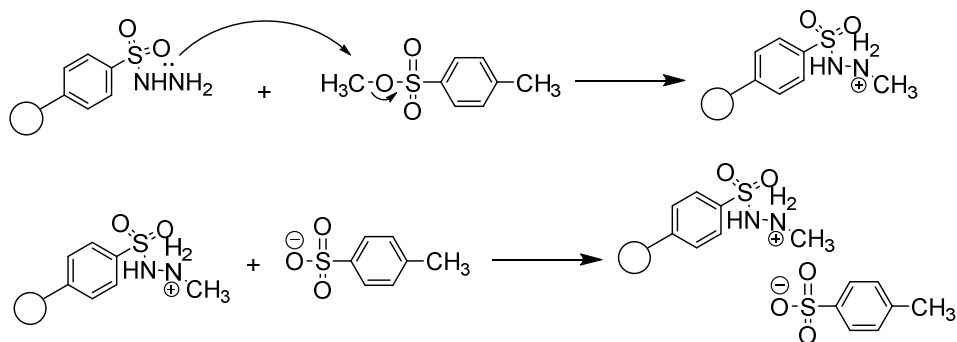
Scheme 5.3: Scavenging mechanism for the removal of methyl p-toluenesulfonate using amine modified scavengers



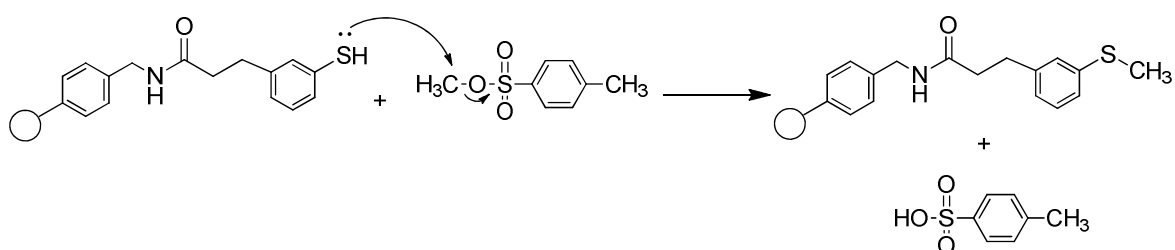
Scheme 5.4: Scavenging mechanism for the removal of methyl p-toluenesulfonate using triamine modified scavengers



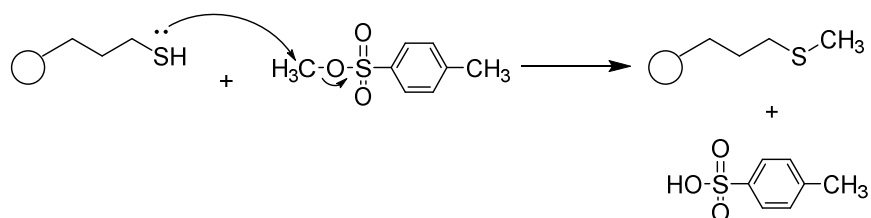
Scheme 5.5: Scavenging mechanism for the removal of methyl p-toluenesulfonate using triamine modified scavengers



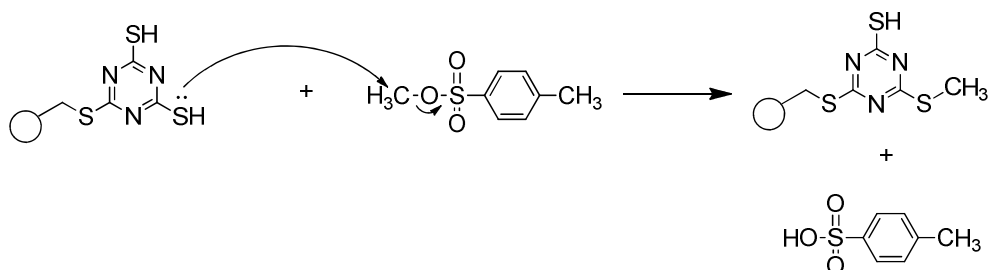
Scheme 5.6: Scavenging mechanism for the removal of methyl p-toluenesulfonate using tosylhydrazine modified scavengers



Scheme 5.7: Scavenging mechanism for the removal of methyl p-toluenesulfonate using thiophenol modified scavengers



Scheme 5.8: Scavenging mechanism for the removal of methyl p-toluenesulfonate using thiol modified scavengers



Scheme 5.9: Scavenging mechanism for the removal of methyl p-toluenesulfonate using trimercaptotriazine modified scavengers

Initially, the experiments were conducted in flow-through mode. It was the intention that the model solution of GTI and API should have a large difference in concentration between those two compounds to reflect a typical case and a ratio of 1:100 was used in the study.

The results of the flow-through scavenging experiments of methyl p-toluenesulfonate from 2-propanol in the presence of 21-chlorodiflorasone using modified polystyrene and silica based scavengers are shown in Figure 5.21.

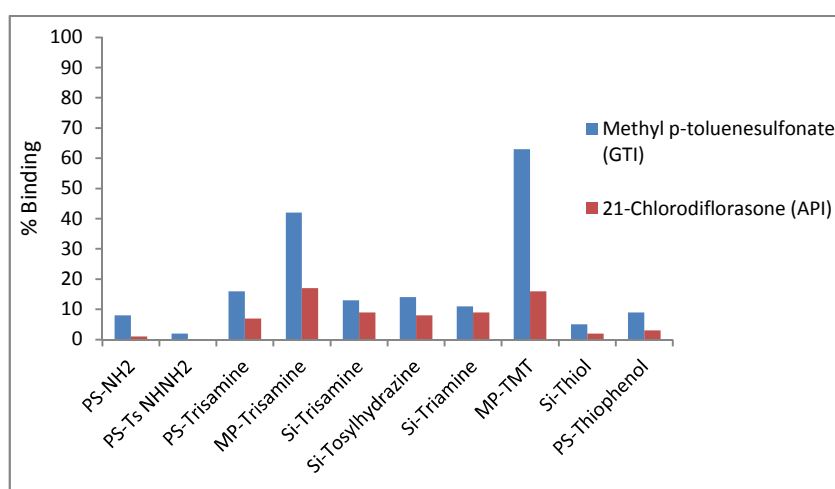


Figure 5.21: Results of flow through scavenging of 5 $\mu\text{g/mL}$ of methyl p-toluenesulfonate in the presence of 500 $\mu\text{g/mL}$ of 21-chlorodiflorasone in 2-propanol using the scavengers

The best results were obtained with trimercaptotriazine (TMT) modified macroporous polystyrene and trisamine modified macroporous polystyrene resins which showed 63 % and 42 % methyl p-toluenesulfonate removal along with 16 % and 17 % loss of 21-chlorodiflorasone in 2-propanol, respectively.

The scavenging was lower than expected; it was expected that GTI at such a low concentration (5 μg) corresponding to only 37 nmol compared to 670 μmol of potential capacity of the MP Trisamine resin would be well removed. One potential reason is the short interaction time in the SPE resin bed between analyte and resin which may have reduced the effectiveness of the scavenging of the GTI.

Based on a flow rate of 0.5 mL/min of the solution through the packed bed in the SPE column, the residence time was estimated to be around 2 min for the various resins. This interaction time may be too short for the scavenging process.

Consequently, batch scavenging experiments of methyl p-toluenesulfonate in the presence of 21-chlorodiflorasone with longer reaction time using modified polystyrene and silica based scavengers were carried out. In the experiments, each scavenger was placed in HPLC vials and a solution of methyl p-toluenesulfonate and 21-chlorodiflorasone in 2-propanol was added. Again, the relative concentration of API and GTI aimed to reflect the industrial scenarios where the API is highly concentrated and the GTI is present in lower concentration and as discussed above, the concentration ratio of API to GTI was set to 100. The suspension mixtures were analyzed by HPLC. The results of these experiments are shown in Figure 5.22.

Trisamine, triamine and trimercaptotriazine modified scavengers showed high removal of methyl p-toluenesulfonate. Si-Trisamine and MP-Trisamine lead to complete methyl p-toluenesulfonate removal with 11 % and 22 % loss of 21-chlorodiflorasone, respectively. Trimercaptotriazine modified macroporous polystyrene scavenger on the other hand also resulted in complete methyl p-toluenesulfonate removal but 96 % of 21-chlorodiflorasone was also removed. This undesired API binding to MP-TMT was likely due to the reaction between the nucleophilic scavenger and electrophilic groups of the API. This covalent capture was later confirmed as the API could not be removed from this scavenger with a washing step. Based on the various moieties on the API, several undesired covalent reactions of MP-TMT with 21-chlorodiflorasone can be envisaged. For example nucleophilic substitution reactions between the thiol groups of the reactive scavenger and the chlorine group of the API can occur. Likewise, nucleophilic conjugate additions of the thiol groups of the reactive scavenger to one of the double bonds in the API may be also possible.

For the PS-based scavengers, there was a relationship between the scavenging efficiency and the type of ligand on the scavenging resin. ie, single amine scavengers, such as PS-Amine have a lower capacity (1.5 mmol/g) and perform

worse than multiple amine scavengers such as PS-Trisamine and MP-Trisamine (~ 4 mmol/g). The scavenging levels were much higher with the high capacity resins compared to the low capacity resins. The capacities of the resins used in these experiments were summarized in Table 5.7.

The most selective scavenging was obtained with Si-Trisamine which removes 100 % of methyl p-toluenesulfonate and 11 % of 21-chlorodiflorasone in 2-propanol. MP-Trisamine also displays a quantitative level of GTI removal but has a slightly higher binding of the API (21 %) under these conditions. The scavenging efficiency was correlated to the reported capacities and also to surface area. However, PS-Trisamine with a capacity of around 4 mmol/g scavenged less GTI than MP-Trisamine that had a capacity of around 2 mmol/g. In this comparison, the permanent porous structure of the MP resins seems more advantageous for GTI scavenging than the gel-type PS resin. On the other hand, silica-based scavengers have more than twice the surface area than MP resins, but are equal in GTI removal. Also, despite the larger surface area, their undesired non-specific binding to the API was lower. Hence, several factors such as morphology and surface chemistry properties of a material govern both scavenging efficiency and selectivity of a given GTI – API pair.

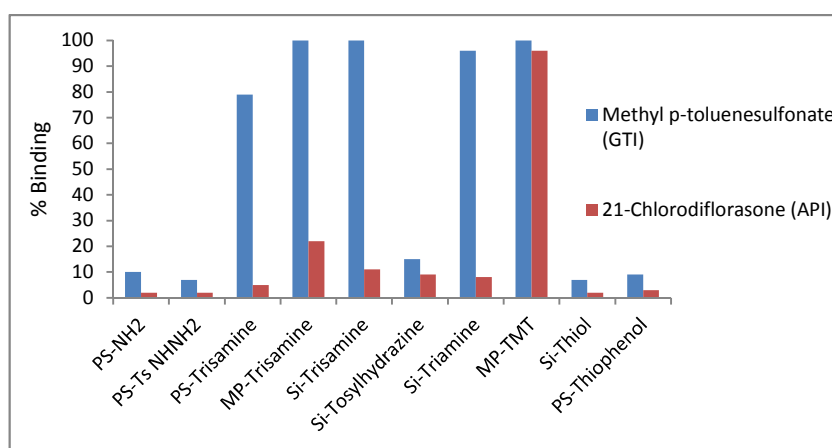


Figure 5.22: Results of batch scavenging of 5 $\mu\text{g/mL}$ of methyl p-toluenesulfonate in the presence of 500 $\mu\text{g/mL}$ of 21-chlorodiflorasone in 2-propanol using the scavengers

Time-course studies of the removal of methyl p-toluenesulfonate using MP-Trisamine, Si-Trisamine, PS-Trisamine and MP-TMT scavengers were then

conducted. In the experiments, a solution of methyl p-toluenesulfonate and 21-chlorodiflorasone in 2-propanol was added to the scavenger resin and aliquots from the sample were taken at different times and analyzed by HPLC

As shown in Figure 5.23, MP-TMT reacts with methyl p-toluenesulfonate very rapidly and removes 78 % within 5 min. After 30 min, 100 % methyl p-toluenesulfonate was removed using MP-TMT. MP-Trisamine required 90 min for complete removal while the other scavengers required even longer times.

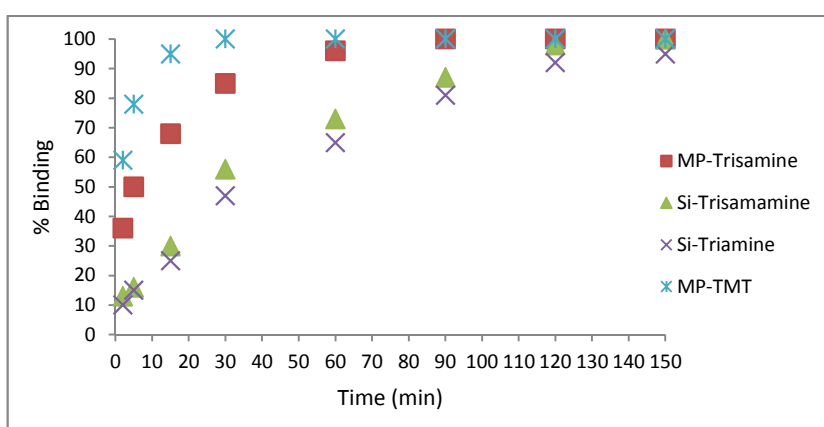


Figure 5.23: Results of kinetic study for 5 $\mu\text{g/mL}$ of methyl p-toluenesulfonate scavenging in 2-propanol

Although not advantageous for this present application, it was observed that use of the scavengers also removed the active pharmaceutical compound.

The kinetics of the undesired scavenging of 21-chlorodiflorasone was therefore examined further. As shown in Figure 5.24, MP-Trisamine, Si-Trisamine and Si-Triamine reach equilibrium after 60 min and bind only a minor proportion of the API while MP-TMT is slower in its scavenging action but goes to completion and removes most of the API.

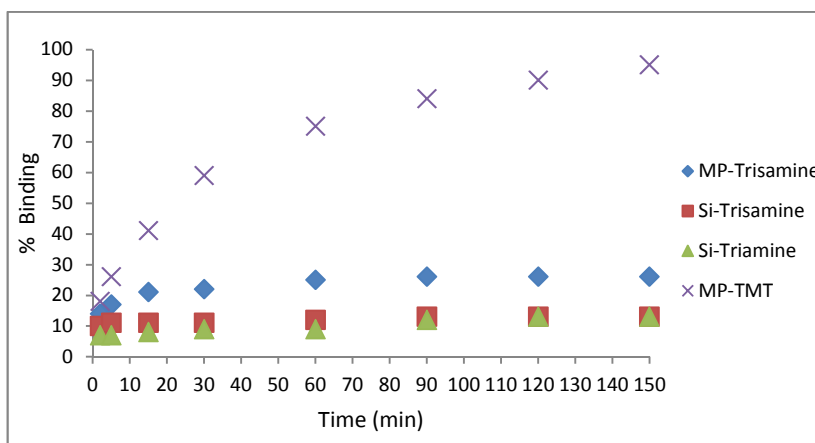


Figure 5.24: Results of the kinetic study for 500 $\mu\text{g/mL}$ of undesired 21-chlorodiflorasone scavenging in 2-propanol

In order to increase API yields, any non-specifically adsorbed API to the scavenger has to be washed off again and pooled with the rest of the API eluate. First, a wash solution was designed to release bound API. 2-propanol with THF as a co-solvent was thought to compete with adsorption to the styrene-based scavenger backbone. Hence, the release of bound API from scavengers was attempted using 2-propanol: tetrahydrofuran (1:1) in equal proportions. After 30 min, 100 % API recovery from the resins MP-Trisamine, Si-Trisamine and Si-Triamine was obtained while, on the other hand, the API was not released from MP-TMT. This shows that a scavenging reaction had occurred between MP-TMT and the API 21-chlorodiflorasone while the API was just bound to the other scavengers by adsorption to the surface.

The kinetics for methyl p-toluenesulfonate (GTI) and 21-chlorodiflorasone (API) removal using the MP-TMT resin are compared in Figure 5.25. As seen from the figure, scavenging is quite rapid for both GTI and API. Hence, while effective for methyl p-toluenesulfonate removal, this scavenger cannot be used in the presence of this particular API. However, for other APIs with which MP-TMT does not react, GTI removal could be very promising application area for this scavenger resin in addition to palladium scavenging

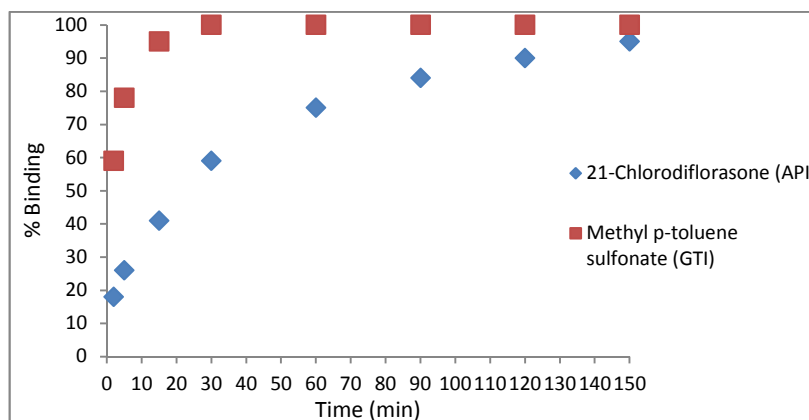


Figure 5.25: Results of the kinetic study for 5 $\mu\text{g/mL}$ of methyl p-toluenesulfonate and 500 $\mu\text{g/mL}$ of 21-chlorodiflorasone in 2-propanol using MP-TMT resin

The capacity is an important characteristic of a resin and important for production process economics. It is obvious that the more compound that can be processed on a given amount of scavenger, the lower the process costs are both in terms of costs to purchase a given amount of adsorbent and also the number of runs required to complete a given separation task.

In order to determine the capacity, the scavenging experiment was repeated with different amounts of the best scavengers. Different amounts of scavengers were put into HPLC vials and a solution of methyl p-toluenesulfonate and 21-chlorodiflorasone in 2-propanol was added. After 2 h, the aliquots of the clear supernatant were taken and assayed by HPLC. The outcome of this experiment is plotted in a binding graph, where the various scavengers can be compared with each other.

As shown in Figure 5.26, MP-Trisamine displays the most efficient scavenging behavior and 75 mg of MP-Trisamine scavenger is sufficient for complete removal of 5 $\mu\text{g/mL}$ of methyl p-toluenesulfonate in 1 mL solution within 120 min. On the other hand, at least 250 mg of Si-Trisamine and Si-Triamine is needed for complete scavenging of methyl p-toluenesulfonate. At large scale this difference of adsorbent required is very significant and MP-Trisamine would be by far the most economical solution.

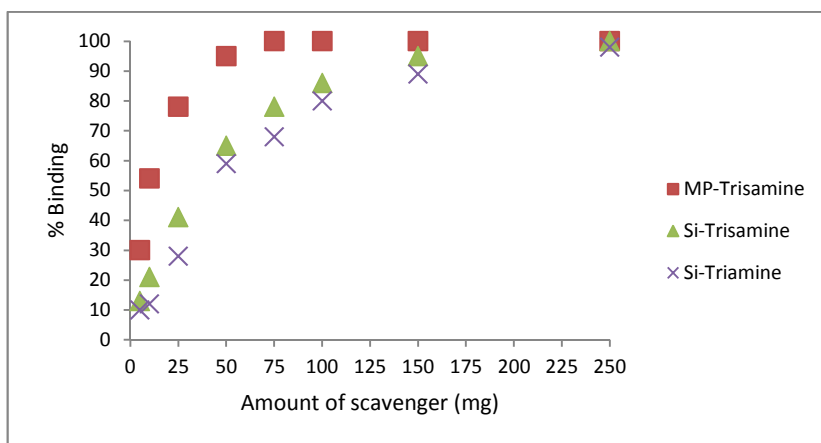


Figure 5.26: Results of batch scavenging of 5 µg/mL of methyl *p*-toluenesulfonate in 2-propanol with different amounts of scavengers

As mentioned before, after the scavenging reaction with methyl *p*-toluenesulfonate, the amine-based scavengers are expected to have the ability to function as ion-exchangers and bind the *p*-toluenesulfonic acid generated in the reaction. The amount of *p*-toluenesulfonic acid was monitored in the reaction medium after scavenging of methyl *p*-toluenesulfonate, but no *p*-toluenesulfonic acid was detected. The ion-exchange capture was confirmed, when it was found to be possible to release *p*-toluenesulfonic acid in an elution step using 5 % NH₃ in IPA:THF (1:1) where after 30 min, 92 % *p*-toluenesulfonic acid could be recovered from the MP-Trisamine resin. This result proves the scavenging mechanisms shown in Schemes 5.3 to 5.6 including that the scavengers behave additionally as ion exchangers and can quantitatively bind the *p*-toluenesulfonic acid formed in the scavenging reaction. This ion exchange property of these resins further simplifies the purification result of such clean-up processes.

5.1.8 Comparison of MIPs and reactive resins for GTI removal

Comparative experiments were carried out in batch mode using small HPLC vials containing resin and GTI and API dissolved in IPA, MeCN or DCM. These suspensions were stirred for 24 h, then they were allowed to settle for 2 min and aliquots of 100 µL were taken and analyzed by HPLC.

The outcome of the comparison experiments is shown in Figure 5.27. As seen from the figure, for all solvent systems, MP-Trisamine and the silica based resin

Si-Trisamine gave almost complete removal of methyl p-toluenesulfonate. Regarding the undesired API adsorption, MP-Trisamine displayed a similar level of adsorption, in all the solvents and the non-specific binding of MP-Trisamine, varies between 20 %, 18 % and 15 % in IPA, MeCN and DCM, respectively.

Silica-based scavengers have much higher surface areas than MP-based resin (Table 5.7), but both are almost equal in GTI removal. But despite the differences of their surface area, undesired non-specific binding of the API to silica based scavenger was lower. Hence, several factors such as morphology and surface chemistry properties of a material govern both scavenging performance and selectivity of a given GTI and its corresponding API.

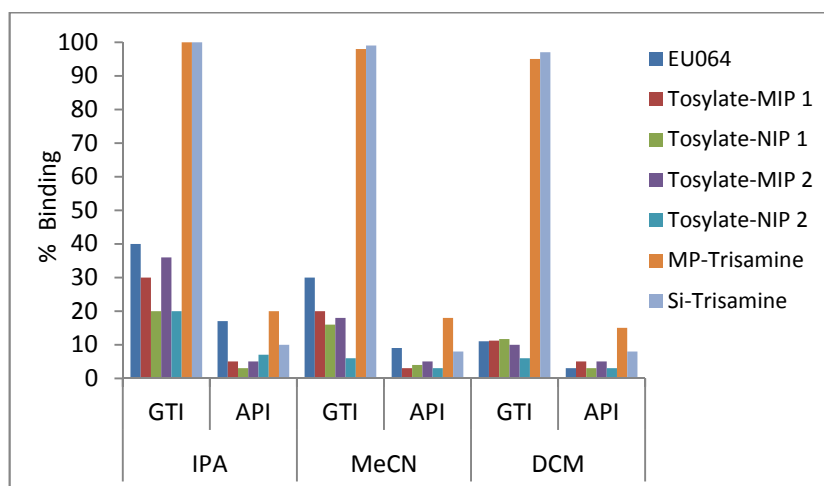


Figure 5.27: Binding of 5 $\mu\text{g/mL}$ of methyl p-toluenesulfonate and 500 $\mu\text{g/mL}$ of 21-chlorodiflorasone by the polymers and reactive resins in various solvents

Compared to the scavengers, the MIPs and NIPs have poor performance in their current state and are probably insufficient for industrial applications and need further material improvement to be competitive for such applications. For example, increasing the pore area and number of active sites may increase the capacity of the MIPs. However, MIPs may have an advantage, where a higher selectivity is required or where the GTI and the API are very similar in structure and chemistry. Scavengers are effective in their action, but are cruder in their selectivity. Scavengers are already used in organic chemistry clean-up in industry,

and MIPs are used in various analytical and preparative clean-up steps, but both material categories will serve their application niches depending on the nature of the clean-up task.

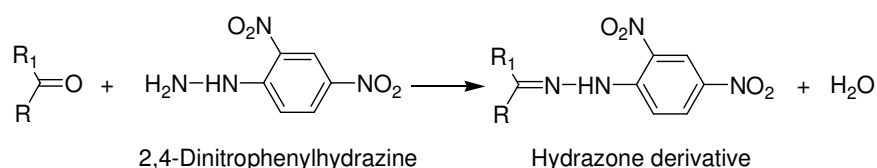
From the comparison experiments it can be concluded that the removal of methyl p-toluenesulfonate from 21-chlorodiflorasone was shown to be most effective using trisamine modified macroporous polystyrene and silica supported trisamine scavengers which give almost complete removal of GTI in IPA, MeCN and DCM with only low concomitant loss of API.

5.2 Removal of acrolein from APIs using designed MIPs and aldehyde scavengers

5.2.1 Analysis of acrolein

Low molecular weight aldehydes are highly volatile and the analysis of these compounds is difficult by HPLC. Many of those compounds do not contain chromophores and can therefore not be detected by UV. Due to the reactive carbonyl group present in those low molecular weight aldehydes and ketones, they can however easily be derivatized with a derivatization agent such as 2,4-dinitrophenylhydrazine (DNPH). Reaction of DNPH with the carbonyl group of acrolein in an acidic solution leads to formation of stable hydrazones containing dinitrophenyl groups which are UV absorbing and can thus easily be detected by HPLC-UV.

In Scheme 5.10, the derivatization reaction of DNPH with an aldehyde or ketone is given.



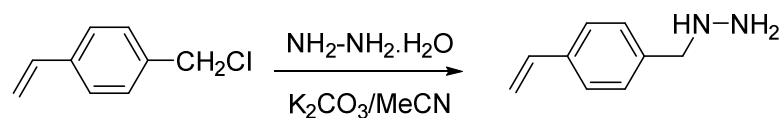
Scheme 5.10: Derivatization reaction of an aldehyde or ketone with DNPH

Derivatization of acrolein with DNPH was carried out according to a published procedure^[156] as described in Section 4.1.1.

5.2.2 Synthesis of functional monomer for acrolein MIPs

Covalent imprinting via hydrazine formation was chosen as the most appropriate technique for MIP towards acrolein. Suitable monomer used in this study is currently not commercially available and thus, a polymerizable vinylbenzyl hydrazine monomer was synthesized according to a published procedure^[160] prior to polymer preparation.

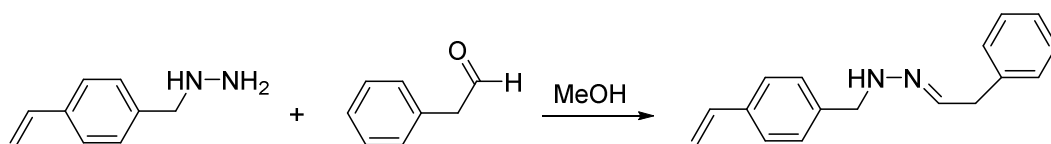
4-Vinylbenzyl chloride and potassium carbonate was added to a solution of hydrazine monohydrate in acetonitrile. After completed reaction, the crude product was purified by silica gel column chromatography using dichloromethane as eluent. The reaction scheme is given in Scheme 5.11.



Scheme 5.11: Synthesis of the vinylbenzyl hydrazine monomer

After vinylbenzyl hydrazine synthesis, the synthesis of the Schiff base with phenyl acetaldehyde was carried out.

Phenyl acetaldehyde was dissolved in methanol and an equimolar amount of vinylbenzyl hydrazine was added to the solution. The reaction was complete after the reaction had been refluxed overnight. Then, the solvent was evaporated and the product was purified by silica gel column chromatography using dichloromethane as the eluent. The reaction scheme is given in Scheme 5.12.



Scheme 5.12: Synthesis of the Schiff base construct used in the preparation of acrolein MIPs

5.2.3 Synthesis of MIPs for acrolein

After the monomers had been synthesized in sufficient quantities, a total of four different imprinted and non-imprinted polymers were prepared towards acrolein. Two different cross-linking monomers, DVB and EDMA were used. The polymers were prepared in the following procedure.

The synthesized monomer was dissolved in chloroform and then DVB or EDMA was added to the solution. After polymerization, cleavage of the N-N bound was carried out with acidified methanol mixture under reflux.

The composition of the polymers for acrolein is given in Table 5.8.

Table 5.8: Composition of the polymers for acrolein

Polymer	Composition	Stoichiometry [mmol]	Porogen	Volume [ml]	Method
MIP I	Schiff Base	0.1	Chloroform	7.5	ABDV 40/60 °C **
	DVB	2			
MIP II	Schiff Base	0.1	Chloroform	7.5	ABDV 40/60 °C **
	EDMA	2			
NIP I	Vinylbenzyl hydrazine	0.1	Chloroform	7.5	ABDV 40/60 °C **
	DVB	2			
NIP II	Vinylbenzyl hydrazine	0.1	Chloroform	7.5	ABDV 40/60 °C **
	EDMA	2			

** The polymerization is started at lower temperature, 40 °C, for 12 h to maximize the interaction between monomer and template and the temperature is then increased to 60 °C for complete polymerization (curing step).

The synthesized polymers were characterized by BET to estimate surface area, pore volume and pore diameter of the synthesized polymers, light scattering for the particle size distribution and finally the shape was characterized by microscopy. FTIR analysis of the polymer was also carried out to verify the molecular structure.

The FT-IR spectra of the imprinted polymers for acrolein are shown in Figures 5.28 and 5.29. In the FT-IR spectra of the DVB based polymer shown in Figure 5.28, the absorption bands due to aliphatic C-H stretching ($\sim 2922\text{ cm}^{-1}$) and aromatic C=C ($\sim 1511\text{ cm}^{-1}$) from the cross-linker DVB were observed.

As seen from the Figure 5.28 which shows the FT-IR spectra of EDMA based polymers, the absorption bands due to carbonyl stretching ($\sim 1719\text{ cm}^{-1}$) from the cross-linker EDMA and C-H stretching ($\sim 2955\text{ cm}^{-1}$) were observed.

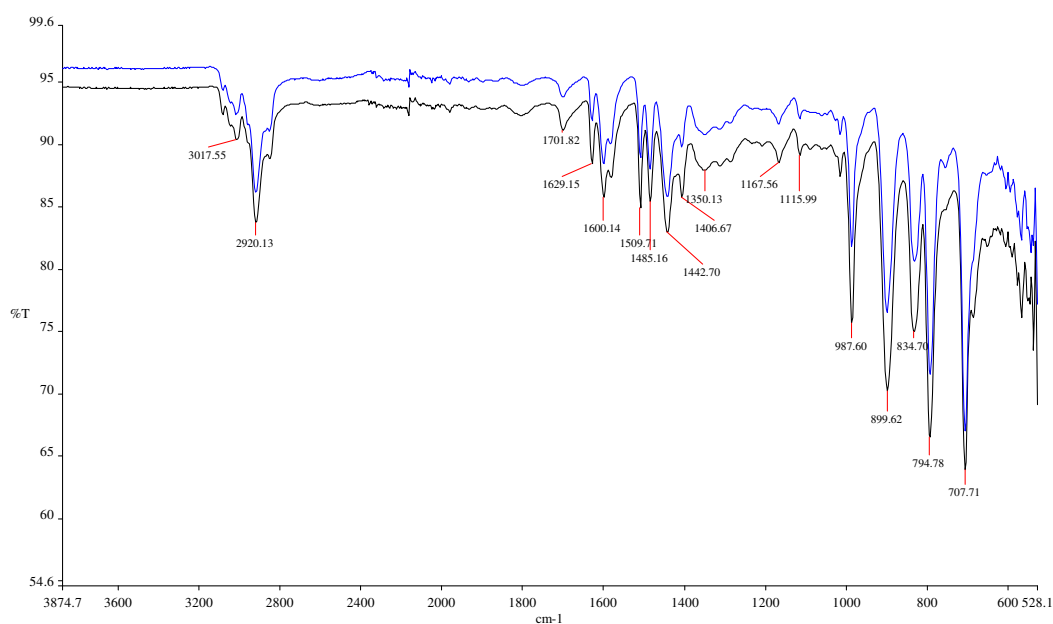


Figure 5.28: FT-IR spectra of MIP1 (blue) and NIP 1 (black)

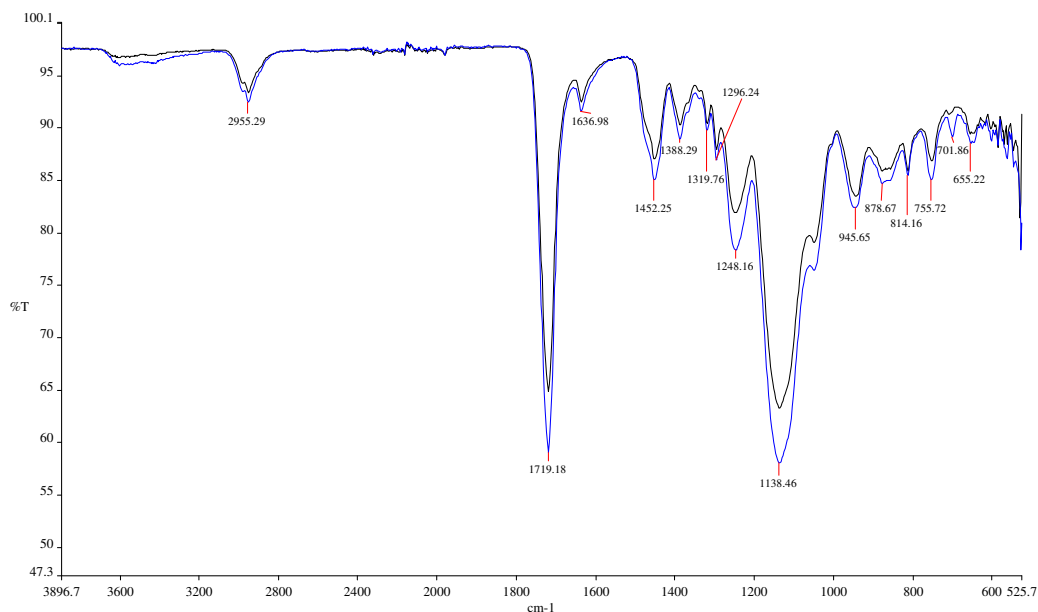


Figure 5.29: FT-IR spectra of MIP 2 (blue) and NIP 2 (black)

An optical microscope image of the acrolein MIP after grinding and sieving is shown in Figure 5.30. As seen in the figure, the imprinted polymer particles are irregular in the size range of 25-36 μm .

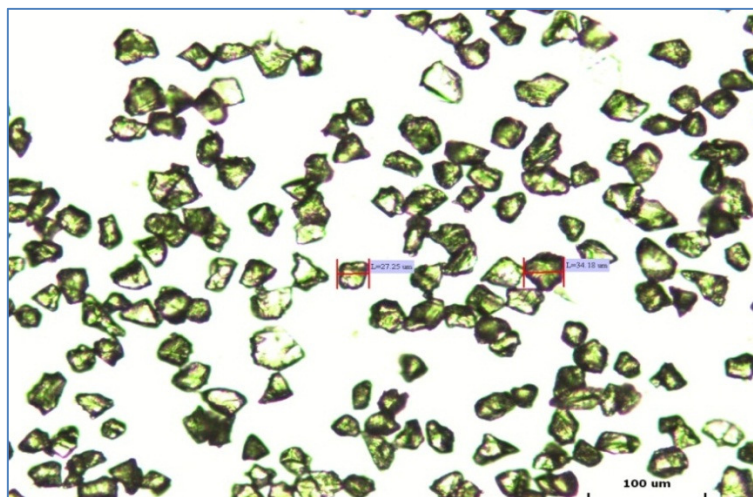


Figure 5.30: Optical microscope image of MIP 1 for acrolein (100 x magnification)

The light scattering measurement is shown in Figure 5.31. The median of the particle size distribution is 40 μm while this value should be between 25-36 μm as the particles were sieved to this particle size distribution. This slightly larger

median of the particle size distribution may be caused by aggregation of the particles.

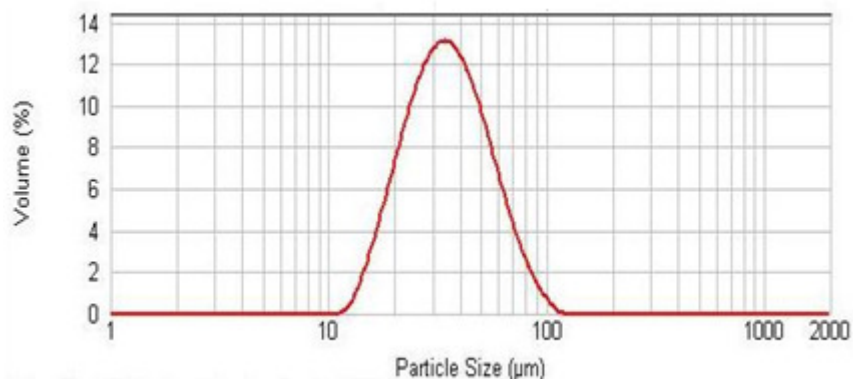


Figure 5.31: Particle size distribution of MIP 1 towards acrolein by laser diffraction technology which is based on the fact that all particles that pass through a laser beam will scatter the light, and the angle of the scattered light is directly related to the particle size

Table 5.9 shows the BET results for the synthesized polymers. As seen from the table, NIP 1, MIP 2 and NIP 2 have almost no surface area and pore volume.

Considering the BET results, this polymerization seems to not be as expected. Typically, MIPs and NIPs have pore volumes of at least 0.25 ml/g and surface area of a few 100 m²/g. Here, it appears that the polymer recipe with a new type of hydrazine monomer does not lead to macroporous polymers except in the case of MIP 1. The imprinting principle is different here than the standard non-covalent imprinting approaches as here, the imprinting step is done by covalent interactions. It is also not clear how the reactive hydrazine monomer behaves during the radical polymerization process and it may be that hydrazine interferes with the polymerization process and thus prohibits complete polymerization. Thus the polymer cross-linking degree may be low and the polymer might be only a gel-type material. As discussed previously for the scavengers, gel-type polymers are non-porous and have negligible surface area, but can work if they can swell appropriately and reveal the interaction capability.

Table 5.9: BET results for the polymers towards acrolein

Polymer	Surface Area (m ² /g)	Pore Volume (ml/g)	Pore Diameter (nm)
MIP 1	720	0.9	9.3
NIP 1	5	0.01	-
MIP 2	1.5	0.002	-
NIP 2	1	0.005	-

In order to evaluate the swelling behavior of the polymers towards acrolein, swelling tests were performed in the solvents MeCN, THF and EtOH which is used in the binding experiments. Volume swelling ratios of the MIPs and NIPs are shown in Table 5.10. As can be seen from the table, imprinted polymer RKM2 and its counterpart non-imprinted polymer RKN2 displayed higher swelling in MeCN, EtOH and THF. Also the non-imprinted polymer RKN1 displayed higher swelling than imprinted polymer RKM1 in all solvents.

Table 5.10: Swelling ratios of the MIPs and NIPs

Solvent	RKM1 (MIP)	RKN1 (NIP)	RKM2 (MIP)	RKN2 (NIP)
MeCN	1.5	1.6	1.7	1.7
EtOH	1.6	1.7	1.9	1.8
THF	1.6	1.8	2.0	1.8

5.2.4 Binding behavior of the polymers towards acrolein

The binding of acrolein using those synthesized polymers is based on a reversible covalent interaction forming hydrazone bonds (Schiff bases) between acrolein and the hydrazine monomer as schematically shown in Figure 5.32.

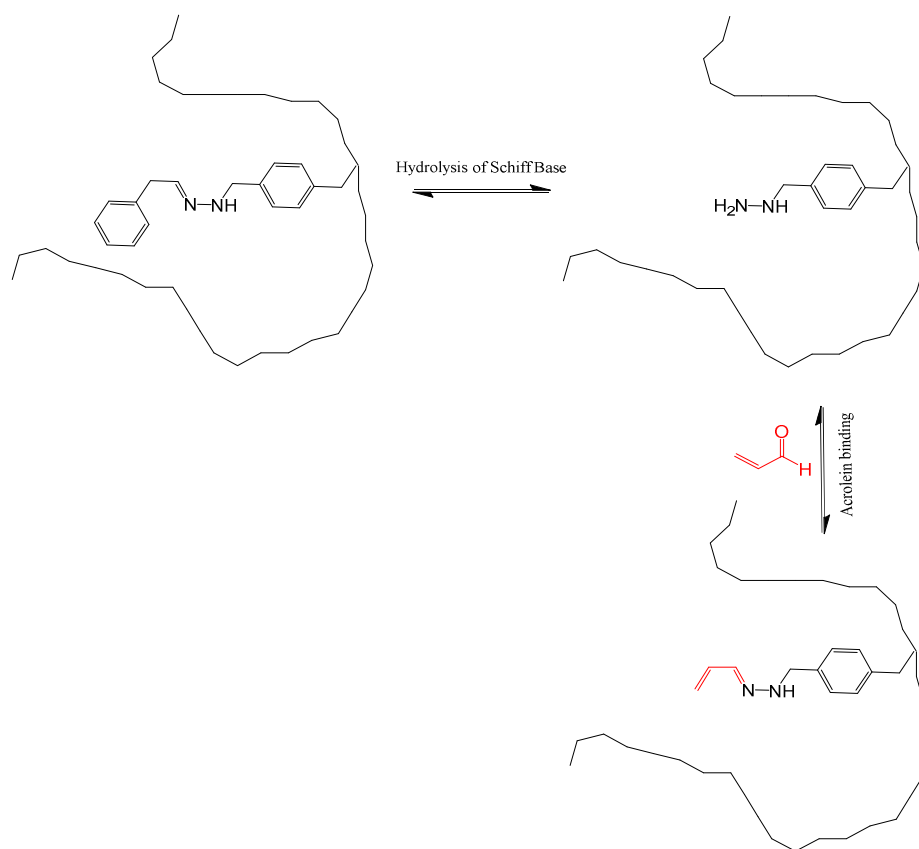


Figure 5.32: Schematic description of acrolein MIP binding cavity. The hydrolysis of the template dummy is shown as well as the binding of acrolein to the cavity

In this part of the study, experiments studying the binding behavior of molecularly imprinted polymers towards acrolein in batch mode were carried out.

Binding experiments were carried out in small HPLC vials contain polymer, GTI and API. This suspension was stirred for 24 h, then allowed to settle for 2 min and aliquots of 100 μ L were taken and analyzed by HPLC.

The results of batch binding of acrolein in EtOH, EtOH:H₂O (1:1) and MeCN are shown in Figure 5.33.

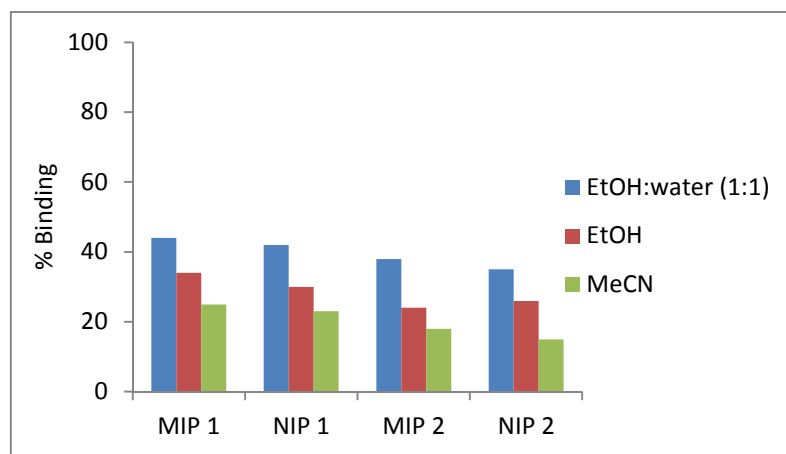


Figure 5.33: Binding of 5 µg/mL of acrolein in EtOH, EtOH:H₂O (1:1) and MeCN to the acrolein MIPs and NIPs.

As seen from the figure, the polymers did not display a high degree of acrolein binding. For example, in EtOH, MIP 1 displayed 34 % binding of acrolein while 30 % acrolein was retained on the non-imprinted polymer NIP 1. When EtOH:H₂O (1:1) was used as a solvent, the level of binding increased. This can be attributed to the fact that the compounds are increasingly adsorbed to the resin by non-specific hydrophobic binding mechanisms. In MeCN, all the polymers displayed less than 25 % binding towards acrolein. Overall, there is no measurable imprinting effect under these conditions.

In order to fully understand the mechanism of the acrolein imprinting and the interaction of free hydrazine in a free radical polymerization environment, further studies have to be conducted. The imprinting efforts described above are a first conceptual study using hydrazine-based interaction modes with aldehydes.

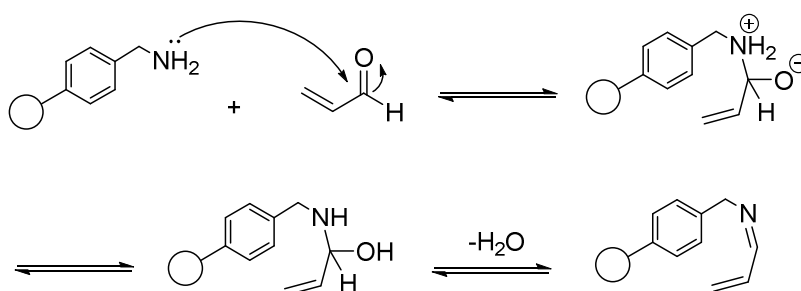
After these preliminary results were obtained with MIPs and NIPs, it was concluded to abandon the imprinting route for this target compound. Instead, commercially available amine-based scavengers were investigated to evaluate the removal of acrolein from pharmaceuticals with the aim to achieve higher levels of GTI removal.

5.2.5 Scavenging behavior of reactive resins

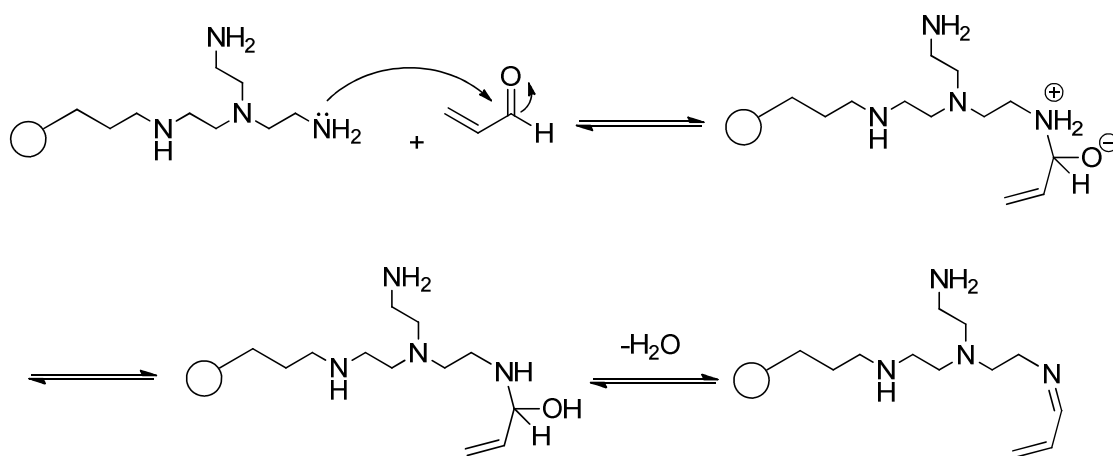
In this part of the study, the nitrogen based polystyrene and silica based reactive resins described in details in Section 5.1.6 were evaluated for the removal of acrolein from the model API iodixanol.

The removal of acrolein using reactive resins is based on a chemical reaction occurring through the formation of imines (Schiff bases). The expected acrolein scavenging mechanisms using the reactive resins are shown in Schemes 5.13 to 5.16.

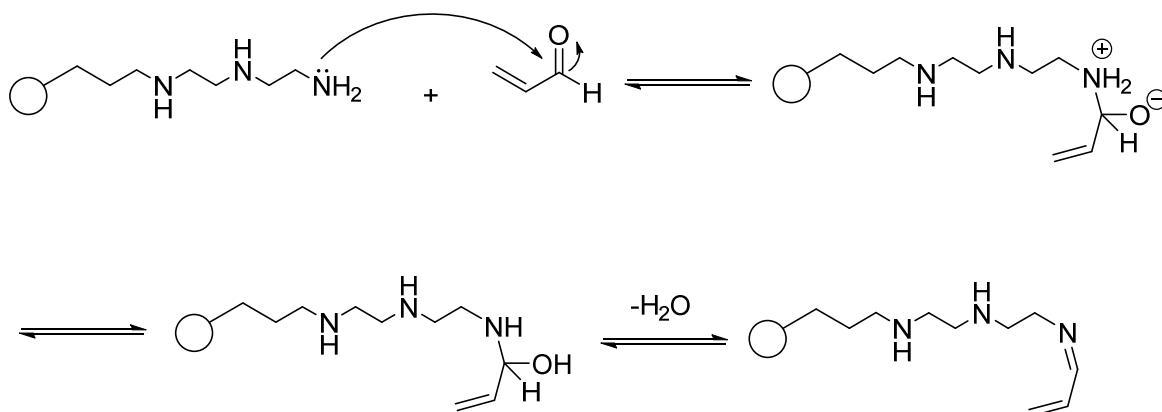
As can be seen from the schemes below, the amino groups of the reactive resins react with the carbonyl carbon of the acrolein via nucleophilic attack. Then the nitrogen is deprotonated and oxygen is protonated and in the last step the C=N double bond is formed through elimination of a water molecule.



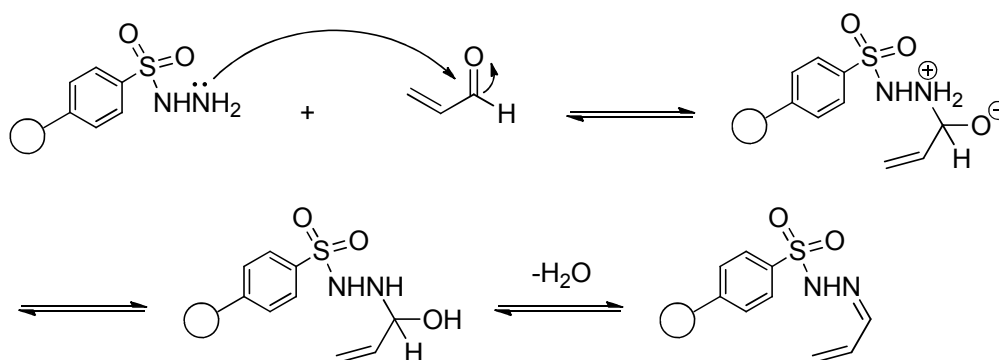
Scheme 5.13: Scavenging mechanism for the removal of acrolein using amine modified scavengers



Scheme 5.14: Scavenging mechanism for the removal of acrolein using trisamine modified scavengers



Scheme 5.15: Scavenging mechanism for the removal of acrolein using triamine modified scavengers



Scheme 5.16: Scavenging mechanism for the removal of acrolein using tosylhydrazine modified scavengers

There are several routes for how resins can be used to remove solutes from a solution. One mode of utilization is in a packed bed, where the resin is packed in a bed and the solvent passes through this bed. While travelling through the packed bed, any dissolved compounds that exhibit an affinity towards this resin are retained. All other dissolved compounds pass through the packed bed and are collected as a purified solution. The flow through mode has the advantage that the process does not require an additional separation of the sorbent from the solution. All in all the operation and handling is easy. However, at a larger scale the capital cost is in many cases higher than in a batch mode process. The capital cost for

flow through processes includes the acquisition of columns and pumps, and during operation, it also requires clean-up processes to regenerate the column. In batch scavenging, resin and mixture containing the target compound are mixed in a vessel and stirred for the time required for the compound to be scavenged. The advantages of the batch scavenging are its conceptual simplicity and that one can easily reach the interaction time which allows the process to reach equilibrium. The backside of the batch process is of the longer process time and that the particles need to be filtered off afterwards which causes additional process handling steps.

The impact of batch and flow through mode on scavenging of acrolein in the presence of iodixanol was evaluated.

In the flow-through scavenging experiments, each scavenger was packed in SPE cartridges and after loading of a solution of acrolein and iodixanol in EtOH, the collected aliquots of the sample were derivatized using DNPH and then analyzed by HPLC.

The outcome of the flow-through scavenging experiments of acrolein in the presence of iodixanol using modified polystyrene and silica based scavengers is shown in Figure 5.34.

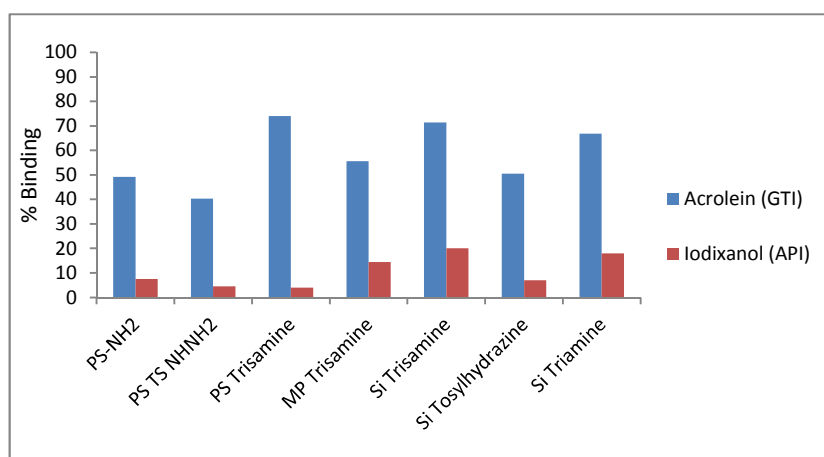


Figure 5.34: Results of flow through scavenging of 5 µg/mL acrolein in the presence of 2 mg/mL iodixanol in EtOH using the suite of scavengers

From the Figure 5.34, it can be seen that trisamine modified polystyrene showed 74 % acrolein removal with only very little loss of iodixanol while trisamine modified silica and triamine modified silica showed 71 % and 67 % acrolein removal, respectively but with extensive removal of iodixanol. This non-specific binding can be expected to be adsorption of iodixanol to the surface of the silica.

It was previously found for the tosylate that, in the flow through mode, the short interaction time (ca 2-5 min) between analyte and resin reduces the effectiveness of the scavenging. As the next step, the batch scavenging mode recommended by the supplier of scavengers was carried out to increase the interaction time and thus the efficiency of scavenging of acrolein.

In the experiments for batch scavenging of acrolein, a small amount of each scavenger was placed in HPLC vials. After addition of a solution of acrolein and iodixanol in EtOH, aliquots were taken after 30 min, derivatized by DNPH and assayed by HPLC.

The results from the batch scavenging experiments of acrolein in the presence of iodixanol using the modified polystyrene and silica based scavengers are shown in Figure 5.35. Most of the scavengers showed near complete removal of acrolein. Amine, multiple amine and hydrazine modified polystyrene scavengers led to higher than 90 % acrolein removal with only very little binding to iodixanol while the silica-based scavengers on the other hand showed in extensive binding of iodixanol. The low cross-linked polymer-bound scavengers displayed a far better selectivity than the silica based scavengers and also than the macroporous highly cross-linked scavenger. Therefore, only the polymer-bound scavengers based on low cross-linked polymer were used for further evaluations. Apparently, under the conditions tested, iodixanol exhibits a certain affinity to both the silica surface and also the surface of the macro-porous highly cross-linked polymer. Binding of iodixanol to the silica backbone can be explained by the interaction of polar groups of the iodixanol such as hydroxyl groups with the acidic silanol moieties on the silica surface. Apparently, the higher surface area of rigid styrene constructs offers a more pronounced binding interaction than loosely cross-linked styrene.

The difference of binding of this particular API to high or low cross-linked polystyrene resins can be compared to other related applications. For example, polystyrene carriers for solid phase amino acid synthesis are also characterized by low cross-linkage. The theory behind this is to provide a material with high swelling which mimics a solvent-like environment and thus high capacity but also to provide very little solid surface for undesired binding.

Other APIs may behave differently and thus other scavengers may display a more advantageous selectivity profile than the currently chosen scavengers.

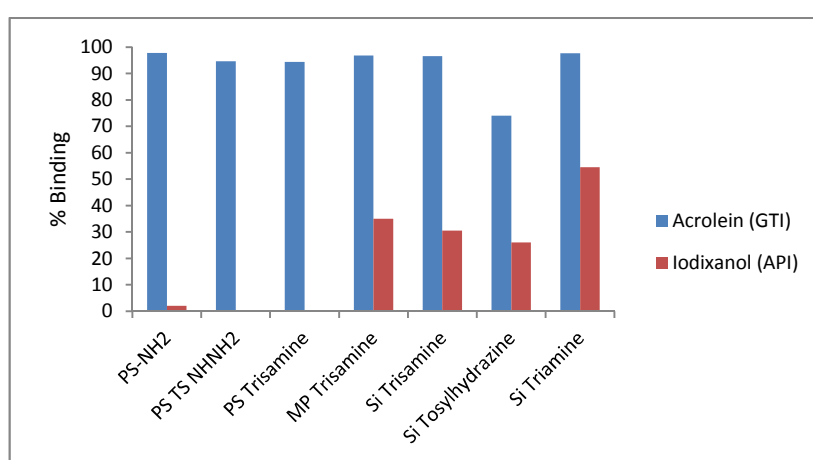


Figure 5.35: Results of batch scavenging of 5 $\mu\text{g/mL}$ acrolein in the presence of 2 mg/mL iodixanol in EtOH

In order to get a preliminary understanding of the kinetics of the scavenging reaction, time course studies for the removal of acrolein using PS-NH₂, PS-Ts-NHNH₂ and PS-Trisamine scavengers were conducted. The aim was to determine the reaction time required for an effective scavenging step.

In the time course studies for acrolein scavenging experiments, a solution of acrolein and iodixanol in EtOH was added to each scavenger. Aliquots of the supernatant were taken at different scavenging time and derivatized by DNPH and assayed by HPLC.

The results from the time course studies are shown in Figure 5.36. As shown in the figure, PS-Trisamine reacts with acrolein very rapidly and removes over 80 % within only 2 min. After 20 min, all scavengers had bound acrolein quantitatively

and exhibited no further significant change in acrolein binding. The highest scavenging level is obtained with PS-NH₂ which removes up to 97.8 % of acrolein and only 2.0 % of iodixanol. If a process can allow scavenging times of 20 minutes or more, then all of the tested scavengers demonstrate a considerably high level of acrolein removal and are very useful and practical. However, if the process interaction time is limited, then the PS-Trisamine is the scavenger that shows the fastest scavenging kinetics and already after 2 minutes around 90 % of acrolein is removed.

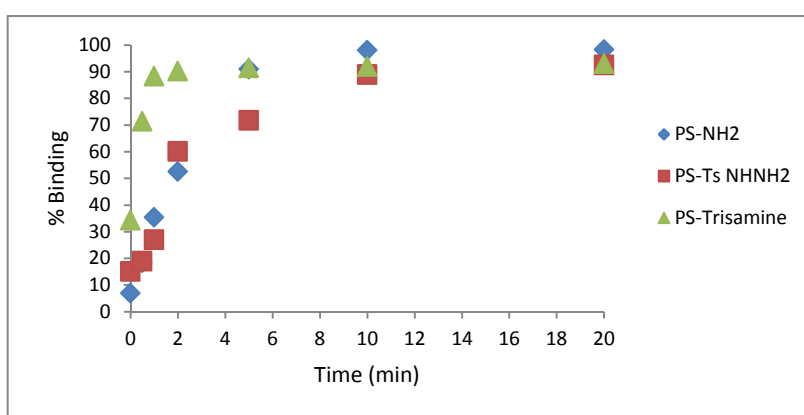


Figure 5.36: Results of time course study for 5 µg/mL acrolein scavenging in EtOH

As discussed earlier in Section 5.1.7, the loading capacity is an important parameter for the resin selection and for production process economics. Therefore, the loading capacity determinations of the polymer based resins were also conducted here as shown in Figure 5.37. For this purpose, small scale experiments were done and scavengers were put into HPLC vials with varying amounts of resins and a solution of acrolein and iodixanol in EtOH was added. After 30 min, samples were collected and derivatized by DNPH and then assayed by HPLC-UV.

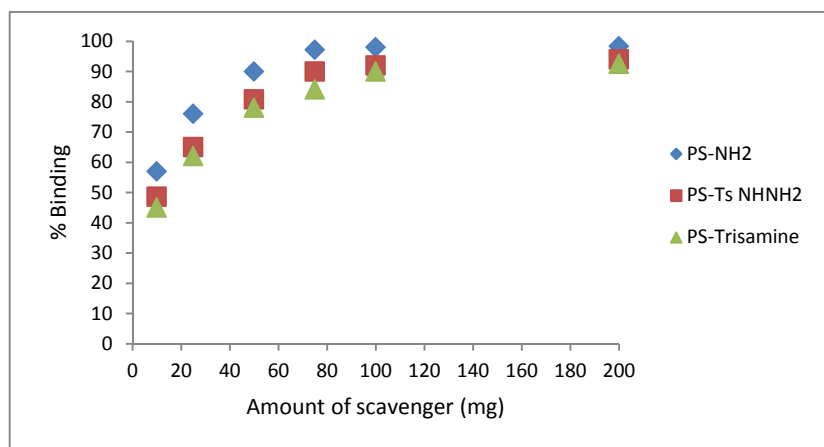


Figure 5.37: Results of loading capacity experiments of the various scavengers; 5 $\mu\text{g/mL}$ acrolein in EtOH

As can be seen in Figure 5.37, at least 75 mg of scavenger is needed to remove most of the acrolein from the solution. Increasing the amount of scavengers gives no major improvement in acrolein removal. Based on the assumption that the reactions are complete, the equilibrium capacity of the scavengers can be estimated to 64.8 $\mu\text{g/g}$ for PS-NH₂, 60 $\mu\text{g/g}$ for PS-TsNHNH₂ and 56 $\mu\text{g/g}$ for PS-Trisamine under these conditions.

Tosylhydrazine, amine and diol modified reactive resins were previously used for removal of an aldehyde impurity in a previously reported study by Welch et al. [171] In this study, various commercial resins were evaluated for the removal of an aldehyde impurity; the reactive scavengers tested were silica functionalized with a diol or with an amine or polystyrene functionalized with tosylhydrazine. Polystyrene based tosylhydrazine resin displayed 86 % binding of the impurity but it is important to consider that leaching of hydrazine and hydrazine derivatives would be a concern with this type of resin.

The results of the present thesis show that PS-NH₂ and PS-Trisamine resins are equally well suited for removal of acrolein without this potential leakage problem. In another work by Emerson et al. [169] the synthesis of macroporous polystyrene based sulfonylhydrazine resin and its use for removal of various aldehydes and ketones from organic reactions was described. Already then in 1979, the group of Emerson proved that resins with immobilized hydrazine are very effective in both

aldehyde and ketone binding. However, this conceptual study does not deal with any genotoxic removal studies where selectivity (i.e. non-binding of active pharmaceuticals) is of interest. The results in the present study show that the choice of backbone is important to minimize loss of API and macroporous resins may not be the best choice.

Based on a model system containing 5 µg/mL acrolein, the capacity can be transferred to larger volumes. A 1 liter API solution with 5 mg/l acrolein (5 ppm) would require 75 g of amine modified polystyrene scavenger to reduce the concentration from 5 ppm down to 0.15 ppm. The initial concentrations correspond to an impure API with 0.25 % of acrolein and to reduce this level to the ICHQ3A limit of 0.05 % (80 % reduction), around 50 g of scavenger would be needed. Thus industrial applicability of this resin is very suitable for real applications.

5.3 Fast identification of selective resins for removal of aminopyridines from APIs

5.3.1 Screening of resin chemistries

In the first experiment, 2-aminopyridine, 3-aminopyridine, 4-aminopyridine, 5-amino 2-methylpyridine and 5-amino 2-chloropyridine were screened on a plate consisting of a wide collection of resins with diverse resin chemistries (e.g containing hydrophobic moieties, urea groups, carboxylic acid groups, boronate groups, imidazole groups, pyridine groups, amide groups, acrylate groups and strong and weak ion exchange moieties) as shown in Table 5.11. This selection of resins was used to determine which resin chemistry displayed best retention and to indicate which further resins should be screened or designed.

Table 5.11: Functional groups of the plate used for resin chemistry screening

Resin Code	Functional group	Resin Code	Functional group
<i>EA090</i>	Carboxylic acid	<i>EH028</i>	Pyridine
<i>EA098</i>	Carboxylic acid	<i>D-NIP24</i>	Pyridine
<i>EA102</i>	Carboxylic acid	<i>NSAID</i>	Urea
<i>A-NIP6</i>	Carboxylic acid	<i>EU064</i>	Urea
<i>A-NIP8</i>	Carboxylic acid	<i>EU066</i>	Urea
<i>A-NIP22</i>	Carboxylic acid	<i>EU086</i>	Urea
<i>A-NIP24</i>	Carboxylic acid	<i>EU090</i>	Imidazole
<i>HLB-WCX</i>	Carboxylic acid	<i>D-NIP2</i>	Imidazole
<i>HLB-WAX</i>	Carboxylic acid	<i>D-NIP25</i>	Imidazole
<i>EC064</i>	Boronate	<i>D-NIP3</i>	Amide
<i>EC072</i>	Boronate	<i>D-NIP26</i>	Amide
<i>HLB</i>	Pyrrolidone	<i>D-NIP28</i>	Amide
<i>EH012</i>	Styrene	<i>D-NIP27</i>	Piperazine
<i>RP125</i>	DVB-Styrene	<i>HLB-SCX</i>	Sulphonic acid
<i>EH016</i>	Pyridine	<i>HLB-SAX</i>	Ammonium
<i>EH018</i>	Pyridine	<i>Acrylate NIP</i>	Hydroxyl

In the screening experiments, a solution of 5 different aminopyridines was prepared in ammonium formate (NH₄FA) buffer and the solution was allowed to pass through SPE columns packed with the polymers. Each fraction was collected and analysed by LC-MS/MS.

Figure 5.38 shows the average binding results from this experiment and it was found that the weak cation exchange resin A-NIP 22 displayed the highest binding which was around 90 % while purely hydrophobic resins and urea resins showed weak binding. Pyridine and amide resins also showed reasonable binding values but not as high as A-NIP 22. On a molecular basis, the retention seems to predominantly be of ionic nature. The secondary amine may get protonated and

the acidic hydrogen of the carboxylic acid is expected to be deprotonated. This can also be assumed to be the case based on their pKa values.

The reason for the lower retention of the other carboxylic acid resins could be explained by the nature and hydrophobicity of the backbone- A-NIP 22 has more acidic backbone than EA090, EA098 and EA102 which have predominantly a styrene backbone.

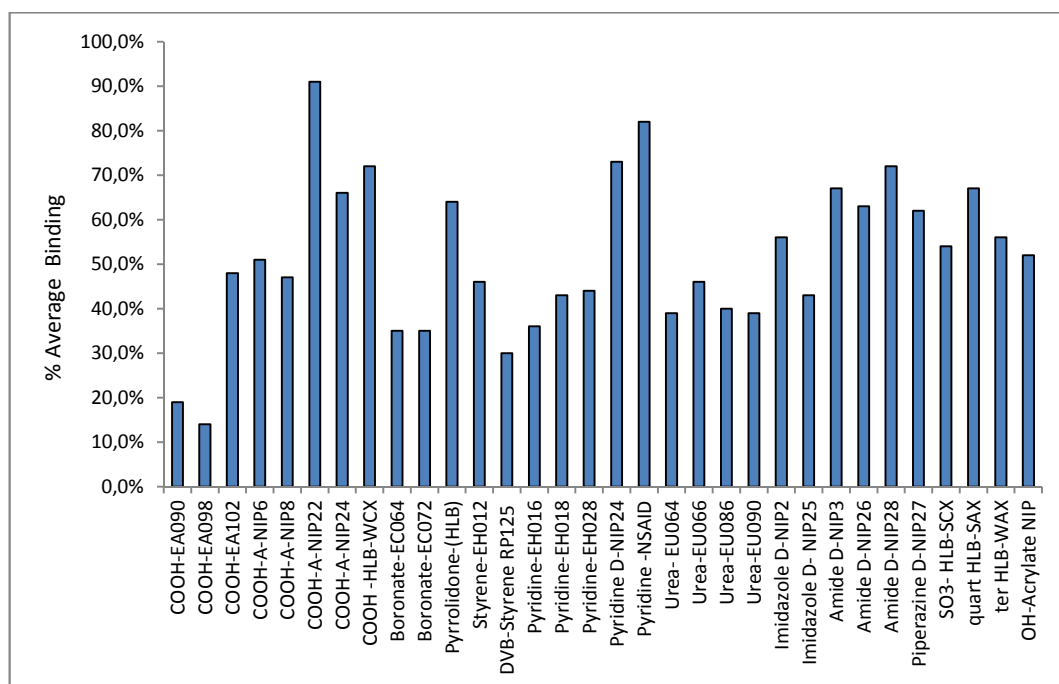


Figure 5.38: Screening of resin chemistries for 5 different aminopyridines; 10 µg/mL aminopyridines mixture loaded in 10mM NH₄FA pH 6.5. Values shown are the average for all 5 aminopyridines.

5.3.2 Screening of carboxylic acid MIPs

After the screening of resin chemistries, the aminopyridines GTIs were screened on a plate containing a series of chemically related MIPs and NIPs which contain both hydrophobic and carboxylic acidic constituents (methacrylic acid).

All polymers coded with EA have 80 % styrene backbone while A-resins are bulk materials with an acrylic cross-linked backbone.

The interaction chemistry to be expected on this plate is ionic interaction between the carboxylic acid functional monomer and the aminopyridine GTIs. A schematic representation of the interaction between aminopyridines and the carboxylic acid monomer used in the carboxylic acid plate is shown in Figure 5.39.

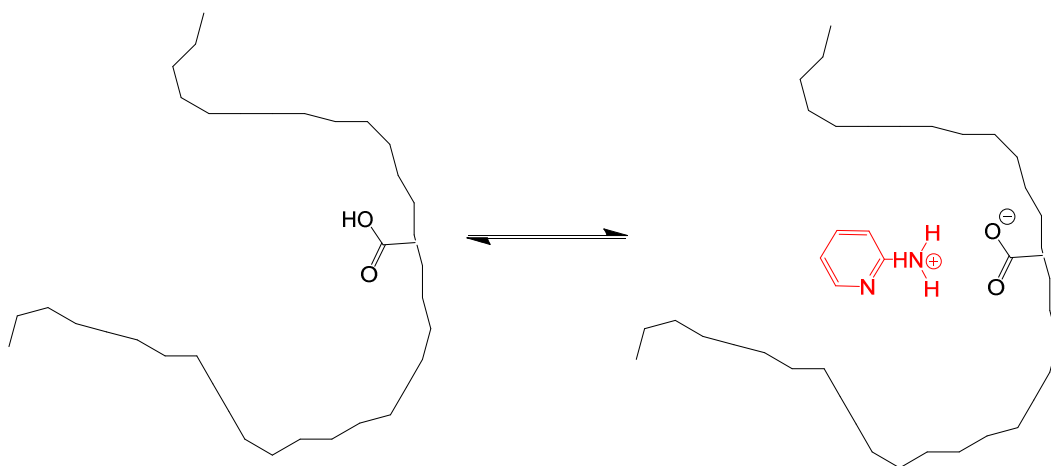


Figure 5.39: Schematic representation of interaction between aminopyridines and the carboxylic acid monomer on the carboxylic acid plate

The results from the screening of the aminopyridines on this plate are shown in Figure 5.40. As can be seen in the figure, A-MIP 22 and A-MIP-24 displayed the strongest overall interaction with the 5 different aminopyridines tested. A-MIP 22 displayed 97 % average binding for 5 different aminopyridines with a clear imprinting effect while A-NIP 22 displayed 78 % average binding. Based on these results, A-MIP 22 and its control polymer A-NIP 22 were chosen as candidate resins for further investigation.

Because the experiments for the screening of resin chemistries brought forward that carboxylic acid based resins displayed the highest binding, these further screening experiments were conducted on a larger variety of carboxylic acid based resins but also the hydrophobic plate with the various pyridine resins (MIPs-NIPs) could have merited attention to evaluate.

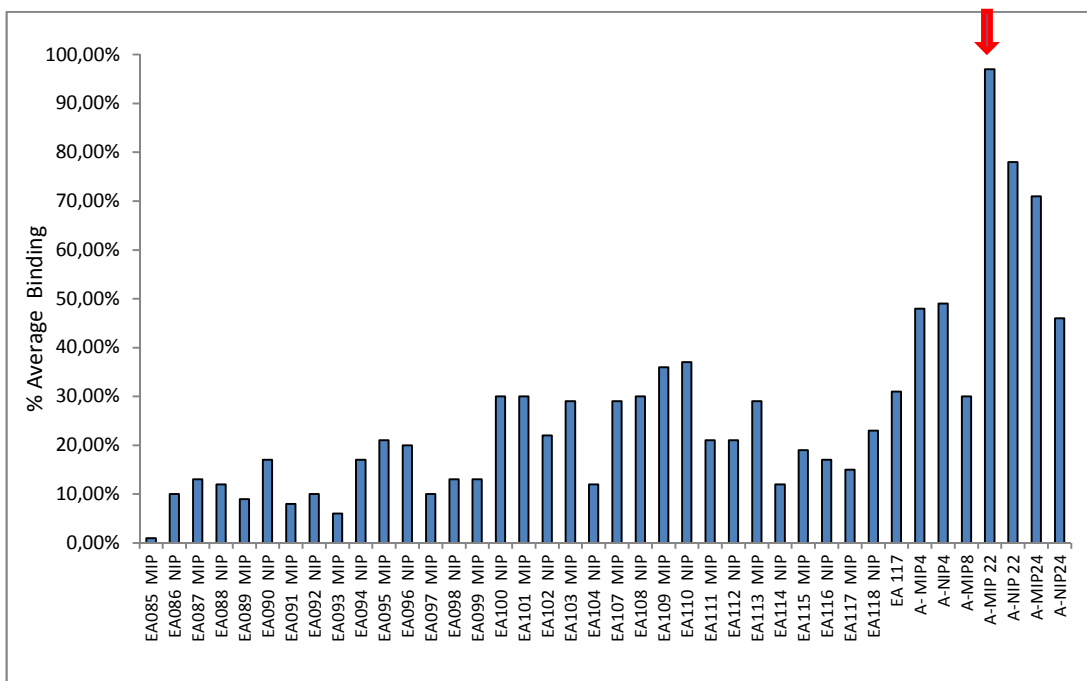


Figure 5.40: Screening of 5 different aminopyridines on the carboxylic acid plate; 10 µg/mL aminopyridines mixture loaded in 10mM NH₄FA pH 6.5. The % Binding shown is the average for all 5 aminopyridines.

5.3.3 Binding and elution of aminopyridines and corresponding APIs from the candidate resins

Binding and elution experiments were performed to understand the binding and elution behaviors of the aminopyridines on the candidate resins A-MIP 22 and A-NIP 22 and to study the selectivity of the resins in more detail. It was already established that the aminopyridines bind well to the A-NIP 22 in buffer. In the next step, binding and elution experiments for aminopyridines were carried out in organic solvent such as DCM.

The subsequent experiments were designed to investigate the elution strength needed to elute the aminopyridines using organic solvent with increasing acid strength. The commercial weakly acidic resin Amberlite CG-50 was included as a reference.

The results from the binding and elution experiments of 2-aminopyridine, 3-aminopyridine and 4-aminopyridine on the resins are shown in Figures 5.41 –

5.43 in the form of cumulative recovery line charts for the resins. As can be seen in the figures, A-MIP 22 gives a 100 % retention for 2-aminopyridine, 3-aminopyridine and 4-aminopyridine in the loading step (DCM) and the first washing step (W1: DCM) indicating very effective binding to the resins.

Elution of 2-aminopyridine, 3-aminopyridine and 4-aminopyridine from A-MIP 22 and A-NIP 22 starts at 5 % HAc in DCM and complete elution was achieved using 5 % FA in DCM.

Furthermore, the retention of 2-aminopyridine and 3-aminopyridine on A-MIP 22 is significantly higher than on its corresponding reference NIP, and thus confirms the imprinting effect and selective binding to the imprinted sites of the MIP.

The non-imprinted polymer A-NIP 22 displayed 100 % binding towards 4-aminopyridine while it shows lower binding towards 2-aminopyridine and 3-aminopyridine. This can be explained by basicity of 4-aminopyridine and steric hindrance on 2-aminopyridine and 3-aminopyridine. Andersson et al. reported that the proximity of the pyridyl nitrogens lead to a steric hindrance which affects the binding between the target molecule and the functional monomer.^[172] The pKa values of 2-aminopyridine, 3-aminopyridine and 4-aminopyridine are 6.86, 6.0 and 9.26, respectively. The nitrogen at para-position on the 4-aminopyridine raises the molecular basicity and leads to stronger interaction with the carboxylic acid groups of the polymer. Thus, 4-aminopyridine is expected to display a strong binding to the polymers via interaction with the functional carboxylic acid groups.

A-MIP 22 is an imprinted polymer with nornicotine as a template (shown in Figure 5.44) and with a backbone of methacrylic acid (MAA), ethylene glycol dimethacrylate (EDMA) and the hydrophilic monomer 2-hydroxyethyl methacrylate (HEMA). Nornicotine contains the pyridine moiety and also an amino group although in a slightly different position than the aminopyridines. In this case, nornicotine imprinted polymer displayed significant cross-reactivity towards aminopyridine GTIs.

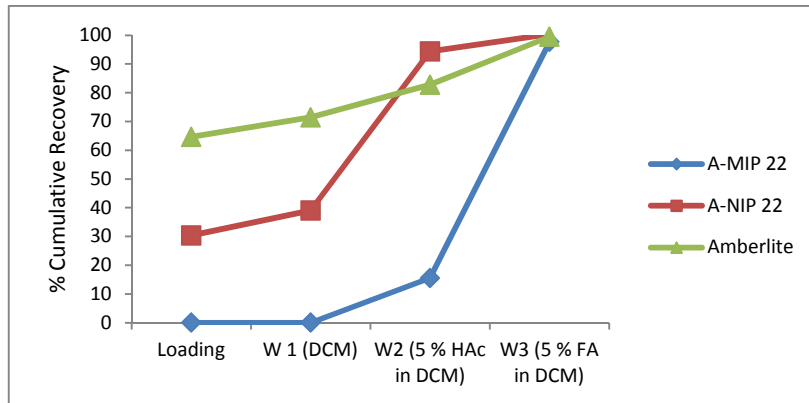


Figure 5.41: Elution profile of 1 µg/mL 2-aminopyridine in DCM from the resins

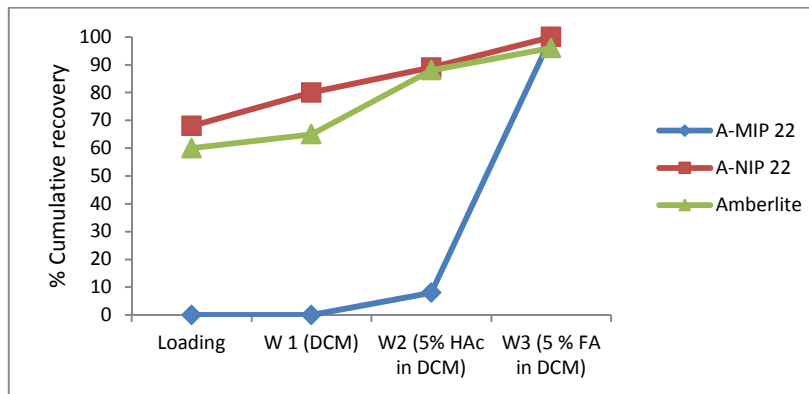


Figure 5.42: Elution profile of 1 µg/mL 3-aminopyridine in DCM from the resins

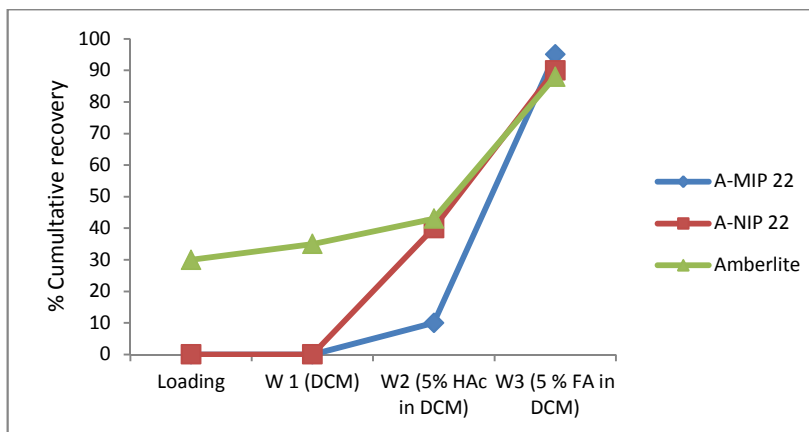


Figure 5.43: Elution profile of 1 µg/mL 4-aminopyridine in DCM from the resins

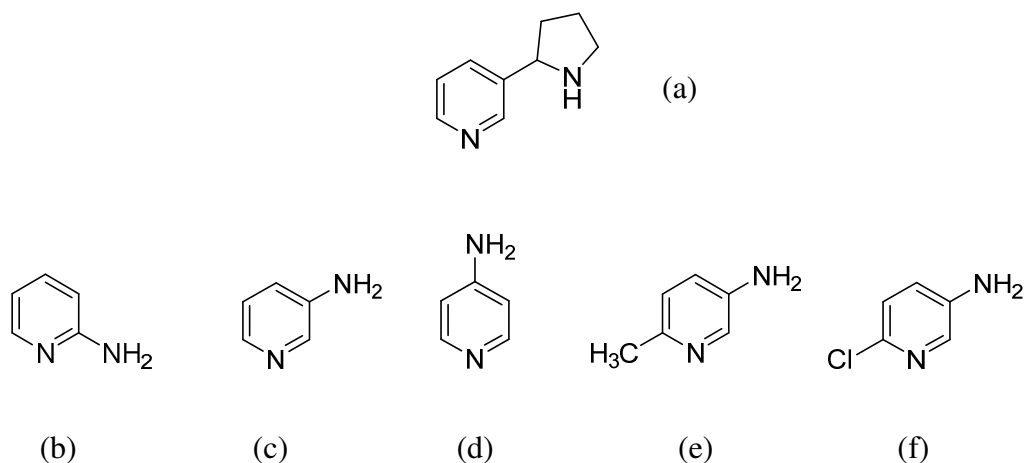


Figure 5.44: Structures of nornicotine (template for A-MIP 22) (a) and aminopyridine GTIs (b-f)

Figure 5.45 shows a schematic depiction of the binding site of A-MIP 22 with the MAA and HEMA functionalities towards 3-aminopyridine. As can be seen from the figure, the interaction chemistry to be expected on A-MIP 22 is ionic interaction of 3-aminopyridine with the carboxylic acid groups and hydrogen bonding with the hydroxyl groups of 2-hydroxyethyl methacrylate.

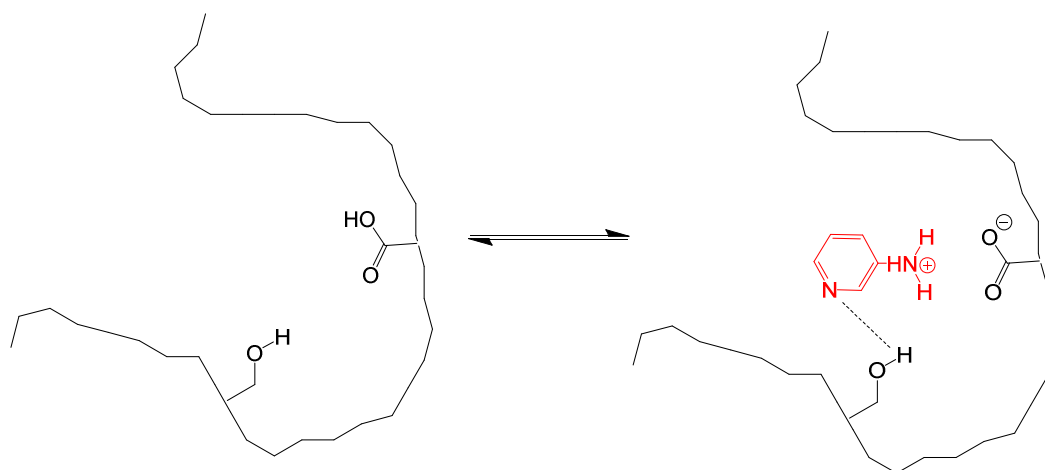


Figure 5.45: Schematic depiction of the binding sites of A-MIP 22 towards 3-aminopyridine.

The results from the elution experiments of 5-amino-2-methylpyridine and 5-amino-2-chloropyridine from the resins are shown in Figure 5.46 and 5.47. As can be seen from the figures, A-MIP 22 showed prominent imprinting effect also for 5-amino 2-methyl pyridine while no imprinting effect was observed for 5-amino 2-chloropyridine.

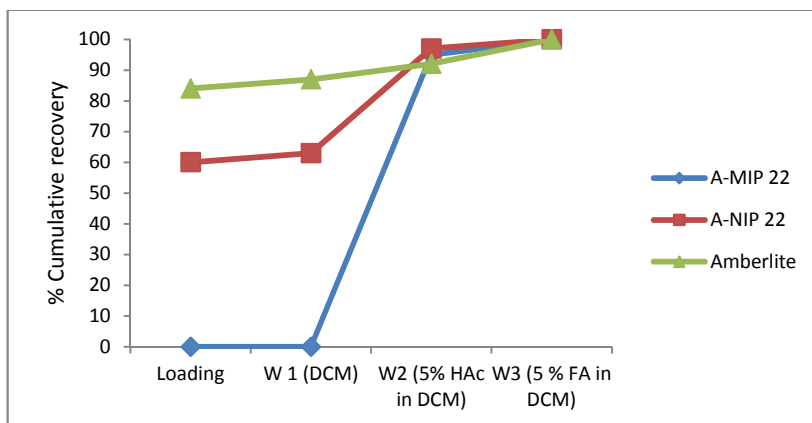


Figure 5.46: Elution profile of 1 µg/mL 5-amino-2-methylpyridine in DCM from the resins

Commercial Amberlite CG-50 (type 1), a 4 % crosslinked methacrylic acid type of weakly acid cation exchange resin, on the other hand showed only 36 % binding for 2-aminopyridine, 40 % binding for 3-aminopyridine and 70 % binding for 4-aminopyridine. Amberlite has the same constituents as the MIP and NIP but binds considerably less to the aminopyridines tested here. It appears to be of high importance that both ion exchange functionality and also a rigid backbone are present to lead to a high binding of aminopyridines. Amberlite showed 16 % and 12 % binding for 5-amino 2-methylpyridine and 5-amino 2-chloropyridine, respectively.

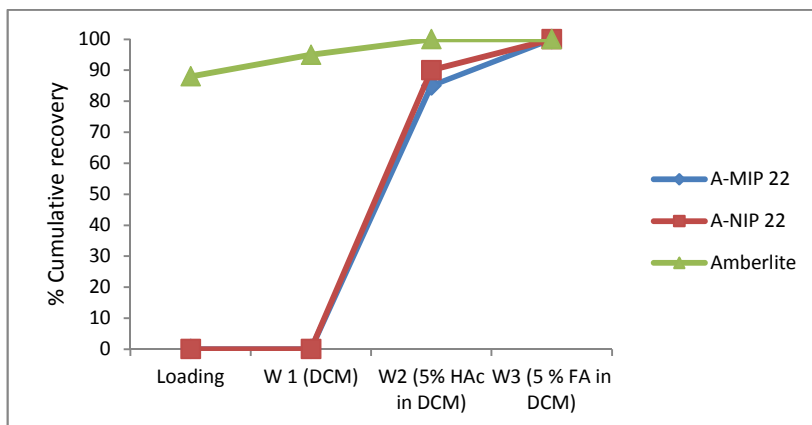


Figure 5.47: Elution profile of 1 µg/mL 5-amino-2-chloropyridine in DCM from the resins

Finally, the results from the same experiments with the corresponding APIs piroxicam and tenoxicam conducted with the resins are shown in Figure 5.48 and 5.49. As can be seen from the figures, all resins displayed very weak retention for both APIs and the weakly bound APIs were completely eluted from the resins in first washing step using DCM.

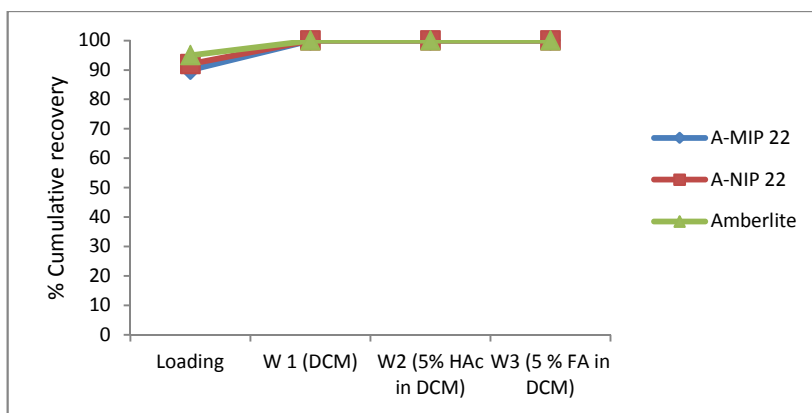


Figure 5.48: Elution profile of 100 µg/mL piroxicam in DCM from the resins

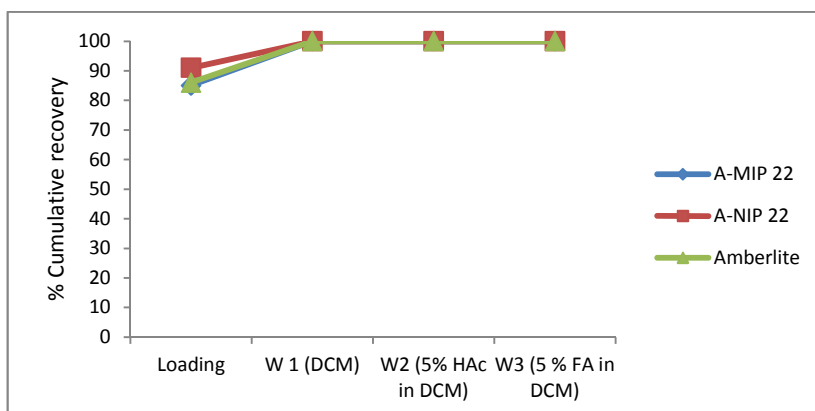


Figure 5.49: Elution profile of 100 µg/mL tenoxicam in DCM from the resins

The specific surface areas of the resins were measured using the BET method and the results are given in the following Table 5.12.

Table 5.12: BET results for the resins

Resin	Surface Area (m ² /g)	Pore Volume (ml/g)	Pore Diameter (nm)
A-MIP 22	150	0.48	13.0
A-NIP 22	178	0.56	12.6
Amberlite CG-50	2	0.002	-

The very weak retention for both GTIs and APIs on the Amberlite CG-50 may be related to its low surface area.

A few reports on aminopyridines recognition have been published so far but no studies have been reported on the removal of genotoxic aminopyridines from pharmaceutical compounds using MIPs.

Jie et al. ^[173] described imprinted polymers towards 2-aminopyridine using methacrylic acid as a functional monomer. The synthesized polymer displayed a clear selectivity towards 2-aminopyridine compared to other test compounds such as aniline, pyridine and 2-methylpyridine. The authors report that the polymer required a long incubation time of 12 hours whereas we have shown that the MIP

found in the present study displayed a clear selectivity already in SPE mode with very short interaction times.

Lai et al. ^[174] reported the preparation of 4-aminopyridine imprinted polymers also using methacrylic acid as functional monomer for chromatographic separation of 4-aminopyridine and 2-aminopyridine. The polymer was synthesized by suspension polymerization and packed into an HPLC column. Simultaneous separation of 4-aminopyridine and 2-aminopyridine in the presence of the interfering compounds pyridine, 4-methyl pyridine and aniline was achieved with the capacity factors 4.2 and 2.4 for 4-aminopyridine and 2-aminopyridine, respectively.

In a study reported by Liu and co-workers, ^[175] temperature responsive imprinted hydrogels towards 4-aminopyridine were synthesized and evaluated for their recognition behavior towards 4-aminopyridine. These hydrogels displayed a higher binding capacity towards 4-aminopyridine compared to other tested similar compounds such as pyridine, 4-methylpyridine and 2-aminopyridine.

Guo et al. ^[176] prepared 4-aminopyridine imprinted polymer membranes via photo-polymerization. The binding properties of these membranes towards 4-aminopyridine, sulfanilamide, pyridine and 2-aminopyridine were investigated. The prepared membranes displayed higher binding towards 4-aminopyridine over the other compounds.

In all the above reported studies, the genotoxic compounds 2-aminopyridine or 4-aminopyridine was used as templates. It is very difficult to remove all the template molecules from the MIPs and under harsh conditions, MIPs may bleed template molecules at very low levels which can be a significant source of false results in trace analysis of the compounds. The possible contamination of samples by the residual template released from the MIPs is also big concern if these MIPs are used for removal of undesired impurities from pharmaceutical compounds.

These problems can also be avoided using the dummy template approach as described in Section 1.3.4.

In the present study, a MIP was found by screening of the libraries. The MIP was made with a non-related template, namely nornicotine. Nornicotine is not a genotoxic compound and can thus not cause the same type of problems as would the genotoxic templates in case it would bleed out of the MIP.

5.3.4 Chromatographic evaluation of the polymers towards aminopyridines

The chromatographic efficiency of the nornicotine-imprinted polymer A-MIP 22 and its non-imprinted polymer A-NIP 22 towards 2-aminopyridine, 3-aminopyridine and 4-aminopyridine has also been evaluated. The chromatographic behavior of the polymers towards aminopyridines GTIs was evaluated using polymer packed in HPLC columns (Figures 5.50-5.52).

Nornicotine imprinted polymer A-MIP 22 displayed imprinting effect for the 2-aminopyridine and 3-aminopyridine as shown in Figures 5.50 and 5.51. Both 2-aminopyridine and 3-aminopyridine are more strongly retained on the imprinted polymer A-MIP 22. However, 2-aminopyridine was retained less than 3-aminopyridine on the non-imprinted polymer A-NIP 22. 4-Aminopyridine was strongly retained on both imprinted and non-imprinted polymers (Figure 5.52). Thus, no imprinting effect was observed for 4-aminopyridine. The reason of this could be explained by the basicity of 4-aminopyridine as already discussed for the SPE results. The pKa value of 4-aminopyridine (9.26) is higher than pKa values of 2-aminopyridine (6.86) and 3-aminopyridine (6.0). The pyridine nitrogen at para position of 4-aminopyridine increases the basicity of the molecule. This leads to strong interaction of 4-aminopyridine with the carboxylic acid moieties also of the non-imprinted polymer. Interaction of the carboxylic acid groups of the non-imprinted polymer with 2-aminopyridine and 3-aminopyridine is lower than for 4-aminopyridine due to the steric hindrance generated by the proximity of the pyridyl nitrogens.^[173]

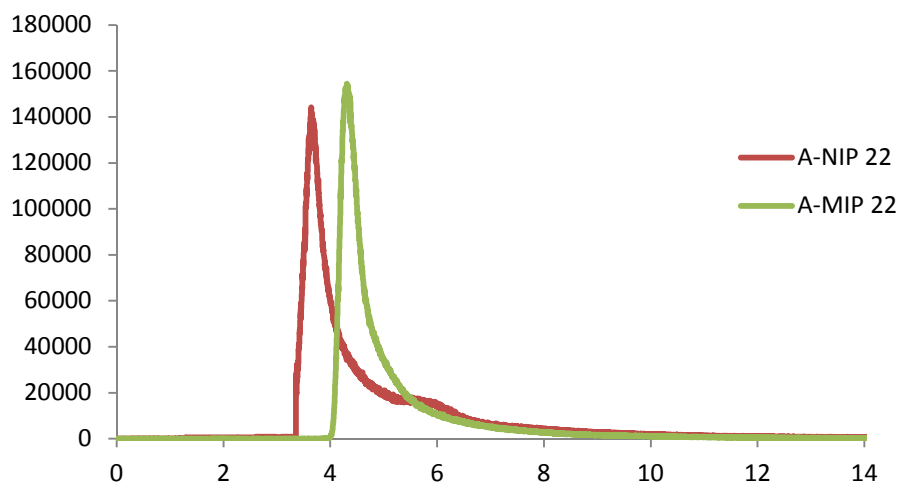


Figure 5.50: Comparison of 10 µg/mL 2-aminopyridine retention on A-MIP 22 and A-NIP 22: Polymers packed in 50x4.6 mm stainless steel HPLC columns; Gradient elution was performed with 10 % FA in water (mobile phase A) and MeCN (mobile phase B).The gradient started from 100 % B to 0 % B over 4 min, then kept at 0 % B for 2 min, then back to 100 % B over 3 min and kept at 100 % B for 6 min ; injection volume: 10 µL; flow rate: 0.5 mL/min

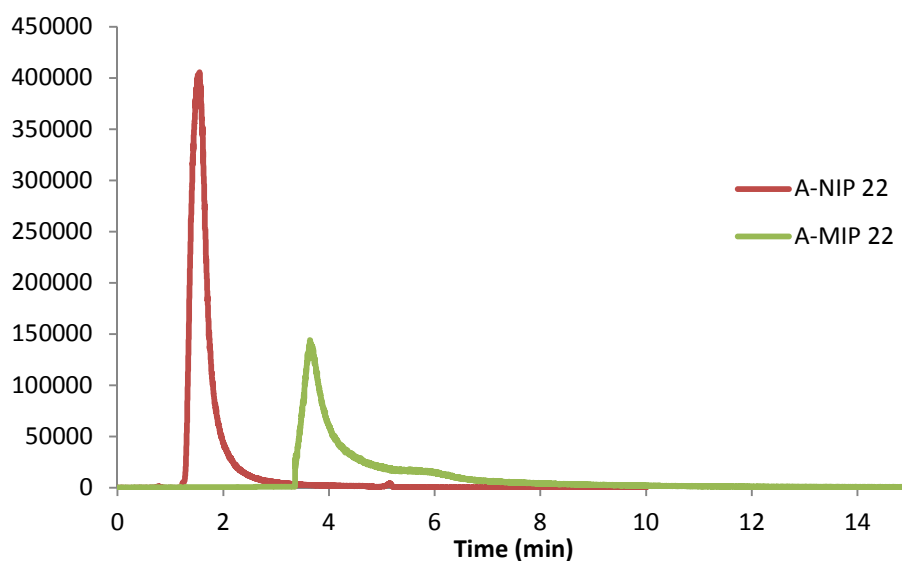


Figure 5.51: Comparison of 10 µg/mL 3-aminopyridine retention on A-MIP 22 and A-NIP 22: Polymers packed in 50x4.6 mm stainless steel HPLC columns Gradient elution was performed with 10 % FA in water (mobile phase A) and MeCN (mobile phase B).The gradient started from 100 % B to 0 % B over 4 min, then kept at 0 % B for 2 min, then back to 100 % B over 3 min and kept at 100 % B for 6 min ; injection volume: 10 µL; flow rate: 0.5 mL/min

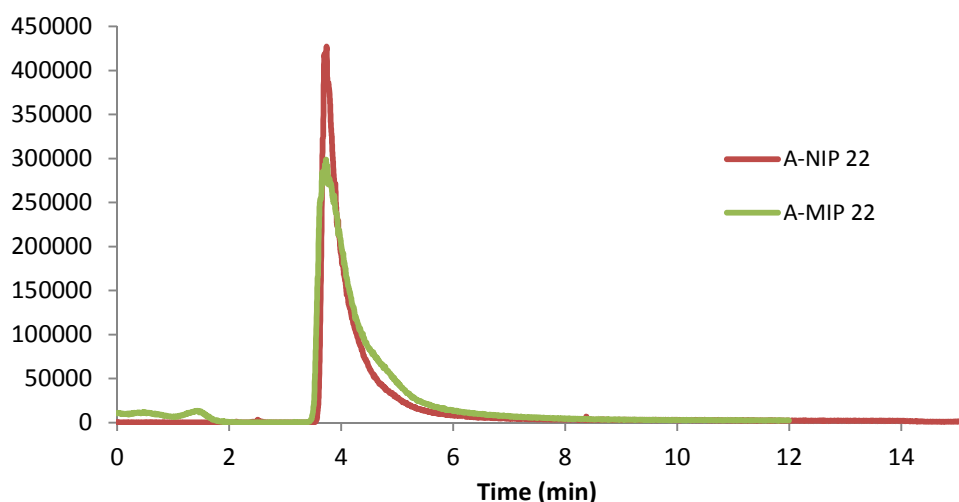


Figure 5.52: Comparison of 10 µg/mL 4-aminopyridine retention on A-MIP 22 and A-NIP 22: Polymers packed in 50x4.6 mm stainless steel HPLC columns; Gradient elution was performed with 10 % FA (mobile phase A) and MeCN (mobile phase B).The gradient started from 100 % B to 0 % B over 4 min, then kept at 0 % B for 2 min, then back to 100 % B over 3 min and kept at 100 % B for 6 min ; injection volume: 10 µL; flow rate: 0.5 mL/min

The capacity factors (k') and the imprinting factors (IF) for the aminopyridine GTIs were calculated according to the following equations ;

$$k' = \frac{t_r - t_0}{t_0} \quad (9)$$

t_r = Retention time of the analyte

t_0 = Retention time of the void marker (e.g acetone)

$$IF = \frac{k'_{MIP}}{k'_{NIP}} \quad (10)$$

The capacity factors and imprinting factors obtained using the MIP and NIP are shown in Table 5.13. As can be seen from the table, A-MIP 22 displayed the highest imprinting factor towards 3-aminopyridine, while it showed only low imprinting factors towards 2-aminopyridine and 4-aminopyridine.

Table 5.13: The outcome of chromatographic evaluation of the polymers

Analyte	Retention Time _{MIP}	Retention Time _{NIP}	k _{MIP}	k _{NIP}	IF
2-Aminopyridine	4.30	3.58	2.58	1.98	1.3
3-Aminopyridine	3.49	1.59	1.90	0.33	5.7
4-Aminopyridine	3.60	3.71	2.0	2.1	--

Another definition of how well target compounds have been separated in the column is provided by calculation of the *resolution (R)*. The resolution of two analytes, x and y is defined as:

$$R = \frac{2[(tr)_x - (tr)_y]}{w_x + w_y} \quad (11)$$

t_r = Retention time of the analyte

w = width of the analyte peak

In order to evaluate the separation, the chromatographic separation of 10 µg/mL 2-aminopyridine (GTI) and 500 µg/mL piroxicam (API) in MeCN was evaluated using A-MIP 22 packed in an HPLC column. In Figure 5.53, the HPLC chromatogram for separation of the GTI and API mixture is shown. As can be seen in the chromatogram, the retention of the GTI in the column is stronger than for its corresponding API and the GTI is therefore eluted later.

The chromatographic separation of GTI and API is quite satisfactory with baseline separation between the peaks. The resolution factor (R) of the separation between GTI and API is 6.05 as calculated from the equation 11.

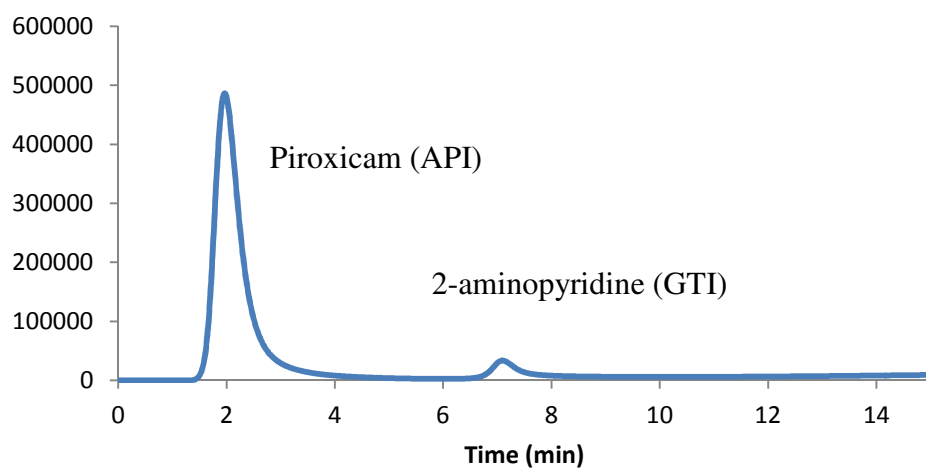


Figure 5.53: Chromatographic separation of 10 $\mu\text{g/mL}$ 2-aminopyridine (GTI) and 500 $\mu\text{g/mL}$ piroxicam (API) using A-MIP 22: A-MIP 22 packed in 50x4.6 mm stainless steel HPLC column; Gradient elution was performed with 10 % FA (mobile phase A) and MeCN (mobile phase B). The gradient started from 100 % B to 0 % B over 4 min, then kept at 0 % B for 2 min, then back to 100 % B over 3 min and kept at 100 % B for 6 min ; injection volume: 10 μL ; flow rate: 0.5 mL/min

6 CONCLUSIONS

In this work, the removal of genotoxic impurities from pharmaceutical compounds using molecularly imprinted polymers (MIPs) and reactive scavengers was evaluated. The results showed that both imprinted polymers and reactive scavengers are useful tools for removal of genotoxic impurities from APIs.

Additionally, the analysis of compounds present at low levels is often not straightforward and especially the trace analysis of genotoxic residues in the presence of far higher concentrations of pharmaceutically active compounds is a demanding task. In the present work, a range of accurate and reliable methods for the analysis and quantification of genotoxic compounds were established.

In the first part of the work, screening experiments using a MIP resin library to identify selective resins and design of new MIP resins and reactive scavengers towards methyl p-toluenesulfonate removal from the model API 21-chlorodiflorasone was carried out. Although the library screening experiments for methyl p-toluenesulfonate did not result in any resin that showed high binding of methyl p-toluenesulfonate, a resin was found that displayed good selectivity for methyl p-toluenesulfonate over the model API 21-chlorodiflorasone. This resin was packed into an HPLC column and satisfactory chromatographic separation of GTI and API was achieved.

New MIPs for selective scavenging of methyl p-toluenesulfonate from APIs were also synthesized, characterized and investigated. Scavenging experiments showed that MIPs displayed good selectivity for methyl p-toluenesulfonate over 21-chlorodiflorasone, although overall binding was low, as is often a drawback of MIPs.

Additionally, a simple, rapid and facile scavenging approach for selective removal of the genotoxic impurity methyl p-toluenesulfonate from the model API 21-chlorodiflorasone was described. Removal of methyl p-toluenesulfonate was

shown to be most effective using trisamine modified macroporous polystyrene and silica supported trisamine and triamine scavengers which give complete removal of GTI and virtually no loss of API after a simple organic wash step. The more reactive trimercaptotriazine (TMT)-based scavenger also removed the GTI but displayed extensive removal of the API as well. Lee et al. ^[23] have previously demonstrated that Si-Triamine can be used to remove p-toluenesulfonate esters, but the results in the present study show that MP-Trisamine and Si-Trisamine may be better choices, especially in cases where the more reactive TMT resin cannot be used.

In the second part of the work, the synthesis, characterization and binding behavior of novel MIPs towards acrolein were evaluated. Also, the performance of modified polystyrene and silica based scavengers and designed MIPs were tested in organic media for the selective removal of acrolein from model API solutions. The selective removal of these genotoxic impurities from model API solutions was successfully achieved by using aldehyde scavengers.

It was found that for the model API process solution system, removal of acrolein was quite fast and effective using both polymer and silica based scavengers. However, low cross-linked polymer based scavengers displayed a more advantageous selectivity profile than highly cross-linked polymers and silica based scavengers as it was observed that those scavengers displayed an undesired high level of non-specific binding to the API.

The use of reactive scavengers for the removal of some other impurities from pharmaceutical compounds has previously been reported. ^[170,171] but removal of acrolein from active pharmaceutical ingredients by using polystyrene and silica based reactive scavengers has first been demonstrated in this work. In essence, an easy and simple procedure for the effective removal of acrolein from contaminated API solutions using iodixanol as a model compound was described.

In the last part of the work, an easy and efficient two-step screening procedure for fast identification of selective resins was described. In the procedure, first a screening of resin chemistries was carried out and then based on the outcome of this screening, further MIPs of this type were screened. Using this screening procedure, a resin with good binding properties towards a range of aminopyridines was identified. Elution experiments showed that this nornicotine imprinted polymer can effectively remove the aminopyridines from the APIs with virtually no loss of APIs after a wash step with DCM and the resin displayed a considerable imprinting effect for 2-aminopyridine, 3-aminopyridine and 5-amino-2-methylpyridine. This MIP could be envisaged to be employed in API purification processes.

So far, only a few reports on aminopyridines recognition have been published [173-176], and also some of studies have focused on the trace analysis of aminopyridines in pharmaceutical compounds [42,43], but until now there has been no reported study on the removal of the genotoxic impurities aminopyridines from pharmaceutical compounds using MIPs.

As a concluding remark, polystyrene and silica based reactive scavengers towards both methyl p-toluenesulfonate and acrolein and selective MIPs towards a group of aminopyridines are promising resins for GTI removal from model API solutions and can be envisaged to be used in real pharmaceutical clean-up processes.

7 APPENDIX

7.1 Abbreviations

ABDV	2, 2'-Azobis (2,4-dimethyl)valeronitrile
AIBN	2, 2'-Azobis isobutyronitrile
API	Active pharmaceutical ingredient
BET	Brunauer-Emmett-Teller
BSA	Benzenesulfonic acid
DCM	Dichloromethane
DMF	Dimethylformamide
DMSO	Dimethylsulphoxide
DNA	Deoxyribonucleic acid
DNPH	Dinitrophenylhydrazine
DVB	Divinylbenzene
EDMA	Ethylene glycol dimethacrylate
ESI	Electrospray ionization
EtAc	Ethyl acetate
EtOH	Ethanol
FA	Formic acid
FTIR	Fourier transform infrared
GTI	Genotoxic impurity
HAc	Acetic acid
HEMA	2-Hydroxyethyl methacrylate
HPLC	High performance liquid chromatography
IPA	Isopropanol
LC-MS	Liquid chromatography-mass spectroscopy
MAA	Methacrylic acid
MeCN	Acetonitrile
MeOH	Methanol
MDD	Maximum daily dose
MIP	Molecularly imprinted polymer
MP	Macroporous polystyrene
MRM	Multiple reaction monitoring
MSA	Methanesulfonic acid
NIP	Non-imprinted polymer
NMR	Nuclear magnetic resonance
PDA	Photodiode array
PGIs	Potentially genotoxic impurities
PS	Polystyrene
p-TSA	p-toluenesulfonic acid
SEM	Scanning electron microscopy
SPE	Solid phase extraction
TEA	Triethylamine
TFA	Trifluoroacetic acid

TFMAA	Trifluoromethacrylic acid
THF	Tetrahydrofuran
TMT	2,4,6-Trimercaptotriazine
TTC	Threshold toxicological concern
UV	Ultraviolet

8 PUBLICATIONS

8.1 Articles

R. Kecili, D. Nivhede, J. Billing, M. Leeman, B. Sellergren and E. Yilmaz “Removal of acrolein from active pharmaceutical ingredients using aldehyde scavengers”, **Organic Process Research & Development**, 16 (6), 1225-1229 (2012)

R. Kecili, J. Billing, D. Nivhede, M. Leeman, B. Sellergren, Anthony Rees, E. Yilmaz, “Selective scavenging of the genotoxic impurity methyl p-toluenesulfonate from pharmaceutical compounds”, **Separation and Purification Technology**, (2012) (in press) <http://dx.doi.org/10.1016/j.seppur.2012.09.028>

R. Kecili, J. Billing, D. Nivhede, M. Leeman, B. Sellergren, E. Yilmaz, “Fast identification of selective resins for removal of genotoxic aminopyridine impurities via screening of molecularly imprinted polymer resin libraries ”, (Manuscript in preparation)

8.2 Posters

E. Yilmaz, D. Nivhede, **R. Kecili**, A. Rees, “Utilizing the cross reactivity of MIPs-ExploraSep™”, MIP 2010 – The 6th International Conference on Molecular Imprinting, New Orleans, USA, Aug 9-12, **2010**

R. Kecili, D. Nivhede, B. Sellergren and E. Yilmaz, “Genotoxic Impurity Removal by using ExploraSep™ Concept” , 4th Graduate Student Symposium on Molecular Imprinting, Imperial College, London, UK, Sep 28-30. **2011**

R. Kecili, J. Billing and E. Yilmaz , “Fast Identification of Selective resins for Genotoxic Impurity Removal via Screening of Molecularly Imprinted Polymers Resins Libraries”, HPLC 2012, Anaheim, California, USA, June 16-21. **2012**

9 REFERENCES

- [1] T. McGovern, K.D. Jacobsen, *Trends Anal Chem.* **2006**, 25, 790.
- [2] K.L. Dobo, N. Greene, M.O. Cyr, S. Caron, W.W. Ku, *Regul.Toxicol. Pharmacol.* **2006**, 44, 282.
- [3] D. Bartos, S. Görög, *Curr. Pharm. Anal.* **2008**, 4, 215.
- [4] D.A. Pierson, B.A. Olsen, D.K. Robbins, K.M. DeVries, D.L. Varie, *Org. Process Res Dev.* **2009**, 13, 285.
- [5] M. Lynch, *Am. Pharm.Rev.* **2011**, 93.
- [6] Guideline on Genotoxic and Carcinogenic Impurities in Drug Substances and Products: Recommended Approaches; US Department of Health and Human Services, Food and Drug Administration, Center for Drug Evaluation and Research (CDER), USA, December, **2008**
- [7] H. M. Bolt, H. Foth, J.G. Hengstler, G.H. Degen, *Toxicol. Lett.* **2004**, 151, 29.
- [8] L. Muller, R.J. Mauthe, C.M. Riley, M.M. Andino, D. De Antonis, C. Beels, J. De George, A.G.M. De Knaep, D. Ellison, J.A. Fagerland, R. Frank, B. Fritschel, S. Galloway, E. Harpur, C.D.N. Humfrey, A.S. Jacks, N. Jagota, J. Mackinnon, G. Mohan, D.K. Ness, M.R. O'Donovan, M.D. Smith, G. Vudathala, L. Yotti, *Regul. Toxicol. Pharmacol.* **2006**, 44, 198.
- [9] K. Kondo, A. Watanabe, Y. Iwanaga, I. Abe, H. Tanaka, M.H. Nagaoka, H. Akiyama, T. Maitani, *Food Addit. Contam.* **2006**, 23, 1179.
- [10] B. Leblanc, C. Charuel, W. Ku, R. Ogilvie, *Int. J. Pharm. Med.* **2004**, 18, 215.
- [11] D. Jacobson-Kram, T. McGovern, *Adv. Drug Deliv. Rev.* **2007**, 59, 38.
- [12] A. Nageswari. K.V. Reddy, K. Mukkanti, *Sci. Pharm.* **2011**, 79, 4, 865.
- [13] A. Roy, S. Nyarady, M. Matchett, *Chim. Oggi.* **2009**, 27, 19.
- [14] S. Reddy, E. Swathi, S. Jyothisri, T. Reddy, P. Monica, T. Sowjanya, *J. Sci. Res. Pharm.* **2012**, 1, 1.
- [15] Guidelines on the Limits of Genotoxic Impurities. CPMP/SWP/5199/02, European Medicines Agency (EMA), London, June, **2006**.
- [16] L. Muller, T. Singer, *Toxicol. Lett.* **2009**, 190, 243.

- [17] D.I. Robinson, *Org. Process Res. Dev.* **2010**, 14, 946.
- [18] International Conference on Harmonization (ICH) guideline - ICH Q3 Q3A(R): impurities in new drug substances (revised guideline), **2003**, 68, 6924.
- [19] International Conference on Harmonization (ICH) guideline - ICH Q3B(R): impurities in new drug products (revised guideline), **2003**, 68, 64628.
- [20] International Conference on Harmonization (ICH) guideline - ICH Q3C: impurities: guideline for residual solvents, **2003**, 68, 64352.
- [21] M.D. LeVan, Ed. *Fundamental of Adsorption*; Kluwer Academic Publishers: Norwell, MA, **1996**.
- [22] F. Rouqueol, J. Rouquerol, K. Sing, *Adsorption by Powders and Porous Solids: Principles, Methodology and Applications*; Academic Press: New York, **1999**.
- [23] C. Lee, R. Helmy, C. Strulson, J. Plewa, E. Kolodziej, V. Antonucci, B. Mao, C.J. Welch, Z. Ge, M.A. Al-Sayah, *Org. Process Res. Dev.* **2010**, 14, 4 , 1021.
- [24] G. Székely, J. Bandarra, W. Heggie, B. Sellergren, F. C. Ferreira, *J. Membr. Sci.* **2011**, 38, 121.
- [25] G. Székely, J. Bandarra, W. Heggie, F. C. Ferreira, B. Sellergren, *Sep. Purif. Technol.* **2012**, 86, 190.
- [26] G. Székely, J. Bandarra, W. Heggie, B. Sellergren, F. C. Ferreira, *Sep. Purif. Technol.* **2012**, 86, 79.
- [27] G. Székely, E. Fritz, J. Bandarra, W. Heggie, B. Sellergren, *J. Chromatogr. A.* **2012**, 1240, 52.
- [28] S.G. Del Blanco, L. Donato, E. Drioli, *Sep. Purif. Technol.* **2012**, 87, 40.
- [29] W. Armarego, *Purification of Laboratory Chemicals*. Elsevier Science, **2003**, 370.
- [30] A. Teasdale, S.C. Eyley, S. Delaney, K. Jacq, K. Taylor-Worth, A. Lipczynski, V. Reif, D.P. Elder, K.L. Facchine, S. Golec, R. Shulte Oestrich, P. Sandra, F. David, *Org. Process Res. Dev.* **2009**, 13, 429.
- [31] E. Eder, W. Kutt, C. Deininger, *Chem.Biol. Interac.* **1989**, 69, 45.
- [32] E. Eder, C. Deininger, W. Kutt, *Mut. Res.* **1989**, 211, 51.
- [33] E. Eder, A. Favre, C. Deininger, H. Hahn, W. Kutt, *Mutagenesis.* **1989**, 4,179.

- [34] D.W. Boerth, E. Eder, G. Rasul, J. Morais, *Chem. Res. Toxicol.* **1991**, 4, 368.
- [35] Arkema : Regulation of Genotoxic Sulfonate Esters in Pharmaceuticals, 2007, 1.
Brochure at www.arkema-inc.com/literature/pdf/819.pdf
- [36] O. Faroon, N. Roney, J. Taylor, A. Ashizawa, M.H. Lumpkin, D.J. Plewak, *Toxicol. Ind. Health*, **2008**, 24, 447.
- [37] I.D. Kozekov, R. J. Turesky, G. R. Alas, C.M. Harris, T.M. Harris, C.J. Rizzo, *Chem. Res. Toxicol.* **2010**, 23, 1701.
- [38] Z. Liu, D.G. Buckanll, M.G. Allen *Mat. Res. Soc. Proc.* **2008**, 1138, 39.
- [39] X. Liu, M. Zhu, J. Xie, *Toxicol Mech. Methods.* **2010**, 20, 36.
- [40] Toxicological profile for acrolein, U.S. Department of Health and Human Services, Service Agency for Toxic Substances and Disease Registry, **2007**
- [41] Impurities testing guideline: Impurities in new drug substances. CPMP/ICH/2737/99, European Medicines Agency (EMA), London, October, **2006**.
- [42] G. Vanhoenacker, E. Dumonta, F. Davida, A. Bakerb, P. Sandraa, *J. Chromatogr. A.* **2009**, 1216, 3563.
- [43] G. Székely, B. Henriques, M. Gil, A. Ramos, C. Alvarez, *J. Pharm. Biomed. Anal.* **2012**, 70, 251.
- [44] H. Tomankova, J. Sabartova, *Chromatographia*, **1989**, 28, 197.
- [45] P.C. Damiani, M. Bearzotti, M. Cabezo'n, A.C. Olivieri, *J. Pharm. Biomed. Anal.* **1998**, 17, 233.
- [46] I.F. Al-Momani, *Anal. Sci.* **2006**, 22, 1611.
- [47] K. Ensing and T. De Boer, *Trends Anal. Chem.* **1999**, 18, 138.
- [48] B. Sellergren, Ed., *Molecularly Imprinted Polymers: Man-made Mimics of Antibodies and Their Application in Analytical Chemistry: Techniques and Instrumentation in Analytical Chemistry*, Elsevier Science, Amsterdam, Netherlands, **2001**.
- [49] G. Wulff, H.G. Poll, *Makromol. Chem.* **1987**, 188, 741.
- [50] B. Sellergren, *Anal. Chem.* **1994**, 66, 1578.

- [51] T. Ikegami, T. Mukawa, H. Nariai, T. Takeuchi, *Anal. Chim. Acta.* **2004**, 504, 13.
- [52] L. Dubey, I. Chianella, I. Dubey, E. Piletska, M. J. Whitcombe, S. Piletsky, *Open Anal. Chem. J.* **2012**, 6, 15.
- [53] T. Ikegami, W.S. Lee, H. Nariai, T. Takeuchi, *J. Chromatogr. B.* **2004**, 804, 197.
- [54] K.J. Shea, T.K. Dougherty, *J. Am. Chem. Soc.* **1986**, 108, 1091.
- [55] M.J. Whitcombe, M.E. Rodriguez, P. Villar, E.N. Vulfson, *J. Am. Chem. Soc.* **1995**, 117, 7105.
- [56] M.A. Khasawneh, P. T. Vallano, V.T. Remcho, *J. Chromatogr. A.* **2001**, 922, 87.
- [57] R. Rajkumar, A. Warsinke, H. Mohwald, F. W. Scheller, M. Katterle, *Biosens. Bioelectron.* **2007**, 22, 3318.
- [58] I. Idziak, D. Gravel, X. Zhu, *Tetrahedron Lett.* **1999**, 40, 9167
- [59] G. Vlatakis, L.I. Andersson, R. Mueller, K. Mosbach, *Nature*, **1993**, 361, 645.
- [60] K. Mosbach, O. Ramström, *Nat. Biotechnol.* **1996**, 14, 163.
- [61] D.A. Spivak, K.J. Shea, *Macromolecules.* **1998**, 31, 2160.
- [62] M.A. Markowitz, G. Deng, B.P. Gaber, *Langmuir*, **2000**, 16, 15, 6148.
- [63] L.I. Andersson, R. Mueller, K. Mosbach, *Macromol. Rapid. Comm.* **1996**, 17, 65.
- [64] A.G. Mayes, L.I. Andersson, K. Mosbach, *Anal. Biochem.* **1994**, 222, 2, 483.
- [65] J. Matsui, T. Takeuchi, *Anal. Comm.* **1997**, 34, 199.
- [66] M. Glad, O. Norrlöv, B. Sellergren, N. Siegbahn, K. Mosbach, *J. Chromatogr.* **1985**, 347, 11.
- [67] A. J. Hall, F. Lanza-Sellergren, P. Manesiotis, B. Sellergren, *Anal. Chim. Acta.* **2005**, 538, 9.
- [68] B. Sellergren, K.J. Shea, *J. Chrom.* **1993**, 654, 31.
- [69] P.K. Dhal, F.H. Arnhold, *Macromolecules*, **1992**, 25, 7051.

- [70] R. Say, E. Birlik, A. Ersöz, F. Yılmaz, T. Gedikbey, A. Denizli, *Anal. Chim. Acta.* **2003**, 480, 251.
- [71] N. Bereli, M. Andac, R. Say, I.Y. Galaev, A. Denizli, *J. Chromatogr. A.* **2008**, 1, 18.
- [72] www.biotage.com
- [73] J.Steinke, D.C. Sherrington, I.R. Dunkin, *Adv. Polym. Sci.* **1995**, 123, 81.
- [74] G. Wulff, A. Sarhan, *Angew. Chem.* **1972**, 84, 364.
- [75] G. Wulff, A. Sarhan, K. Zabrocki, *Tetrahedron Lett.* **1973**, 44, 4329.
- [76] G. Wulff, R. Vesper, R. Grobe-Einsler, A. Sarhan, *Makromol. Chem.* **1977**, 178, 2799.
- [77] G. Wulff, S. Schauhoff, *J. Org. Chem.* **1991**, 56, 395
- [78] G. Wulff, *Angew. Chem. Int. Ed.* **1995**, 34, 1812.
- [79] G.Wulff, A. Biffis Molecular imprinting with covalent or stoichiometric non-covalent interactions. In Sellergren B. (ed.), *Molecularly Imprinted Polymers: Man-Made Mimics of Antibodies and their Applications in Analytical Chemistry, Techniques and Instrumentation in Analytical Chemistry*, **2001**, (p.p. 71-111). Amsterdam: Elsevier
- [80] G. Wulff, H. Poll, *Makromol. Chem. Physic.* **1977**, 178, 2799.
- [81] M.J. Whitcombe, M.E. Rodrigez, P. Villar, E.N. Vulfson, *J. Am. Chem. Soc.* **1995**, 7105.
- [82] Y.Q. Xia, T.Y. Guo, H.L. Zhao, M.D. Song, B.H. Zhang, B.L. Zhang, *J. Sep. Sci.* **2007**, 30, 1300.
- [83] D.K. Alexiadou, N.C. Maragou, N.S. Thomaidis, G.A. Theodoridis, M.A. Koupparis, *J. Sep. Sci.* **2008**, 31, 2272.
- [84] R. Arshady, K. Mosbach, *Makromol. Chem.* **1981**, 182, 687.
- [85] E. Yilmaz, O. Ramström, P.Möller, D. Sanchez, K. Mosbach, *J.Mater. Chem.* **2002**, 12, 1577.
- [86] B. Sellergren, *Anal. Chem.* **1994**, 66, 1578.
- [87] B. Sellergren, *Trend.Anal. Chem.* **1999**, 18, 164.
- [88] L. I. Andersson, *J. Chromatogr. B.* **2000**, 739, 163.
- [89] F. Lanza, B. Sellergren, *Chromatographia*, **2001**, 53, 599.

- [90] F. Chapuis, V. Pichon, M.C. Hennion, *LC-GC Europe*, **2004**, 408.
- [91] F. Qiao, H. Sun, H. Yan, K. Row, *Chromatographia*, **2006**, 64, 625.
- [92] E. Caro, R.M. Marce, F. Borrull, P.A.G. Cormack, *Trend.Anal. Chem.* **2006**, 24, 143.
- [93] E. Caro, M. Marce, P.A.G. Cormack, D.C. Sherrington, F. Borrull, *J. Chromatogr. A.* **2003**, 995, (1–2), 233.
- [94] F.Chapuis, V. Pichon, F. Lanza, B. Sellergren, M.C Hennion, *J. Chromatogr. B.* **2004**, 804, 1, 93.
- [95] E. Caro, M. Marce, P.A.G. Cormack, D.C. Sherrington, F. Borrull, *J. Chromatogr. A.* **2004**, 1047, 2, 175.
- [96] F.Chapuis, V. Pichon, F. Lanza, B. Sellergren, M.C Hennion, *J. Chromatogr. A.* **2003**, 999 (1–2), 23.
- [97] J.P Lai, R. Niessner, D. Knopp, *Anal. Chim. Acta.* **2004**, 522, 2, 137.
- [98] O Brüggemann, A. Visnjevski, R. Burch, P. Patel, *Anal. Chim. Acta.* **2004**, 504, 1, 81.
- [99] A. Berezki, A. Tolokan, G. Horvai, V. Horvath, F. Lanza, A.J. Hall, B. Sellergren, *J. Chromatogr. A.* **2001**, 930, 31.
- [100] W.M. Mullett, M.F. Dirie, E.P.C. Lai, H. Guo, X. He, *Anal. Chim. Acta.* **2000**, 414, 123.
- [101] S.G Wu, E.P.C. Lai, P.M. Mayer, *J. Pharm. Biomed. Anal.* **2004**, 36, 483.
- [102] L.I. Andersson, E. Hardenborg, S.M. Sandberg, K. Moller, J. Henriksson, S.I. Bramsby, L.I. Olsson, R.M. Abdel, *Anal. Chim. Acta.* **2004**, 526, 147.
- [103] S.Y. Feng, E.P.C. Lai, E. Dabek-Zlotorzynska, S. Sadeghi, *J. Chromatogr. A.* **2004**, 1027, 155.
- [104] G. Theodoridis, A. Kantifes, P. Manesiotis, N. Raikos, H. Tsoukali-Papadopoulou, *J. Chromatogr. A.* **2003**, 987, 103.
- [105] L.I. Andersson, M. Abdel-Rehim, L. Nicklasson, L. Schweitz, S. Nilsson, *Chromatographia*, **2002**, 55, 65.
- [106] J. Matsui, K. Fujiwara, S. Ugata, T. Takeuchi, *J. Chromatogr. A.* **2000**, 889, 25.
- [107] A. Ersöz, R. Say, A. Denizli, *Anal. Chim. Acta.* **2004**, 502, 91.

- [108] C. Baggiani, C. Giovannoli, L. Anfossi, C. Tozzi, *J. Chromatogr. A.* **2001**, 938, 35.
- [109] C.R.T. Tarley, L.T. Kubota, *Anal. Chim. Acta.* **2005**, 548, 11.
- [110] D.M. Han, G.Z. Fang, X.P. Yan, *J. Chromatogr. A.* **2005**, 1100, 131.
- [111] N. Masque, R.M. Marce, F. Borrull, P.A.G. Cormack, D.C. Sherrington, *Anal Chem.* **2000**, 72, 4122.
- [112] A. Zurutuza, S. Bayouhd, P.A.G. Cormack, L. Dambies, J. Deere, R. Bischoff, D.C. Sherrington, *Anal. Chim. Acta.* **2005**, 542, 14.
- [113] T. Pap, V. Horvath, A. Tolokan, G. Horvai, B. Sellergren, *J. Chromatogr. A.* **2002**, 973, 1.
- [114] C. Nicholls, K. Karim, S. Piletsky, S. Saini, S. Setford, *Biosens. Bioelectron.* **2006**, 21, 1171.
- [115] F. Puoci, C. Garreffa, F. Iemma, R. Mazzalupo, U.G. Spizzirri, N. Picci, *Food Chem.* **2005**, 93, 349.
- [116] X. Dong, W. Wang, S. Ma, H. Sun, Y. Li, J. Guo, *J. Chromatogr. A.* **2005**, 1070, 125.
- [117] C. Schirmer, H. Meisel, *J. Chromatogr. A.* **2006**, 1132, 325.
- [118] C. Baggiani, P. Baravalle, G. Giraudi, C. Tozzi, *J. Chromatogr. A.* **2007**, 1141, 158.
- [119] F. Chapuis, J. U Mullot, V. Pichon, G. Tuffal, M.C. Hennion, *J. Chromatogr. A.* **2006**, 1135, 127.
- [120] F. Puoc, G. Cirillo, M. Curci, F. Iemma, U.G. Spizzirri, N. Picci, *Anal. Chim. Acta.* **2007**, 593, 164.
- [121] www.sigma-aldrich.com
- [122] www.polyintell.com
- [123] L.I. Andersson, A. Paprica, T. Arvidsson, *Chromatographia*, **1997**, 46, 57.
- [124] J. Matsui, K. Fujiwara, T. Takeuchi, *Anal. Chem.* **2000**, 72, 1810.
- [125] K. Haupt, A. G. Mayes, K. Mosbach, *Anal. Chem.* **1998**, 70, 3936.
- [126] P.D. Martin, T.D. Wilson, I.D. Wilson, G.R. Jones, *Analyst*, **2001**, 126, 757.
- [127] G. Wulff, S. Schauhoff, *J. Org. Chem.* **1991**, 56, 395.

- [128] E.Turiel, A. Martin-Esteban, P. Fernandez, C. Perez-Conde, C. Camara, *Anal. Chem.* **2001**, 73, 5133.
- [129] A. J. Hall, F. Lanza-Sellergren, P. Manesiotis, B. Sellergren, *Anal. Chim. Acta.* **2005**, 538, 9.
- [130] S.Jin, Y. Cheng, S. Reid, M. Li, B. Wang, *Med. Res. Rev.* **2010**, 30, 171.
- [131] J. P. Lorand, J. O. Edwards, *J. Org. Chem.* **1959**, 24, 769.
- [132] T. D. James, K. R. Sandanayake, S. Shinkai, *Nature*, **1995**, 374, 345.
- [133] T. D. James, K. R. Sandanayake, R. Iguchi, S. Shinkai, *J. Am. Chem. Soc.* **1995**, 117, 8982.
- [134] T. D. James, H. Shinmori, S. Shinkai, *Chem. Commun.* **1997**, 71.
- [135] J. Zhao, M. G. Davidson, M. F. Mahon, G. Kociok-Kohn, T. D. James, *J. Am. Chem. Soc.* **2004**, 126, 16179.
- [136] S. Arimori, M. Bell, C. S. Oh, T. D. James, *Org. Lett.* **2002**, 4, 4249.
- [137] S. Arimori, M. L. Bell, C. S. Oh, K. A. Frimat, T. D. James, *Chem. Commun.* **2001**, 1836.
- [138] S. Gamsey, A. Miller, M.M. Olmstead, C.M. Beavers, L.C. Hirayama, S. Pradhan, R.A. Wessling, B. Singaram, *J. Am. Chem. Soc.* **2007**, 129, 1278.
- [139] Z. Wang, D.Q. Zhang, D.B. Zhu, *J. Org. Chem.* **2005**, 70, 5729.
- [140] C.W. Gray, T.A. Houston, *J. Org. Chem.* **2002**, 67, 5426.
- [141] A. Jabbour, D. Steinberg, V.M. Dembitsky, A. Moussaieff, B. Zaks, M. Srebnik, *J. Med. Chem.* **2004**, 47, 2409.
- [142] R. Aharoni, M. A. Bronstheyn Jabbour, B. Zaks, M. Srebnik, D. Steinberg, *Bioorg. Med. Chem.* **2008**, 16, 1596.
- [143] R.P. Singhal, B. Ramamurthy, N. Govindraj, Y. Sarwar, *J. Chromatogr.* **1991**, 543, 117.
- [144] V. Bouriotis, J. Galpin, P.D.G. Dean, *J. Chromatogr.* **1981**, 210, 267.
- [145] P.R. Westmark, L.S. Valencia, B.D. Smith, *J. Chromatogr.* **1994**, 664, 123.
- [146] V. Adamek, X.C Liu, Y.A. Zhang, K., Adamkova, W.H. Scouten, *J. Chromatogr.* **1992**, 625, 91.
- [147] W. Yang, X. Gao, B.Wang, *Med. Res. Rev.* **2003**, 23, 346.
- [148] H. Fang, G. Kaur, B. Wang, *J. Fluoresc.* **2004**, 14, 481.

- [149] E. Yilmaz, Expanding the utility of MIPs by screening, 12th International Symposium on Hyphenated Techniques in Chromatography and Hyphenated Chromatographic Analyzers (HTC-12), 1-3 February 2012, Bruges, Belgium
- [150] A. Cheminat, C. Benezra, M. J. Farral, and J. M. J. Frechet, *Tetrahedron Lett.* **1980**, 21, 617.
- [151] D. L. Flynn, J. Z. Crich, R. V. Devraj, S. L. Hockerman, J. J. Parlow, M. S. South, S. Woodard, *J. Am. Chem. Soc.* **1997**, 119, 4874.
- [152] S. W. Kaldor, M. G. Siegel, J. E. Fritz, B. A. Dressman, P. J. Hahn, *Tetrahedron Lett.* **1996**, 37, 7193.
- [153] C. Lin, Z. Zhang, J. Zheng, M. Liu, X. Xia Zhu, *Macromol. Rapid Commun.* **2004**, 25, 1719.
- [154] M. G. Siegel, P. J. Hahn, B. A. Dressman, J.E. Fritz, J. R. Grunwell, S. W. Kaldor, *Tetrahedron Lett.* **1997**, 38, 3357
- [155] G.M. Coppala, *Tetrahedron Lett.* **1998**, 39, 8233.
- [156] R. Andreoli, P. Manini, M. Corradi, A. Mutti, W.M. Niessen, *Rapid Commun. Mass Spectrom.* **2003**, 17, 7, 637.
- [157] A.J. Hall, P. Manesiotis, M. Emgenbroich, M. Quaglia, E. De Lorenzi, B. Sellergren, *J. Org. Chem.* **2005**, 70, 1732.
- [158] S. Brunauer, P.H. Emmett, E. Teller, *J. Am. Chem. Soc.* **1938**, 60, 309.
- [159] E. P. Barrett , L. G. Joyner , P. P. Halenda, *J. Am. Chem. Soc.* **1951**, 73, 1, 373.
- [160] A. Costoyas, J. Ramos, J. Forcada, *J. Polym. Sci - Pol. Chem.* **2009**, 47, 6201.
- [161] K. Hwang, T. Sasaki, *J. Mater. Chem.* **1998**, 8, 2153.
- [162] M. C. Etter, Z. Urbanczyk-Lipkowska, M. Zia-Ebrahimi, T.W. Panunto, *J. Am. Chem. Soc.* **1990**, 112, 8415.
- [163] M. C. Etter, T.W. Panunto, *J. Am. Chem. Soc.* **1998**, 110, 5897.
- [164] B. Pirard, G. Baudoux, F. Durant, *Acta Cryst.* **1995**, 51, 103.
- [165] D.A. Haynes, J. A. Chisholm, W. Jones, W. D. Samuel Motherwell, *Cryst Eng Comm.* **2004**, 6, 584.
- [166] M.H. Abraham, *Chem. Soc. Rev.* **1993**, 22, 73.
- [167] I. Langmuir, *J. Am. Chem. Soc.* **1918**, 40, 1361.

- [168] Booth, R. J.; Hodges J. C. *J. Am. Chem. Soc.* **1997**, 119, 4882.
- [169] D.W. Emerson, R.R. Emerson, S.C. Joshi, E.M. Sorensen, J. Nrek, *J. Org. Chem.* **1979**, 44, 4634.
- [170] C. J. Welch, J. Albaneze-Walker, W. R. Leonard, M. Biba, J. DaSilva, D. Henderson, B. Laing, D.J. Mathre, S. Spencer, X. Bu, T. Wang, *Org. Process Res. Dev.* **2005**, 9, 198
- [171] C.J. Welch, M. Biba, A. Drahus, D. A. Conlon, H. Hsin Tung, P. Collins, *J. Liq. Chrom. & Rel. Technol.* **2003**, 26, 12, 1959.
- [172] H. S. Anderson. A.C. Koch-Schmidt, S. Ohlson, *J. Mol. Recognit.* **1996**, 9,675.
- [173] Z. Jie, H. Xiwen, *Anal. Chim. Acta.* **1999**,381, 85.
- [174] J-P. Lai, X-Y.Lu , C-Y. Lua, H-F. Ju , X-W. Hea. *Anal. Chim. Acta.* **2001**,442, 105.
- [175] X. Liu, T. Zhou, Z. Du, Z. Weia , J. Zhang, *Soft Matter*, **2011**, 7, 1986.
- [176] H. Guo , X. He, H. Liang, *Fresenius J. Anal. Chem.* **2000**, 368, 763.

Curriculum Vitae

Rüstem Keçili

PERSONAL DETAILS

Nationality : Turkish
Date of Birth : 10.04.1980
Marital Status : Single

EDUCATION

Doctor of Philosophy (Ph.D)

Technical University of Dortmund, Faculty of Chemistry
Dortmund, Germany September 2009-present

Master of Science (MSc)

Anadolu University, Faculty of Science
Chemistry Department, Eskişehir, Turkey September 2003- August 2006

University of Palermo, Chemistry Department, Italy February 2005 –June 2005
(By Socrates-Erasmus Student Exchange Programme)

Anadolu University, Department of Secondary School
Education September 2003- August 2004

Bachelor of Science

Anadolu University, Faculty of Science
Chemistry Department, Eskişehir, Turkey September 1999 – June 2003

WORKING EXPERIENCE

Researcher : Biotage AB, Lund, Sweden September 2009- October 2012

Researcher: Anadolu University Plant, Drug and Scientific Researches Center,
Eskisehir, Turkey July 2005- August 2009

AWARDS

Ph.D Fellowship - Early Stage Researcher, Marie Curie Fellowship funded by European Commission (September 2009- September 2012)

M.Sc Fellowship - Sokrates-Erasmus Student Exchange Programme, Fellowship funded by European Commission (February 2005-June 2005)

PUBLICATIONS

1. R. Keçili, D. Nivhede, J. Billing, M. Leeman, B. Sellergren and E. Yilmaz “Removal of acrolein from active pharmaceutical ingredients using aldehyde scavengers” , **Organic Process Research & Development**, 16 (6), 1225-1229 (2012)

2. R. Keçili, J. Billing, D. Nivhede, M. Leeman, B. Sellergren, Anthony Rees, E. Yilmaz, “Selective scavenging of the genotoxic impurity methyl p-toluenesulfonate from pharmaceutical compounds”, **Separation and Purification Technology**, (2012) (in press) <http://dx.doi.org/10.1016/j.seppur.2012.09.028>

CONFERENCES

1. E. Yilmaz, D. Nivhede, **R. Keçili**, A. Rees, “Utilizing the cross reactivity of MIPs-ExploraSep™”, MIP 2010 – The 6th International Conference on Molecular Imprinting, New Orleans, USA, Aug 9-12, **2010**

2. R. Keçili, D. Nivhede, B. Sellergren and E. Yilmaz, “Genotoxic Impurity Removal by using ExploraSep™ Concept” , 4th Graduate Student Symposium on Molecular Imprinting, Imperial College, London, UK, Sep 28-30. **2011**

3. R. Keçili, J. Billing and E. Yilmaz , “Fast Identification of Selective resins for Genotoxic Impurity Removal via Screening of Molecularly Imprinted Polymers Resins Libraries”, HPLC 2012, Anaheim, California, USA, June 16-21. **2012**